AD/SSC/Tech. No. 89

Accelerator Development Department

BROOKHAVEN NATIONAL LABORATORY

Associated Universities, Inc.

Upton, New York 11973

SSC Technical Note No. 89
368-16 (RHIC-MD-107)
SSCL-N-742

INSTABILITIES OF BELLOWS: DEPENDENCE ON INTERNAL PRESSURE, END SUPPORTS, AND INTERACTIONS IN ACCELERATOR MAGNET SYSTEMS

R.P. Shutt and M.L. Rehak

November 20, 1990

Table of Contents

for

Instabilities of Bellows: Dependence on Internal Pressure, End Supports, and Interactions in Accelerator Magnet Systems

Summary and Conclusions		1
I.	Introduction	6
II.	Basic Derivation for Bellows under Pressure	8
IIIa.	Axial and Lateral Spring Constants, and Convolution Wall Stresses and Deflections under Bellows Compression or Tension	16
IIIb.	Deflections and Stresses of Bellows Convolutions under Internal Pressure	28
IV.	Spring-Supported Bellows Model	34
V.	Magnet End Misalignment and Lateral Spring Constants	40
VI.	Bellows Interactions in Magnet Systems	45
VIIa.	Numerical Results: Spring Constants, Wall Stresses and Deflections	53
VIIb.	Numerical Results: Spring-Supported Bellows Model	59
VIIc.	Numerical Results: Bellows Interactions in Magnet Systems	68
VIII.	Numerical Method	74
References		76
Appendix:	MACSYMA Code for Magnet Bellows Assembly	126
Appendix:	Fortran Code for Magnet Bellows Assembly	128
Appendix:	File Names of Additional Codes	130

Instabilities of Bellows: Dependence on Internal Pressure, End Supports, and Interactions in Accelerator Magnet Systems

R.P. Shutt and M.L. Rehak

Summary and Conclusions

In this paper we are dealing with internally pressurized bellows which are to be used extensively for SSC and RHIC magnet interconnections. In Section II we show how an internally pressurized bellows whose ends are not free to move but are supported more or less rigidly can become unstable at some well-determined critical pressure p_{cr}, similarly to a bar that is compressed axially, resulting in Euler-type buckling.

Interconnection bellows must not only accommodate helium coolant flow and pressures, but also must be axially precompressed when warm and extended when cold in order to allow for the thermal shrinkage of superconducting magnets during cooldown. From manufacturers one can obtain pressure ratings, spring constants, diameters, length, convolution geometry, cycling fatigue properties and manufacturing inaccuracies. Making use of our requirements for the mentioned parameters, we give in Sections IIIa,b an approximate theory for bellows, having assumed that, for our purposes, radial widths of convolutions are small compared to bellows diameters. This gives us a possibility to specify bellows details that will satisfy our requirements for spring constants, compressions and extensions, and pressures including margins. We can thus test whether our requirements will enable us to obtain reasonably available bellows. Specifically, we will be able to calculate convolution wall stresses and motions (without collapsing convolutions) under operating conditions and beyond, when instability occurs. Based on the results, we can write our specifications for manufacturers to consider. Large numbers of small or large, and expensive, bellows will be needed, and they must not fail since need for replacement will mean a major interruption of accelerator operation.

Sections IV to VI are valid for any size of bellows, since the derivations given there require knowledge of only easily obtainable bellows parameters. In Section IV bellows ends are assumed to be supported by two kinds of springs, namely springs acting perpendicularly to the bellows axis and others acting torsionally, providing a torque when the bellows ends' angle is varied. If the torsion springs were not provided, the ends would be considered "hinged". This "spring-support" model has provided much insight into the various conditions under which a bellows can become unstable. The importance of proper bellows support becomes apparent, in addition to selection of proper bellows design parameters. Manufacturing inaccuracies resulting in prebent shapes of purchased bellows, and installation inaccuracies resulting in lateral or angular offsets of bellows ends are also investigated. Instabilities are due to the mentioned Euler-type buckling and end support spring properties. End-to-end offsets and initial bellows prebends (before installation) reinforce these instabilities and increase bellows distortions and stresses even at operating pressures.

In Section V we address possible misalignments of adjacent magnet ends due to bellows and installation inaccuracies. For instance, assuming that magnet ends are well-aligned before bellows installation, prebends or offsets of bellows ends can disturb the alignment, especially if the bellows' lateral spring constant is large or if the magnet end stiffness is small. The latter could, in principle, be increased by moving magnet supports as close to the ends as possible. Interconnection installation difficulties would then have to be considered. Nevertheless, accelerator performance is quite sensitive to magnet misalignments, especially concerning quadrupoles, and therefore affects requirements for bellows behavior under operating conditions.

In Section VI, we have studied a model consisting of three magnets interconnected by two bellows. Each magnet can be supported by up to five supports whose lateral stiffness is taken into account in addition to the magnet stiffness. (Vertical magnet support stiffness is larger than lateral.) A resulting magnet end stiffness can then be calculated and used for comparison with the spring-support model discussed in Section IV. Some of the instabilities already found in the spring-support model can be split into two peaks here, due to

asymmetries of components or bellows inaccuracies. In particular, however, interactions between bellows are of interest here; what is the effect of a buckling bellows on bellows in neighboring interconnections? To answer this question, we have also introduced the possibility of large forces acting at bellows ends in a direction perpendicular to the magnet axis. This would model the effect of a grossly distorted, but still pressurized, bellows on the magnet system. Since the effect is transmitted through supported magnets, the number and stiffness of magnet supports will thus also play an important role.

Calculations were performed using a symbolic algebra manipulation code called MACSYMA (Section VIII) which has been extremely valuable in solving the many algebraic equations following from the previous Sections. The program provided matrix inversions and thus algebraic solutions or matrix coefficients which could be entered into a numerical FORTRAN program. The algebraic solutions for the spring-support model allowed us to understand many of the features that can cause bellows collapse or rupture. The FORTRAN program provided the large matrix inversion needed for Section VI, and of course, all the numerical output data. MACSYMA and FORTRAN program codes are described in the Appendices.

In Section VII we discuss numerical results as well as some algebraic expressions including limiting values for some quantities such as spring values. Examples are given for SSC as well as for RHIC. Additional details concerning each accelerator will be presented in separate Magnet Division Notes.

Our calculations confirm that bellows wall stresses generally will have to be very high ($\leq 1.8 \times 10^5$ psi) if one wants to obtain bellows that are usable in applications of the kind required here. Therefore, in many cases the material will be allowed to yield somewhat during every operating cycle (axial deflection, bending, pressurizing, cool-down/warm-up). Material fatigue must then be taken into account, which usually is included in manufacturers' specifications. For our purpose, we would specify about 2000 cycles.

In the spring-support model we find that a prebent shape of a bellows (we use sine, cosine and parabolic shapes) can stimulate the instabilities that may algebraically appear as indeterminate, even for ideally straight shapes. Our bellows are "designed" for the first

instability to occur at a lowest pressure of 450 psi. (Another "peak" will then appear at 1800 psi, and more at still higher pressures.) We are mostly concerned that the stresses or strains in the bellows walls will not exceed specifications. An indication is the maximum axial compression or elongation, uniform for a whole bellows or localized somewhere along the bellows convolution. We therefore present maximum convolution elongations found in the calculations, which are compared with manufacturers' specifications. As the pressure is raised in a bellows wall, elongations increase gradually and can reach large values at our critical pressure of 450 psi. To us the value reached at our maximum operating pressure of 300 psi is particularly important. Thus, after a bellows is designed for the critical pressure, we must also meet the criterion not to exceed allowable elongation at operating pressure, which is determined by the rate of rise of the elongation vs. pressure function.

The rise rate is very much affected by the end support of a bellows. The two ends may be forced into laterally or angularly offset positions during installation. Furthermore, equivalent lateral and torsional spring properties of the support structure play a very important role. These spring properties produce additional peaks, usually at higher pressure, but also below 450 psi if, especially, the torsional support is not stiff enough. Torsional stiffness as high as 5×10^5 lb inch/radian is required for some of the large bellows and magnets considered here, independent of lateral stiffness or pressure. Fortunately, we can easily provide values $> 10^7$.

Due to the possible end offsets and due to "support peaks" the rise rate of the bellows elongation increases: support peaks can be placed above 450 psi by sufficient torsional stiffness of end supports. However, the presence of the support peaks increases the rise rate of elongation vs. pressure. The presence of pre-bent shapes additionally increases the rise rate.

The spring support model findings recur in the magnet assembly model (Section VI), except that now, as already mentioned above, because of assembly asymmetries and due to the presence of two bellows, some peaks found previously will be split into double peaks.

The magnet assembly model allows us to study the effects of one bellows on a neighboring one. Any such effects would, of course, also depend on the rigidity of the

magnet supports. Using Fermilab as well as BNL supports, we find that interactions are very small in the pressure region (≤ 450 psi) of interest to us.

One can simulate a "catastrophe" at one bellows by applying one or more large forces there laterally and look at the distortion of the neighboring one. We show that such a disturbance in one bellows affects the other one little at or below operating pressure.

Our general conclusion is that, with sufficient attention to bellows design and support detail (also including the magnet supports if large bellows are used), practically all sizes, large or small, of bellows can be used for interconnections between magnets. However, we recommend strongly that any of the bellows that are to be used in the large quantities required for the accelerators should still be tested very carefully in test set-ups that simulate conditions to which the bellows will be exposed.

I. *Introduction*

Bellows represent one of the most commonly used components in engineering structures. They are used to contain vacuum, or gases or liquids under pressure. They can provide for accommodation of differences in thermal expansion between different structures. Bellows can be bent, stretched, or compressed in various ways when used to connect adjoining but not well-aligned assemblies. They can be obtained in a multitude of shapes, sizes, and materials. They may consist of single or multiple layers.

Many applications of bellows merely require design of adjoining components, resulting specifications for connecting bellows, and making proper selections from catalogues available from a large number of manufacturers. In other cases, special, not readily available bellows may have to be manufactured.

As vital components in much of modern technology, bellows must be as carefully considered in design as other parts in an assembly. They must satisfy all requirements, including a sufficient margin. They must not be overstressed in any direction, must not be damaged in transit, during installation or operation. They must not leak gases or fluids, and their ends must be properly supported. Material fatigue must be taken into account if cycling is intended.

When axially compressed or internally pressurized, bellows can become unstable, leading to gross distortion or complete failure. If several bellows are contained in an assembly, failure modes might interact. (Of course, external pressure can also "buckle" a bellows, but only similarly to a plain cylinder.)

In particle accelerators used for high energy physics research, bellows have been used successfully for a long time to connect beam tubes passing through magnets whose magnetic field, interacting with accelerated electrically charged particles, provides the required circular paths for the particles. In recent times, accelerator magnets have been built to be superconducting (Tevatron at Fermilab, HERA at DESY). In the design stage in the U.S.A. are the Superconducting Super Collider (SSC) in Texas and the Relativistic Heavy Ion Collider (RHIC) at Brookhaven National Laboratory. RHIC will contain many hundreds of superconducting magnets and SSC about 10,000.

For superconducting magnets, one needs many bellows for connection of various helium cooling transfer lines in addition to beam tube connecting bellows.

Large bellows are also considered as a very feasible and strong possibility for connecting the large tubular shells that support the magnet iron yokes and superconducting coils and contain supercritical helium for magnet cooling. In principle, every magnet could be self-contained, with endplates closing off the ends of the shells. These endplates would then be connected by much smaller bellows for the beam tube connections and other bellows to pass cooling fluid, electric bus bars, and instrumentation connections. However, the space available in the magnet interconnection region may be quite limited, and to reduce it further by introduction of the mentioned end plates, transitions, extra bellows, etc., would seem not justified unless it turns out that direct magnet connection with large bellows is not feasible.

It should be mentioned that, with large interconnection bellows full use is made of available volume to limit helium pressure increase when a magnet "quenches", when much of the magnetic field energy is transferred to the helium coolant in a short time. In this event a helium reservoir, such as the interconnection volume, also serves to reduce pressure by reduction of temperature due to partial mixing and helium compressibility.

Assuming that a large bellows has been designed properly concerning stresses, support, availability, etc., we intend to present in this report, (1) a suitable theoretical treatment of bellows properties, (2) a spring-supported bellows model, in order to develop necessary design features for bellows and end supports so that instabilities will not occur in the bellows pressure operating region, including some margin, (3) a model consisting of three superconducting accelerator magnets connected by two large bellows, in order to ascertain that support requirements are satisfied, and in order to study interaction effects between the two bellows. Reliability of bellows for our application will be stressed.

The calculations have been performed with computer programs analytically and numerically, whichever approach seemed most suitable for a particular phase of this work.

The programs are equally adaptable to RHIC and SSC magnet configurations, such as dipole-quadrupole-dipole (DQD), QDQ, DDD, etc.

II. *Basic Derivation for Bellows under Pressure*

Here we wish to derive an analytic expression which will take into account the possibly destabilizing effect of internal pressure on a bellows. (External pressure has a stabilizing effect up to a limit.) The bellows will be assumed to have an arbitrarily bent shape before installation, due to manufacturing inaccuracies. For simplicity, the bent bellows axis is to remain in a plane.

The ends of the bellows are to be quite rigidly supported but are to be open towards adjoining pipes. Figure 1 shows an element of a bellows with average diameter D, local axial bend-radius ρ, and length $\Delta s = \rho\Delta\chi$. Pressure p produces a force $df_o = p\ dA$ on element dA of the bellows wall, when integrated over convolutions, as for a plain cylinder. (*Local forces due to pressure inside convolutions will be treated below.*) With $dA = \frac{1}{2}(D\ d\psi\Delta s_w)$, where Δs_w = length along wall at angle ψ, and expressing

$$\Delta s_w = \left(\rho + \frac{D\cos\psi}{2}\right)\Delta\chi\ ,$$

we obtain for the component of df_o, *in a direction that is parallel to the bending plane,*

$$df = p\frac{D}{2}\cos\psi\left(\rho + \frac{D\cos\psi}{2}\right)d\psi\ \Delta\chi.$$

Integration from $\psi = 0$ to 2π results in

$$\Delta f = \frac{\pi D^2 p}{4}\ \Delta\chi$$

for the total force due to p on the length element Δs. (Integral of components of df_o perpendicular to the bending plane is zero.) Note that this force depends only on the bending angle $\Delta\chi = \Delta s/\rho$. Using Cartesian coordinates,

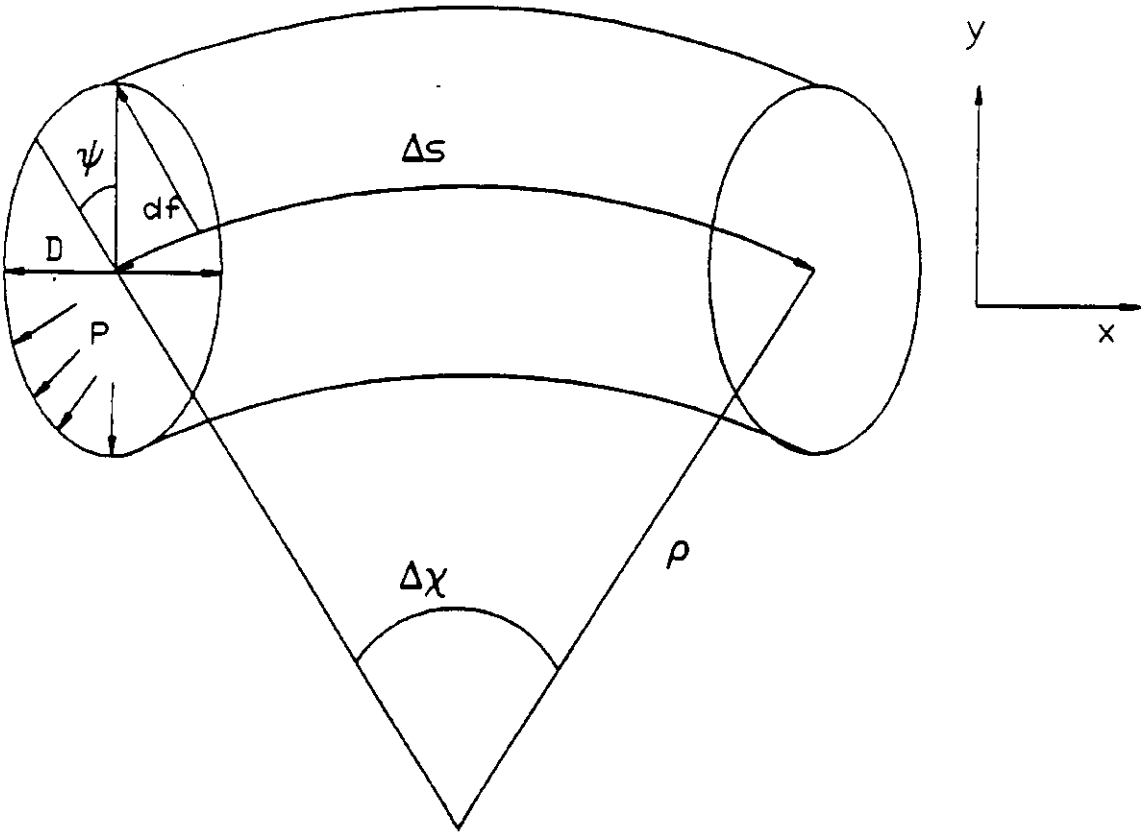

Figure 1.

$$\frac{1}{\rho} = \frac{y''}{(1 + y'^2)^{3/2}}$$
$$\Delta s = (1 + y'^2)^{1/2}\Delta x$$
$$\Delta f = \frac{\pi D^2 p}{4} \frac{y''\Delta x}{(1 + y'^2)}$$

We will be interested only in small bellows deflections. Large deflections are not admissible because wall bending stresses become large and, also the bellows may then interfere with various structures contained in it. Therefore simply

$$\Delta f = -\frac{\pi D^2 p}{4} y''\Delta x \tag{1}$$

(x, y plane to coincide with bending plane) which now acts only in the y-direction, neglecting small components along x. The negative sign is used here since we shall assume that df > 0 when y" is < 0.

We can now set up the equation for bending of a bellows under pressure. In Fig. 2, the central axis of a bellows is shown in an arbitrarily bent plane shape supported by forces $\pm F_{xo}$, $\pm F_{yo}$, and moments M_{c1} and M_{c2}, where

$$-M_{c1} + M_{c2} - F_{xo}y(0) + F_{yo}\ell - \int_o^\ell (\ell - x')df = 0 \tag{2}$$

for equilibrium. Here, the bellows is assumed to be straight, not preshaped before installation.

Bending deflection y at x can be found by solving the differential equation

$$y'' = -\frac{M}{EI} = \frac{1}{EI}\left(F_{xo}(y(0)-y) - F_{yo}x + M_{c1} + \int_o^x (x-x')df\right) \tag{3}$$

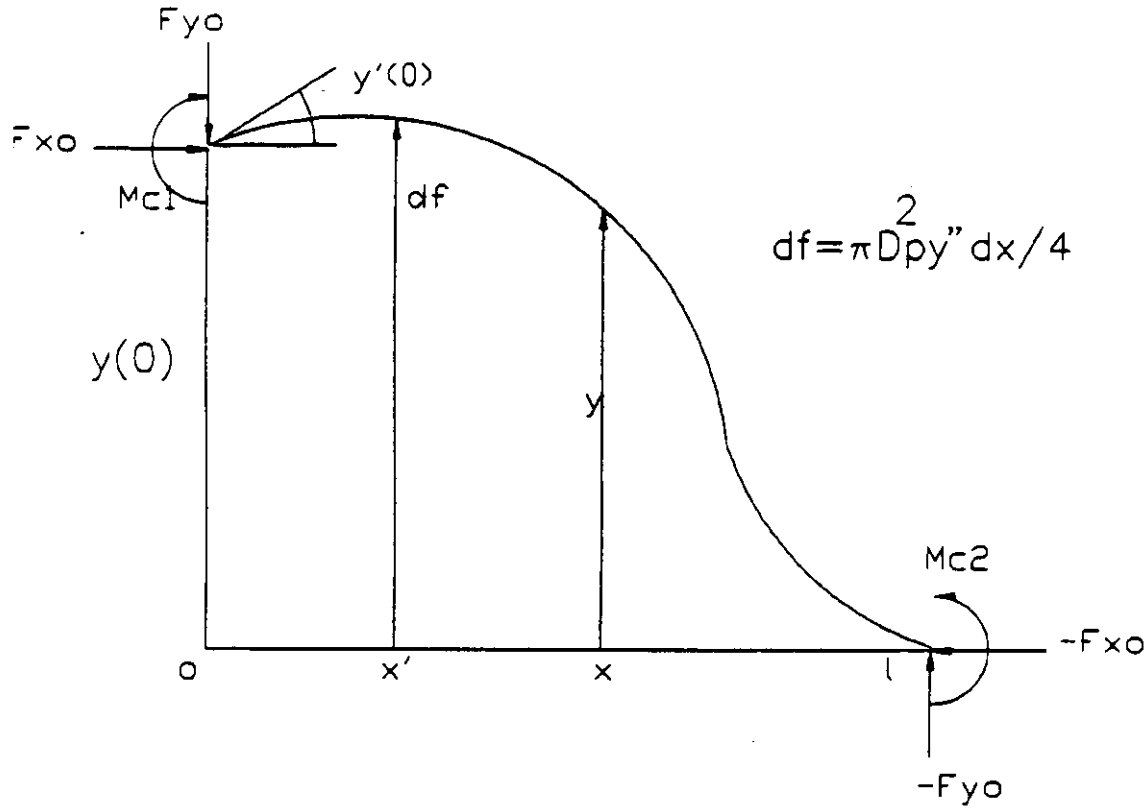

Figure 2.

where E, I are "equivalent" values for elastic modulus and moment of inertia for a bellows represented by a cylinder as discussed below. According to eq. 1

$$\int_o^x (x-x')\,df = -\frac{\pi D^2 p}{4}\int_o^x (x-x')\,y''(x')\,dx'$$
$$= -\frac{\pi D^2 p}{4}\left(y'(x')(x-x') + y(x')\right)\Big|_o^x$$
$$= -\frac{\pi D^2 p}{4}\left(y(x)-y(0)-y'(0)x\right)$$

Therefore

$$y'' = \frac{1}{EI}\left(F_x(y(0)-y)-F_y x + M_{cl}\right) \tag{4}$$

where

$$F_x = F_{xo} + \frac{\pi D^2 p}{4} \tag{4a}$$

$$F_y = \left(F_{yo} - \frac{\pi D^2 p}{4}y'(0)\right) \tag{4b}$$

F_{xo} is the axial bellows end support force before pressure is introduced, for instance due to axial precompression. F_{yo} gives lateral support at x = 0. y(0) and y′(0) are given as boundary conditions or can be determined as a part of the solution of eq. 4. Assume, for instance, that we give as boundary conditions at x = 0

$$y = y(0)$$
$$y' = y'(0)$$

and at $x = \ell$

$$y = y(\ell)$$
$$y' = y'(\ell)$$

Solution of eq. 4 requires determination of two integration constants. Furthermore we must find M_{c1} and F_{yo}. Thus the four boundary conditions suffice. Moment M_{c2} can be found from eq. 2, if required.

Equation 4 is an Euler-type equation describing the effect of an axial end force F_x on a bar. For a sufficiently large end force buckling can occur. Thus, for a bellows internal pressure p can result in buckling ("squirming"), if the bellows is supported at the ends as was assumed.

So far we have neglected the effect of shear forces on bending of the bellows. Axially, the bellows acts like a spring whose spring constant depends on various parameters. To be called "K", it will be derived below. Laterally, without bending, the bellows must act approximately like a cylinder of diameter D with the bellows convolution wall thickness t, but with a much smaller equivalent elastic modulus than that of a cylinder.

Considering bending of a bar whose ends are fixed and which is loaded axially by forces $\pm F$, a critical force F_{cr} exists where the bar becomes unstable. A simple expression, due to Euler gives eq. 5,

$$F_{cr} = \frac{4\pi^2 E_r I_r}{\ell_r^2} \tag{5}$$

where E_r, I_r, ℓ_r are elastic modulus, moment of inertia of cross section, and length, respectively. Ends are assumed to be fixed. Equation 5 does not take shear forces into account. An expression taking deflections due to both bending and shear forces into account has been given by Timoshenko[1]. The critical force is now expressed by

$$P_{crs} = \left(\left(1+\frac{16\pi^2}{\ell_r^2}\frac{E_rI_r}{A_rG_r}\right)^{1/2}-1\right)\frac{A_rG_r}{2} \tag{6}$$

where A_r and G_r are cross section and shear modulus of the bar.

Concerning pure shear, we have to treat the bellows as a cylinder whose average cross section is $A_r = \pi Dt$.

$$G_r = \frac{E_s}{2(1+\nu)}$$

where E_s will be the elastic modulus of the bellows material. If $\nu \approx 0.25$ = Poisson's ratio, $G_r \approx 0.4\ E_s$.

The product E_rI_r concerns the axial behavior of the bellows. Particularly, E_r must be an "equivalent" number referring to the axial bellows spring constant K. The spring constant (also called "stiffness") of a bar would be

$$K = \frac{\textit{Elastic modulus} \times \textit{cross section}}{\textit{length}}$$

For a spring, or bellows, one can <u>define</u> then an equivalent elastic modulus

$$E = \frac{K\ell}{A} \tag{6a}$$

if K is given. ($A = A_r$, $\ell = \ell_r$). Therefore, in eq. 6 we will set $E_r = E$. I_r will have an average value

$$I_r = I = \frac{\pi}{64}\left((D+\frac{t}{2})^4-(D-\frac{t}{2})^4\right) = \frac{\pi D^3 t}{8} \tag{6b}$$

if $t << D$. Therefore

$$EI = \frac{KD^2\ell}{8} \tag{6c}$$

It follows that

$$P_{crs} = \left(\left(1+\frac{2\pi KD}{0.4\ell tE_s}\right)^{1/2}-1\right)\frac{0.4\pi DtE_s}{2}$$

Typical average values for bellows considered in this report will be

K	= 3000 lbs./inch
D	≈ 13.5" or less
ℓ	≈ 10" or less
t	≈ 0.03"
E_s	= 3 x 10^7 psi

which results in

$$\frac{16\pi^2}{\ell^2}\frac{EI}{AG_r} = \frac{2\pi KD}{0.4\ell tE_s} = 0.071<1$$

Therefore it follows from eq. 6 that

$$P_{crs} \approx \frac{4\pi^2 EI}{\ell^2} = P_{cr} \tag{6d}$$

for our case; deflections due to shear are small here, thus justifying the simple approach taken to derive eq. 3. The reason is that here $E_r << G_r$. If D were considerably larger or ℓ smaller, eq. 6 would have to be used.

IIIa. Axial and Lateral Spring Constants, and Convolution Wall Stresses and Deflections under Bellows Compression or Tension.

Bellows manufacturers provide information on bellows parameters in their catalogues and upon inquiries. However, sometimes parameters for a particular application, such as ours, are not readily available. Also, interconnecting large numbers of superconducting magnets requires as much attention to and quality of design, and reliability of components, as the magnets themselves; repair of a failed interconnection can require nearly as much time as replacing a faulty magnet. In order to judge details of a bellows under consideration, such as spring constants, stresses and deflections under pressure, etc., derivations are given in the present section enabling us to correlate obtainable parameters. Since in our applications the radial bellows convolution width d will be much smaller than diameter D, it is admissible (Timoshenko[1], et al.) to reduce the problem from three to two dimensions: We consider a "corrugated sheet" of width πD. The results agree numerically well with some formulas given in the literature.

One-half of a suitable shape for a convolution is drawn in Fig. 3. We define

d	=	convolution width
r_i	=	"valley" radius between convolutions
t	=	wall thickness
r	=	$r_i + t/2$ = average convolution radius
b_c	=	straight section length in convolution
F	=	force applied at bellows ends
M_c	=	moment required to satisfy boundary conditions
D	=	average diameter of bellows
$w_{1,2}(\theta_{1,2})$	=	radial deflections, to be >0 when directed toward center of circle formed by r
$v_{1,2}(\theta_{1,2})$	=	azimuthal deflection, to be <0 when directed toward $\theta_{1,2} = 0$
$y(x)$	=	deflection of straight section
N_b	=	number of convolutions in bellows

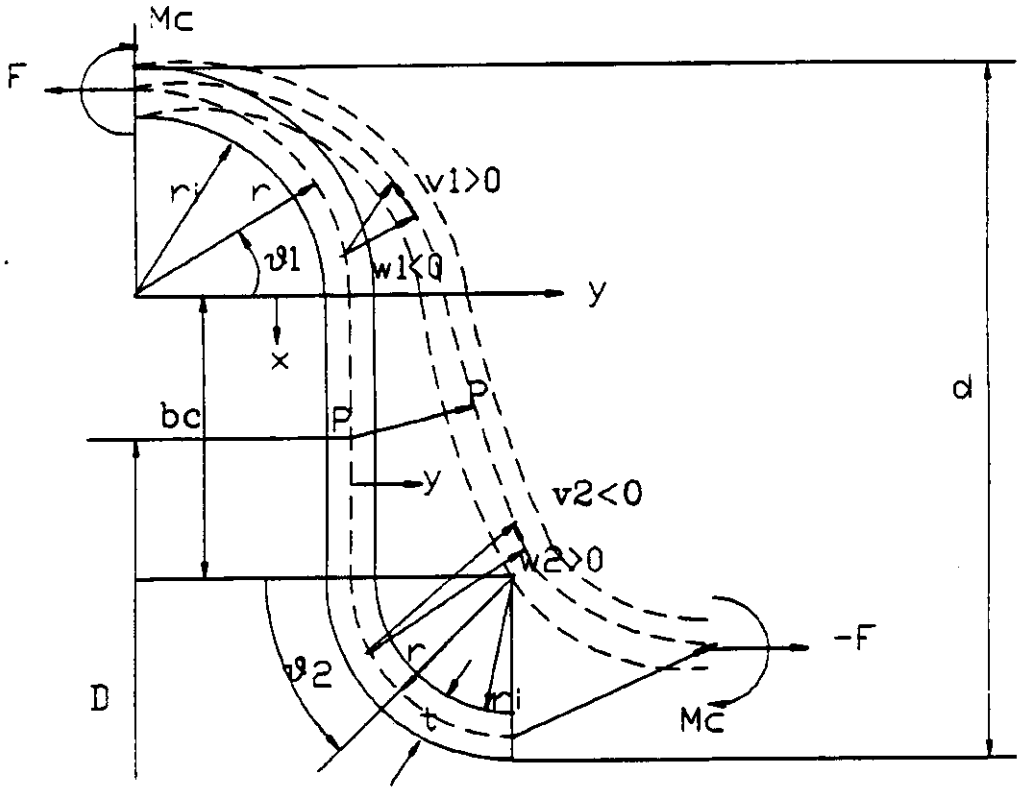

Figure 3.

Since we have assumed that d << D, we expect symmetry around point P at the center of the straight section (when no pressure is applied in the bellows). We will be interested in the axial elongation of the bellows upon application of force F and in accompanying maximum stresses, expected to occur at $\theta_{1,2} = \pi/2$. Because of the indicated symmetry, the elongation of one convolution should be $4y(x = b_c/2)$ and of the bellows:

$$\lambda = 4N_b y\left(\frac{b_c}{2}\right) \tag{7}$$

The axial spring constant is then

$$K = \frac{F}{\lambda} \tag{8}$$

Without symmetry one would have to write $\lambda = 2N_b\ (y(b_c) + v_2(\pi/2))$. ($v_2$ was defined, is indicated in Fig. 3, and will be treated below.)

For equilibrium we have

$$2M_c = F(b_c + 2r)$$

According to Timoshenko[2], for a bent curved bar of radius r

$$w_1'' = \frac{d^2 w_1}{r^2 d\theta_1^2} = -\frac{w_1}{r^2} - \frac{M(\theta_1)}{E_b I_b} \tag{9}$$

which is also valid for a section of a cylinder if

$$E_b = \frac{E_b'}{(1-\nu^2)}$$

where ν = Poisson's ratio and E_b' the elastic modulus of the material.

$$I_b = \frac{\pi D t^3}{12}$$

From Fig. 3 we obtain

$$\frac{d^2 w_1}{d\theta_1^2} = -w_1 + \frac{r^2}{E_b I_b}\left(Fr\left(1-\sin\theta_1\right)-M_c\right) \tag{10}$$

(The positive sign for the second term is due to F and M_c acting at $\theta_1 = \pi/2$, not at $\theta_1 = 0$.) Solution for eq. 10:

$$w_1 = A_1\cos\theta_1 + B_1\sin\theta_1 - \frac{c_1}{2}\left(\theta_1\cos\theta_1 - \sin\theta_1\right) + d_1 \tag{11}$$

if

$$c_1 = -\frac{Fr^3}{E_b I_b}$$

$$d_1 = -\left(M_c - Fr\right)\frac{r^2}{E_b I_b}$$

For the convolution straight section:

$$y'' = -\frac{1}{E_b I_b}\left(Fx - \left(M_c - Fr\right)\right) \tag{12}$$

$$y = Ax + B - \frac{1}{E_b I_b}\left(F\frac{x^3}{6} - \left(M_c - Fr\right)\frac{x^2}{2}\right) \tag{13}$$

Boundary conditions:

$$\theta_1 = \frac{\pi}{2}: \qquad w_1 = 0$$
$$w_1' = 0$$

$$\theta_1 = 0: \qquad y = -w_1$$
$$w_1' = y'$$

For the resulting deflection at x = $b_c/2$:

$$y\left(\frac{b_c}{2}\right) = \frac{F\gamma}{4E_b I_b}$$

$$\gamma = b_c^3/6 + b_c^2 r + 3b_c r^2 + \pi r^3 \tag{13a}$$

This is the deflection in the axial direction for one-quarter of a convolution. For the axial spring constant we obtain then

$$K = \frac{\pi E_b t^3 r D}{3\ell\gamma} \tag{14}$$

since $N_b = \ell/4r$ if the bellows straight sections are parallel to each other (which they are not necessarily (see below)).

The maximum tension/compression stress in the convolution wall is

$$\sigma_m(\theta_1) = \frac{M(\theta_1)}{Z_b} = \frac{M(\theta_1)t}{2I_b}$$

and the maximum for σ_m occurs at $\theta_1 = \pi/2$, leading to

$$\sigma_{max} = \frac{2E_b tr(r+b_c/2)\lambda}{\ell\gamma} \tag{15}$$

where λ was defined as the total axial deflection of the bellows (eq. 7).

One can show that our simple calculation is valid by estimating the hoop stress on the bellows that would ensue without approximation. For this purpose we will calculate $v_1(\theta_1 = 0)$, for which Timoshenko and Gere give

$$\frac{dv_1}{d\theta_1} - w_1 = 0 \tag{16}$$

Therefore

$$v_1 = \int w_1 d\theta_1 + G_1$$

G_1 is found from the boundary condition

$$\theta_1 = \frac{\pi}{2}: \qquad v_1 = 0$$

$v_1(0)$ is then easily calculated and by about this amount the outer convolution diameter would be compressed (and the inner diameter expanded) if no approximation had been used. The resulting hoop stress would amount to only 2 to 3% of the calculated bending stress. We conclude that for our bellows ($d << D$) the above-given calculation is a good approximation. (More general calculations, including d not $<<$ D, often approximate the shape of the convolutions by alternating flat sheets and short cylinders. For our present purpose we prefer the procedure used above. See, however, also A. Laupa and N.A. Weil[8].)

According to manufacturers, the convolution straight sections are not quite parallel, meaning that N_b is not quite $= \ell/4r$. Figure 4 shows the actual shape of a convolution. The "pitch" of a bellows is thus given by

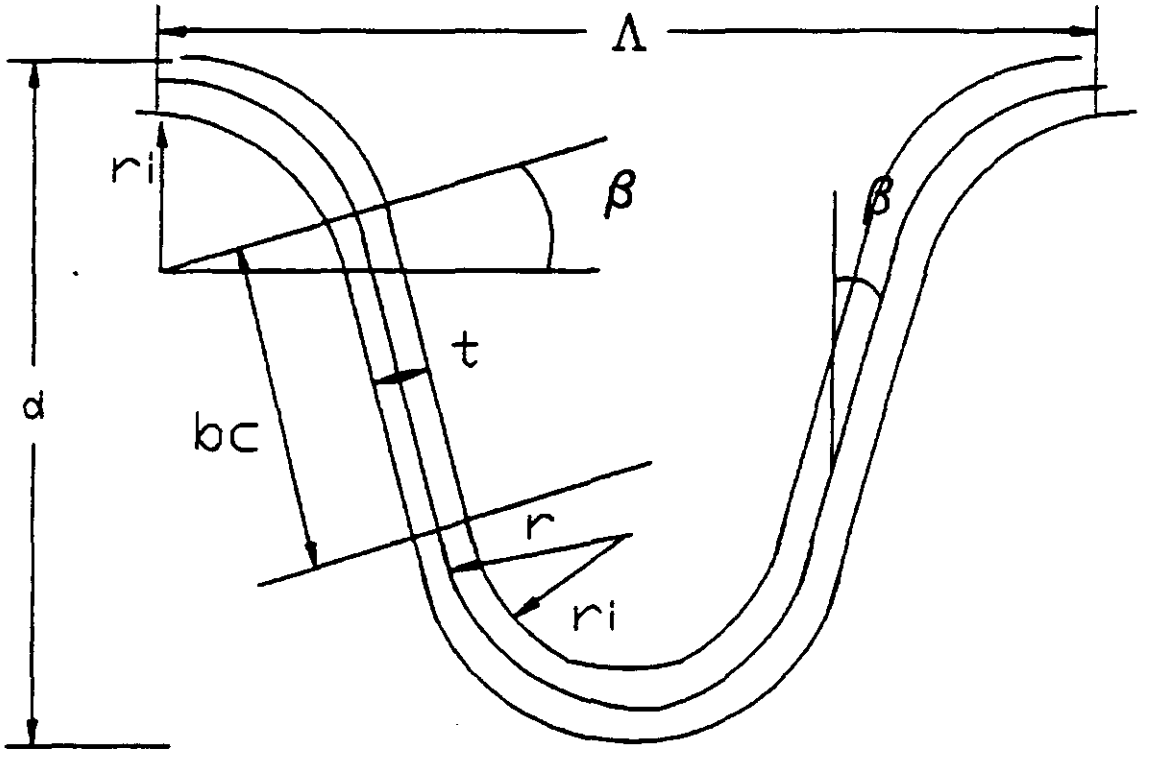

Figure 4.

$$\Lambda = 4r + 2b_c\beta \tag{17}$$

from which angle β can be calculated if Λ, r (or r_i and t), and b_c are given. Radial convolution width d is

$$d = 2r(1-\beta) + b_c + t \tag{18}$$

From eqs. 17 and 18:

$$\beta = \frac{d-t-2r}{4r}\left(\left(1+\frac{4r(\Lambda-4r)}{(d-t-2r)^2}\right)^{1/2}-1\right) \tag{19}$$

$$b_c = d-t-2r(1-\beta) \tag{20}$$

From manufacturers' data, we obtain

$$\beta = 0.094\ rad\ (5.4°)$$
$$b_c = 0.340''$$

for some relevant bellows.

This value for β we shall use for our calculations. For different bellows parameters β may also be different but can be calculated from eq. 19. If then r_i, t and b_c are given, we can determine Λ, d, and $N_b = \ell/\Lambda$.

We can now modify our original procedure, remembering that β is small. First, eq. 5 gave the critical buckling force F_{cr} at the ends of a bar which are fixed. For our calculations we will not be allowed to assume that ends are rigidly fixed; the bellows will be welded to magnet ends which are somewhat flexible, laterally as well as rotationally. Therefore we will encounter buckling modes where

$$F_{cr} = \frac{\pi^2 EI}{\ell^2}$$

Making use of eq. 6c,

$$F_{cr} = \frac{\pi^2 K D^2}{8\ell} \tag{21}$$

Thus, in order not to exceed the critical state we must demand that

$$K \geq 8\ell F_{cr}/\pi^2 D^2 \tag{21a}$$

At installation, at room temperature, bellows will be precompressed by an amount λ. Magnets and bellows are designed for a maximum operating pressure p_{op}. Adding some margin to p_{op} we obtain p_{cr}. Then we can set

$$F_{cr} = K\lambda + \frac{p_{cr}\pi D^2}{4} \tag{22}$$

from which follows, with eq. 21a,

$$F_{cr} = \frac{\pi D^2 p_{cr}}{4\left(1 - \frac{8\lambda\ell}{\pi^2 D^2}\right)} \tag{23}$$

We can now chose critical pressure p_{cr} for a bellows and use the resulting F_{cr} to determine the bellows parameters.

Summarizing, we shall now assume that for a bellows

valley radius r_i

inner diameter D_i

radial convolution width d

angle β of convolution straight sections

bellows length ℓ

maximum pressure $p_{cr} = p_{op}$ + margin

precompression λ

are given. Then we can calculate

average diameter $D = D_i + d$

$$F_{cr} = p_{cr}\pi D^2\left(4\left(1-\frac{8\lambda\ell}{\pi^2 D^2}\right)\right)^{-1} \quad (eq.\ 23)$$

Assume (guess) a likely value for wall thickness t and find

$r = r_i + t/2$

straight section length

$b_c = d-t-2r\,(1-\beta)$ (eq. 20)

$$\gamma = \left(\frac{b_c^3}{6}+b_c^2 r+3b_c r^2+\pi r^3\right) \qquad (eq.13a)$$

pitch length $\Lambda = 4r + 2\,(d-t-2r(1-\beta))\beta$ (eq. 17)

number of convolutions:

$$N_b = \frac{\ell}{\Lambda} \tag{24}$$

improved value for t:

$$t = \frac{4}{\pi D}\left(\frac{6N_b^2 r\gamma F_{cr}}{E_b}\right)^{1/3} \tag{25}$$

where

$$E_b = E_b'/(1-\nu^2)$$

The obtained value for t can now be substituted for the first-guessed value for iteration (convergence will occur after very few iterations).

The maximum wall stress is, substituting t (eq. 25) into eq. 15,

$$\sigma_{max} = \frac{2\lambda}{\pi D}\left(\frac{E_b}{\gamma}\right)^{2/3}\left(r+\frac{b_c}{2}\right)\left(\frac{6rF_{cr}}{N_b}\right)^{1/3} \tag{26}$$

For axial spring constant K we use eq. 21a(23):

$$K = \frac{8\ell F_{cr}}{\pi^2 D^2}\left(= \frac{2\ell p_{cr}}{\pi\left(1-\frac{8\lambda\ell}{\pi^2 D^2}\right)}\right)$$

For a lateral spring constant, both bellows ends fixed to be parallel to bellows axis:

$$K_\ell = 1.5\left(\frac{D}{\ell}\right)^2 \tag{27}$$

which can be proved easily by an appropriate bending calculation, or by applying results for the spring-support model to be considered below (see Section V).

Finally, a simple calculation, considering the total integrated length of the bellows convolutions, gives for the average hoop stress due to pressure p_{cr}

$$\sigma_h = \frac{p_{cr}D}{2t\left(\frac{2N_b}{\ell}(d-t)+\frac{\pi}{2}-1\right)} \tag{28}$$

(Note that σ_h increases when the magnet system is cooled down, due to an increase of bellows length ℓ, without adding to the number of convolutions, N_b.)

Results of calculations for different possible parameters will be given below, after stability calculations have indicated what values are required for K, K_ℓ, σ_{max}. Special attention will have to be paid to availability of wall thicknesses, convolution shapes, etc.

IIIb. *Deflections and Stresses of Bellows Convolutions under Internal Pressure*

In Section IIIa. we have discussed effects on bellows due to forces applied at the ends of the bellows. Here we will consider effects of internal pressure. Total deflections and stresses can be obtained by superposition. Figures 5a and 5b illustrate the problem, showing half a convolution. (The small effect of angle β is neglected here.) We assume that the bellows ends are supported against axial motion. This means that at $\theta_1 = \theta_2 = \pi/2$ no axial motion is allowed:

$$v_1\left(\frac{\theta_1}{2}\right) = v_2\left(\frac{\theta_2}{2}\right) = 0$$

Pressure p is supported at $\theta_1 = \theta_2 = \pi/2$ by forces F_1, F_2 and G, and since at $\theta_{1,2} = \pi/2$, $dw_1/d\theta_1 = dw_2/d\theta_2 = 0$ due to required symmetry, moments M_{c1} and M_{c2} are also required. For equilibrium:

$$F_1+F_2-p(d-t) = 0 \tag{29}$$

$$G = pr \tag{29a}$$

$$-M_{c1}+M_{c2}+F_1(d-t)+2Gr-p(d-t)\left(\frac{d}{2}-t\right)-2pr^2 = 0 \tag{30}$$

(In this Section all quantities (F_1, F_2, M_{c1}, M_{c2}, G) refer only to a one-inch length of the bellows circumference.) Referring to Fig. 5b, the moment due to pressure force element $pr_1 d\theta_1'$ acting at θ_1 is, using components of the force element,

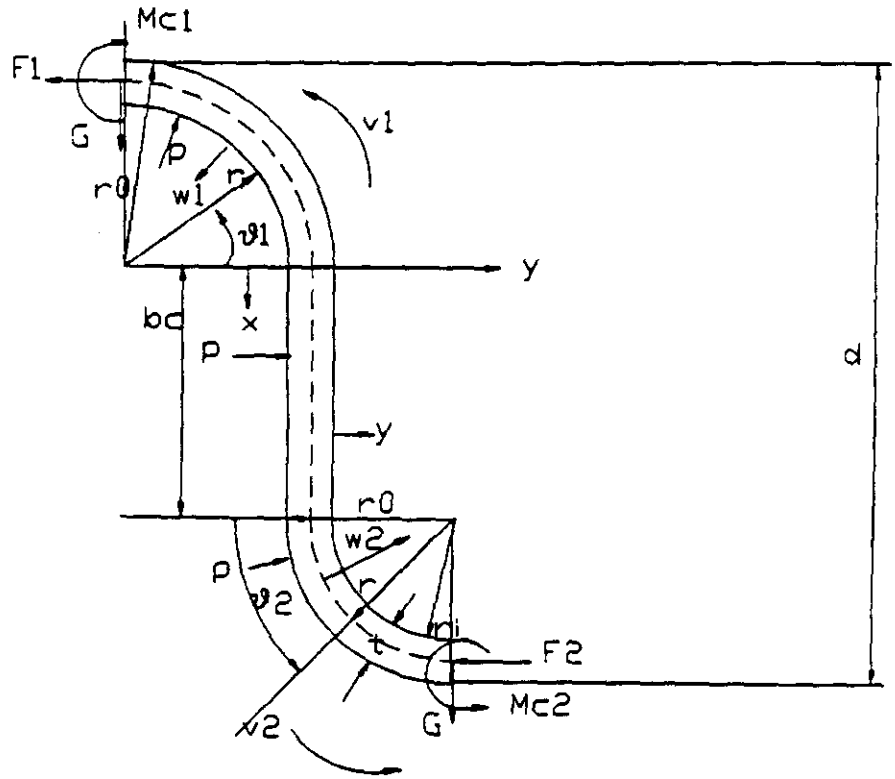

Figure 5a.

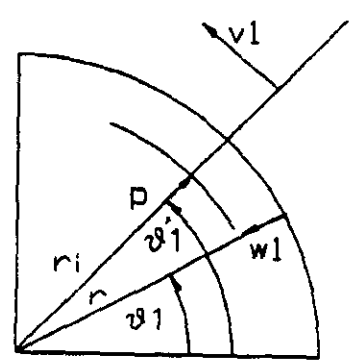

Figure 5b.

$$dM_\theta(\theta_1',\theta_1) = -pr_i d\theta'\left(\sin\theta_1'\left(r\cos\theta_1 - r_i\cos\theta_1'\right) + \cos\theta_1'\left(r_i\sin\theta_1' - r\sin\theta_1\right)\right)$$
$$= -pr_i r\sin\left(\theta_1' - \theta_1\right)d\theta_1'$$

Integrating from θ_1 to θ_1', total moment at θ_1:

$$M_\theta(\theta_1) = -pr_i r(1-\sin\theta_1) \tag{31}$$

Following eqs. 9, 10, and 12, we can now set up the bending equations $\left[here\ I_b = \frac{t^3}{12}\right]$:

$$\frac{d^2w_1}{d\theta_1^2} = -w_1 + \frac{r^2}{E_bI_b}\left(-pr_i r(1-\sin\theta_1) + F_1 r(1-\sin\theta_1) + Gr\cos\theta_1 - M_{cl}\right)$$

or

$$\frac{d^2w_1}{d\theta_1^2} = -w_1 + \frac{r^2}{E_bI_b}\left((F_1 - pr_i)r(1-\sin\theta_1) + Gr\cos\theta_1 - M_{cl}\right) \tag{32}$$

$$y'' = \frac{1}{E_bI_b}\left(p\left(\frac{(x+r_i)^2}{2} + r_i\left(r - \frac{r_i}{2}\right)\right) - F_1(r+x) - Gr + M_{cl}\right) \tag{33}$$

$$\begin{aligned}\frac{d^2w_2}{d\theta_2^2} = {} & -w_2 + \frac{r^2}{E_bI_b}\left(pr_o r(1-\cos\theta_2) - F_1\left(\ell + r(1+\sin\theta_2)\right)\right. \\ & -Gr(2-\cos\theta_2) + M_{cl} \\ & +pr_i\left((\ell + r\sin\theta_2) + r(2-\cos\theta_2)\right) \\ & \left.+p\ell\left(\frac{\ell}{2} + r\sin\theta_2\right)\right)\end{aligned} \tag{34}$$

In addition we have

$$\frac{dv_1}{d\theta_1} = w_1 \tag{35}$$

$$\frac{dv_2}{d\theta_2} = w_2 \tag{36}$$

as given in eq. 16.

Boundary equations are

$$\theta_1 = \frac{\pi}{2} \qquad \begin{aligned} w_1 &= 0 \\ w_1' = \frac{dw_1}{rd\theta_1} &= 0 \\ v_1 &= 0 \end{aligned}$$

$$\begin{aligned} \theta_1 &= 0 & w_1 &= -y \\ x &= 0 & w_1' &= y' \\ x &= \ell & w_2 &= y \\ \theta_2 &= 0 & w_2' &= y' \\ \theta_2 &= \frac{\pi}{2} & w_2 &= 0 \\ & & w_2' &= 0 \\ & & v_2 &= 0 \end{aligned} \tag{36a}$$

Solutions for eqs. 32 and 34 are

$$\begin{aligned} w_{1,2} = A_{1,2}\cos\theta_{1,2} + B_{1,2}\sin\theta_{1,2} - \frac{c_1'}{2}(\theta_{1,2}\cos\theta_{1,2} - \sin\theta_{1,2}) \\ + \frac{c_{1,2}''}{2}\theta_{1,2}\sin\theta_{1,2} + d_{1,2} \end{aligned} \tag{37}$$

if one has written eqs. 32 and 34 in the form

$$\frac{d^2w_{1,2}}{d\theta_{1,2}^2} = -w_{1,2}+c'_{1,2}\sin\theta_{1,2}+c''_{1,2}\cos\theta_{1,2}+d_{1,2}$$

Integrating eqs. 35, 36 results in

$$\begin{aligned} v_{1,2} = A_{1,2}\sin\theta_{1,2}-B_{1,2}\cos\theta_{1,2}-\frac{c'_{1,2}}{2}(\theta_{1,2}\sin\theta_{1,2}+2\cos\theta_{1,2}) \\ -\frac{c''_{1,2}}{2}(\theta_{1,2}\cos\theta_{1,2}-\sin\theta_{1,2})+d_{1,2}\theta_{1,2}+E_{1,2} \end{aligned} \tag{38}$$

Equation 33 leads to

$$y = \frac{\alpha' x^4}{12}+\frac{b' x^3}{6}+\frac{d' x^2}{2}+C_1 x+D_1 \tag{39}$$

We will have to determine integration constants $A_{1,2}$, $B_{1,2}$, $E_{1,2}$, C_1, D_1, and also F_1, F_2, G, M_{c1}, M_{c2}, a total of 13 values for which we have equilibrium conditions 29, 29a, 30, and the 10 given boundary conditions. Substituting equilibrium condition 29a into the boundary conditions results in 10 linear equations which are solved numerically as described below. (M_{c2} and F_2 can be found directly from eqs. 29, 30). Having determined w_1, w_2, y, one can determine stresses from

$$\sigma = \frac{M}{Z_b}$$

where $Z_b = 2I_b/t$. For M use either side of eqs. 32, 33, 34. For instance,

$$\begin{aligned} \sigma_{1,2}(\theta_{1,2}) &= -\left(\frac{d^2w_{1,2}}{d\theta_{1,2}^2}+w_{1,2}\right)\frac{E_b t}{2r^2} \\ \sigma(x) &= -y''\frac{E_b t}{2} \end{aligned} \tag{40}$$

All results will be discussed below. Besides maximum stresses, the maximum value of y will

be of particular interest; if y_{max} is too large, neighboring straight sections may contact each other, in which case the properties of the bellows will change drastically.

IV. *Spring-Supported Bellows Model*

In order to understand and explain the behavior of bellows used for interconnecting accelerator magnets, it has been useful to treat a model consisting of a bellows whose ends are supported by springs. These springs are to model the effects on the magnet ends which could be deflected laterally by forces acting perpendicularly to the magnet axis, and rotationally by moments. Both forces and moments can produce lateral deflections as well as rotations of the bellows ends.

For the spring supported bellows model we will use two straight springs at the bellows ends, with spring constants k_1 and k_2 (lbs./inch), and two torsion springs with spring constants k_{t1} and k_{t2} (lbs. inch/radian).

Manufactured items can adhere to ideal shapes only within tolerances. Thus, we cannot assume that bellows can be ideally straight but will be obtained pre-bent to some shape that could be expressed by a Fourier series. For our purpose it is not necessary to carry the higher harmonics but it is sufficient to carry two of the lowest ones. The prebent shape shall be

$$y_o = d_1 \sin\frac{\pi x}{\ell} + d_2\left(1-\cos\frac{2\pi x}{\ell}\right) \tag{41}$$

with d_1, d_2 the amplitudes, ℓ the bellows length. $y_o = 0$ at $x = 0$ and ℓ. The lowest mode (also representative of a possible offset mode $d_3 \cos \pi x/\ell$) will cause buckling of the bellows at the lowest pressure. The higher mode ($\cos 2\pi x/\ell$) would cause buckling only at 4 times the lowest pressure but it significantly affects the deflections of the bellows, and therefore stresses, even at much lower pressures, in the bellows operating region.

In Section II it was shown that the effect of internal pressure on an arbitrarily shaped bellows can be represented by an axial force that may cause buckling and a lateral force that depends on the pressure and the angle ($y'(0)$) that the bellows axis subtends at $x = 0$ (see eq. 4a,b).

Figure 6 shows the axis of a bellows, which departs from straightness by a function y_o such as given in eq. 41. In addition, due to (small) fabrication errors of the bellows

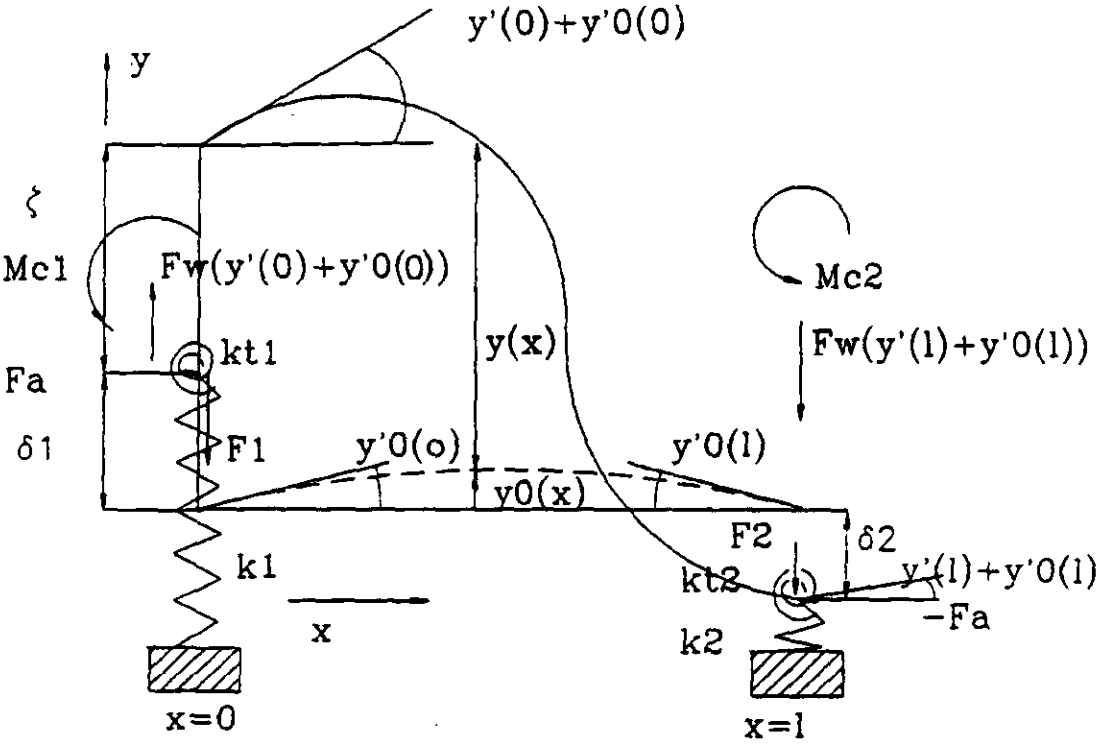
y'(0)+y'0(0)
y
ζ
Mc1
Fw(y'(0)+y'0(0))
Mc2
kt1
y(x)
Fw(y'(l)+y'0(l))
Fa
δ1
F1
y'0(o)
y'0(l)
y0(x)
F2
δ2
k1
kt2
y'(l)+y'0(l)
x
-Fa
k2
x=0
x=l

Figure 6.

mountings, the ends are to be offset laterally by length ς. At the ends, the bellows is mounted on laterally acting springs, k_1 and k_2, and rotation of the ends is limited by torsion springs k_{t1}, k_{t2}. The bellows is to be axially compressed by length λ and internally pressurized to pressure p. The bellows ends are then exposed to equivalent axial end forces (eqs. 4a)

$$\pm F_x = \pm F_a = \pm\left(\lambda K + \frac{\pi D^2 p}{4}\right) \tag{42}$$

Lateral support is to be given by forces F_1 and F_2. Deflection y is to be measured from the unstressed, prebent shape $y_o(x)$ of the bellows. If

$$y'(0)+y_o'(0) = 0 \text{ and } y'(\ell)+y_0'(\ell) = 0$$

we have $F_1 = F_2$. If the end slopes are not zero, then, similarly to eq. 4b, F_1, F_2 become

$$F_1 \to F_1 - F_w\left(y_o'(0)+y'(0)\right)$$
$$F_2 \to F_2 + F_w\left(y_o'(\ell)+y'(\ell)\right)$$

as the total lateral forces on the bellows ends, due to the spring supports and non-zero end slopes. $\left(F_w = \frac{\pi D^2}{4} p\right)$ For equilibrium:

$$F_1 + F_2 = F_w\left(y'(0) - y'(\ell) + \frac{2\pi d_1}{\ell}\right) \tag{43}$$

making use of eq. 41. (Signs in eq. 43 are consistent with Fig. 6.)

Moments M_{c1}, M_{c2} are also required for end support. For equilibrium:

$$M_{c1} + M_{c2} - F_a(\delta_1 - \delta_2) + \left(F_1 - F_w\left(y'(0) + \frac{\pi d_1}{\ell}\right)\right)\ell = 0 \tag{44}$$

Bending deflections y at x, due to the applied forces, are now found from

$$y'' = -\frac{1}{EI}\left(F_a(y+y_o-\delta_1) + F_1 x - F_w\left(y'(0) + \frac{\pi d_1}{\ell}\right)x + M_{c1}\right) \tag{45}$$

F_1 is the force that is due to compression or extension of support spring k_1. Therefore

$$\delta_1 = \frac{F_1}{k_1}$$

similarly

$$\delta_2 = \frac{F_2}{k_2}$$

For boundary conditions, M_{c1} and M_{c2} determine the end slopes due to the bending forces:

$$y'(0) = \frac{M_{c1}}{k_{t1}} \tag{46a}$$

$$y'(\ell) = \frac{M_{c2}}{k_{t2}} \tag{46b}$$

and for the total end deflections:

$$y(0) = \zeta + \delta_1 = \zeta + \frac{F_1}{k_1} \tag{46c}$$

$$y(\ell) = \delta_2 = \frac{F_2}{k_2} \tag{46d}$$

Boundary conditions 46a to 46d, together with equilibrium conditions 43 and 44 will be used to determine y(x). The six conditions suffice to find F_1, F_2, M_{c1}, M_{c2}, and two integration constants for eq. 45 whose solution is

$$y = A\cos\omega x + B\sin\omega x + C_1\sin\frac{\pi x}{\ell} + C_2\cos\frac{2\pi x}{\ell} + Dx + G \tag{47}$$

Substitution into eq. 45 results in

$$\omega = (F_a/EI)^{1/2} \tag{47a}$$

and expressions for C_1, C_2, D_1, and G, while A and B are the integration constants that need to be addressed. Of special interest are

$$C_1 = d_1\left(\frac{\omega\ell}{\pi}\right)^2 / \left(1-\left(\frac{\omega\ell}{\pi}\right)^2\right) \tag{47b}$$

$$C_2 = -d_2\left(\frac{\omega\ell}{2\pi}\right)^2 / \left(1-\left(\frac{\omega\ell}{2\pi}\right)^2\right)$$

which are due to the prebent shape of the bellows (see eq. 41). We can therefore expect buckling (squirming) of the bellows when

$$\omega\ell = \pi \ \ if\ d_1 \neq 0$$

and

$$\omega\ell = 2\pi \ \ if\ d_2 \neq 0$$

or when

$$F_a = \frac{\pi^2 EI}{\ell^2} \tag{48}$$

$$F_a = \frac{4\pi^2 EI}{\ell^2} \tag{49}$$

in agreement with Euler-type buckling.

We must not exceed allowed extension or compression of the bellows, to be called $\Delta\ell_{max}$.

Maximum bellows stress σ due to bending (excluding stress due to local pressure on convolution wall (see Section IIIb), which must be added).

$$\sigma = -\frac{M}{Z} = \frac{y''EI}{Z} = y''\frac{K\ell}{2\pi t}$$

Strain ϵ is

$$\epsilon = \frac{\sigma}{E} = y''\frac{D}{2}$$

Thus

$$\Delta \ell = e\ell = \frac{y'' D\ell}{2}$$

and, including precompression λ:

$$\Delta \ell_{max} = \lambda + \frac{|y''| D\ell}{2} \tag{50}$$

which must be checked for all cases.

In addition to the buckling modes (eqs. 48, 49) due to bellows prebending, there are important additional ones due to the end supports (k_1, k_2, k_{t1}, k_{t2}) which will be considered in detail below, when the procedure for solution of the boundary condition matrix and numerical results are discussed.

V. *Magnet End Misalignment and Lateral Spring Constants*

The accelerator magnets must be aligned within strict tolerances. If bellows mountings are misaligned, making it necessary to distort the bellows laterally, the magnet ends may be misaligned in an opposite direction, depending on lateral bellows and magnet end stiffnesses. This occurs mostly during bellows installation, when it may be necessary to force the bellows to a shape with offset ends.

Refer to Fig. 7. Let k_m be the lateral spring constant of the magnet ends and 2d their relative misalignment. Then $\pm F = k_m d$ are the forces on the bellows ends. Moments M are given by $2M = F\ell$ for equilibrium. Then the bending equation is simply

$$y'' = -\frac{1}{EI}(-Fx+M) = \frac{F}{EI}\left(x-\frac{\ell}{2}\right)$$

At

$$\begin{aligned} x = 0: \quad & y = \zeta - d \\ & y' = 0 \\ x = \ell: \quad & y = d \\ & y' = 0 \end{aligned}$$

One obtains

$$F = \frac{12(\zeta-2d)EI}{\ell^3} \tag{51}$$

and for the total misalignment of the magnet ends

$$2d = \frac{\zeta}{\left(1+\frac{k_m\ell^3}{24EI}\right)} = \frac{\zeta}{\left(1+\frac{k_m}{3K}\left(\frac{\ell}{D}\right)^2\right)} \tag{52}$$

If $k_m \to \infty$, d would have to $\to 0$, and, from eq. 51

$$\frac{F}{\zeta} = \frac{12EI}{\ell^3} = 1.5K\left(\frac{D}{\ell}\right)^2 = K_\ell$$

as was given for the lateral bellows spring constant K_ℓ in eq. 27 and is proved here. Thus

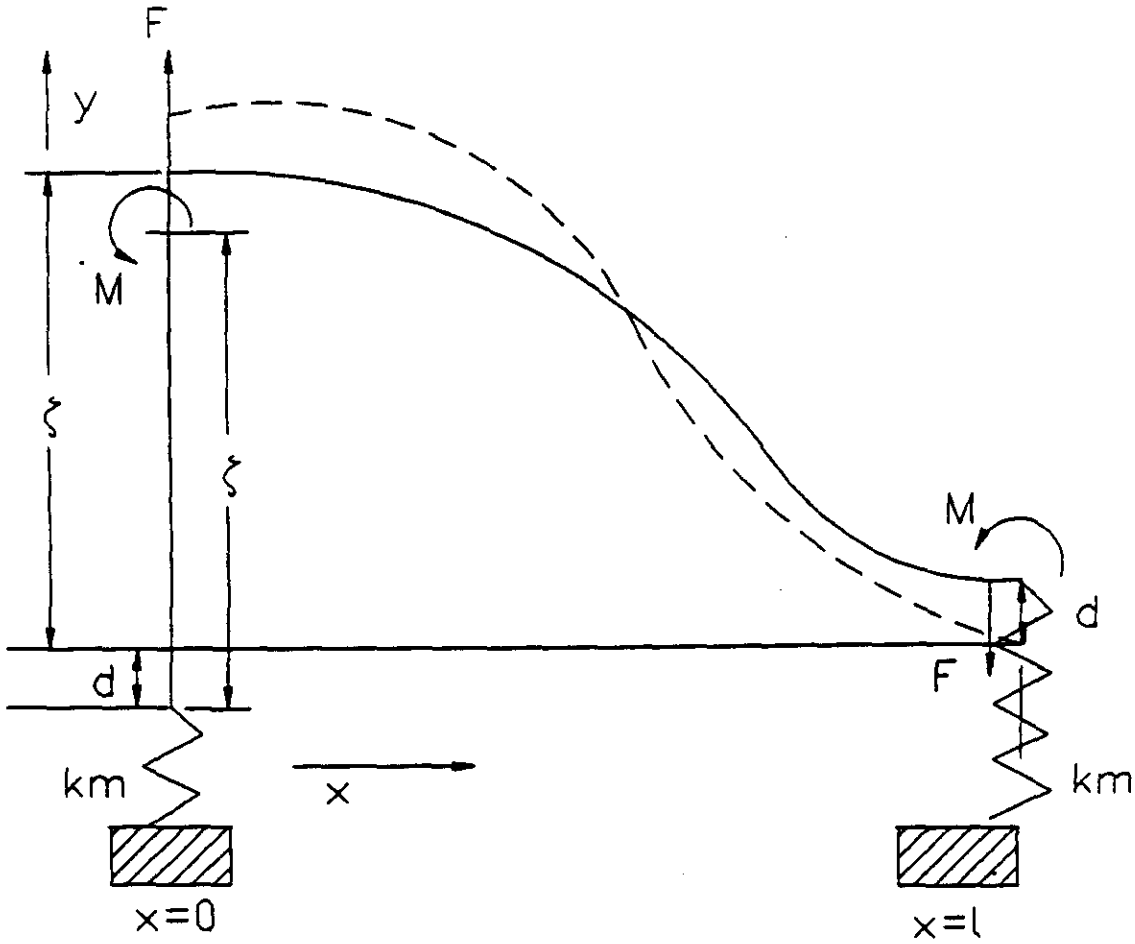

Figure 7.

also

$$2d = \frac{\zeta}{\left(1+\frac{k_m}{2K_\ell}\right)} \tag{52a}$$

It is seen here (eq. 52) that, in order to keep magnet end misalignment small, ζ must remain small, lateral magnet end stiffness (magnet support and shell stiffnesses) should be large, and K_ℓ should not be large. Since $K_\ell \sim K$ and, as will be seen, buckling of bellows occurs at pressures that are proportional to K, the latter should only be as large as necessary. The "slenderness ratio" for the bellows (D/ℓ) occurring in eq. 52 is determined by the required geometry of the interconnection. For bellows dimensions considered for magnet interconnections we may have $2d \approx \zeta/1.5$. If magnet end misalignment 2 d is to be $\leq$ 1 mm, ζ must be < 1.5 mm $\approx$ 0.06". Magnet support stiffness could be increased by moving magnet supports closer to the bellows ends. However, this would most likely interfere with assembly of the interconnections.

Bellows mounting misalignments can occur in random directions. The magnet supports are considerably stiffer vertically than horizontally so that 2 d would be smaller vertically for a given ζ. It must be remembered that ζ must also remain small because lateral bellows stiffness K_ℓ times ζ is the force needed to adjust the bellows before welding to the magnet ends. For $\zeta \approx 0.06$", $K_\ell\zeta$ could be $\approx$ 500 lbs. This lateral force must be provided in addition to the force needed to precompress the bellows axially, namely $K\lambda$, which, for instance, for K = 3000 lbs./inch and λ = 0.5" becomes 1500 lbs. Necessary jigs will have to be provided, and the bellows end mounting designed to minimize ζ.

Some have suggested an alternate way to mount the bellows, so that the latter would not have to be distorted laterally. Figure 8 indicates the arrangement, by using ring sections, cut from cylinders at proper angles. The large axial compression force must, of course, still be provided. It is not clear that this method, requiring additional welding, would result in a substantial decrease of ζ. When internal pressure is applied, moments are produced on bellows and magnet ends due to the asymmetrical mounting.

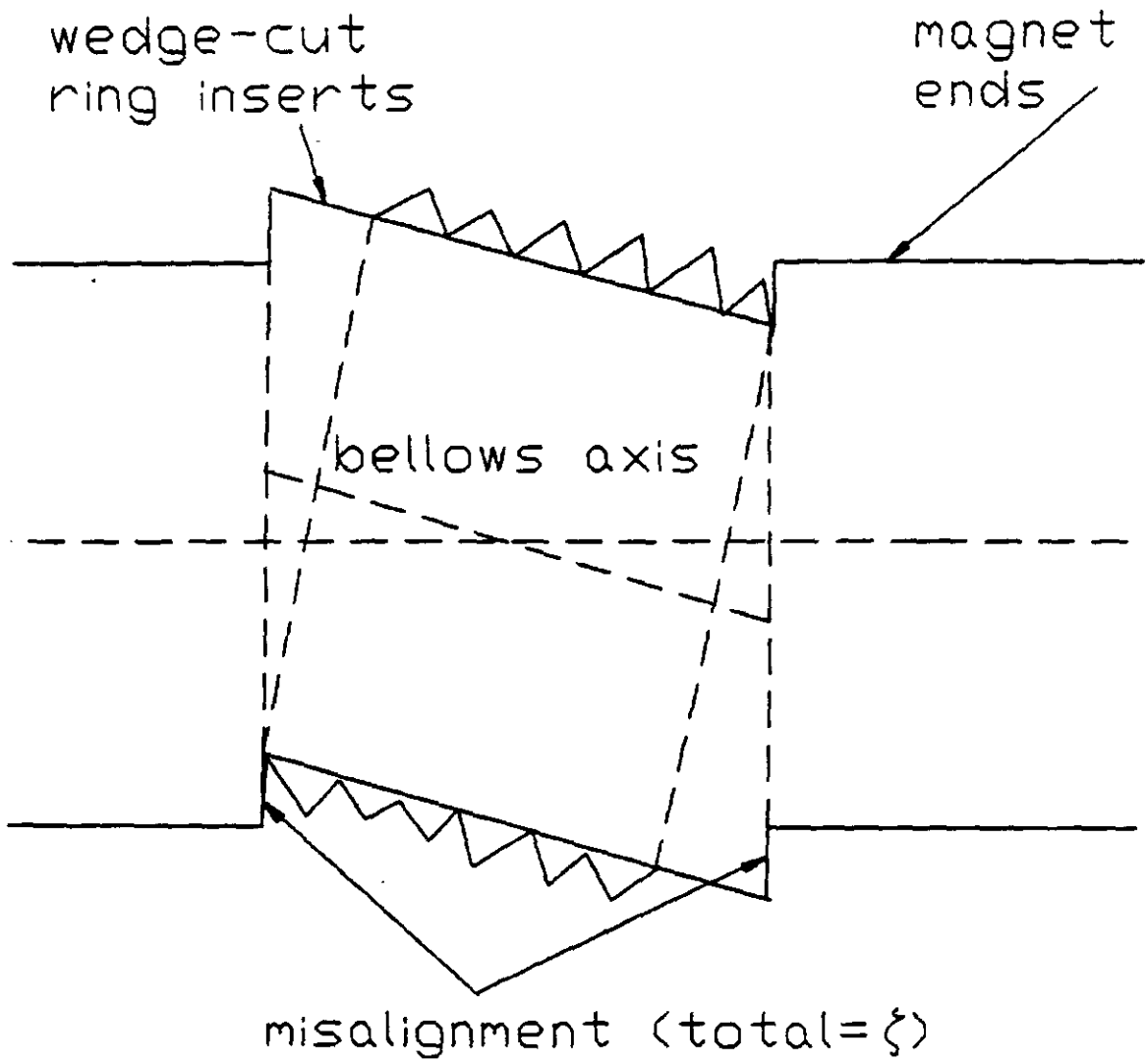
wedge-cut
ring inserts
magnet
ends
bellows axis
misalignment (total=ζ)

Figure 8.

A possibility to eliminate any offset of the bellows would be to butt-weld one end of it to a narrow flange welded to one end of the magnet shell. (This possibility has been tested successfully.)

VI. *Bellows Interactions in Magnet Systems.*

In Fig. 9 we show schematically three magnets and two bellows interconnecting the magnets. Supports for the magnets are shown at locations x_1 to x_{19}. Support forces are F_1 to F_{19}. The whole system is assumed to be preshaped (before applying forces) according to a function $y_o(x)$. Deflections $y_n(x)$ ($1 \le n \le 19$) are to be measured, starting at $y_o(x)$, so that the total deviation from abscissa x is $y_n(x) + y_o(x)$. Concerning $y_o(x)$, dipoles are circularly curved, quadrupoles (packaged together with sextupole and corrector magnets) are straight, but much shorter than dipoles, and interconnections are straight. $y_o(x)$ shall represent an average curve of the system. For $1 \le n \le 18$, forces F_n will be expressed by

$$F_n = k_n \delta_n \tag{53}$$

if the k_n are the support spring constants, and having called $\delta_n = y_n(x_n)$. For n = 19,

$$F_{19} = k_{19} y_{18}(x_{19}) \equiv k_{19} \delta_{19} \tag{53a}$$

Note that forces F_n act only approximately in the y-direction as shown in Fig. 9. For the present problem (small deflections) this approximation is adequate.

Two bellows are located between x_6 and x_7, and x_{13} and x_{14}. At these locations $k_{6,7,13,14} = 0$ so that there are no magnet support forces (eq. 53). However, one can apply forces $F_{6,7,13,14}$ for the purpose of analyzing effects of "bellows catastrophes" on adjacent magnets and other bellows. Such a "catastrophe" may be collapse of a bellows due to buckling, resulting in gross distortion of the bellows and therefore possibly large laterally acting forces due to the internal pressure. When a bellows buckles, it will not necessarily rerlease the pressure in it but rather deform the convolutions until they are either compressed till contact or "straightened" to become a smooth surface.

In our calculations we assume that large diameter bellows are employed. Therefore forces on bellows and adjacent components can become large. On smaller bellows the forces of concern to us are, of course, also smaller, decreasing proportionally to the average bellows cross section.

In Fig. 9, the bellows ends are shown to be offset laterally from the magnet ends, at $x_{6,7,13,14}$ by $\varsigma_{6,7,13,14}$, and by angle $\eta_{6,7,13,14}$. While adjacent magnets must be aligned within

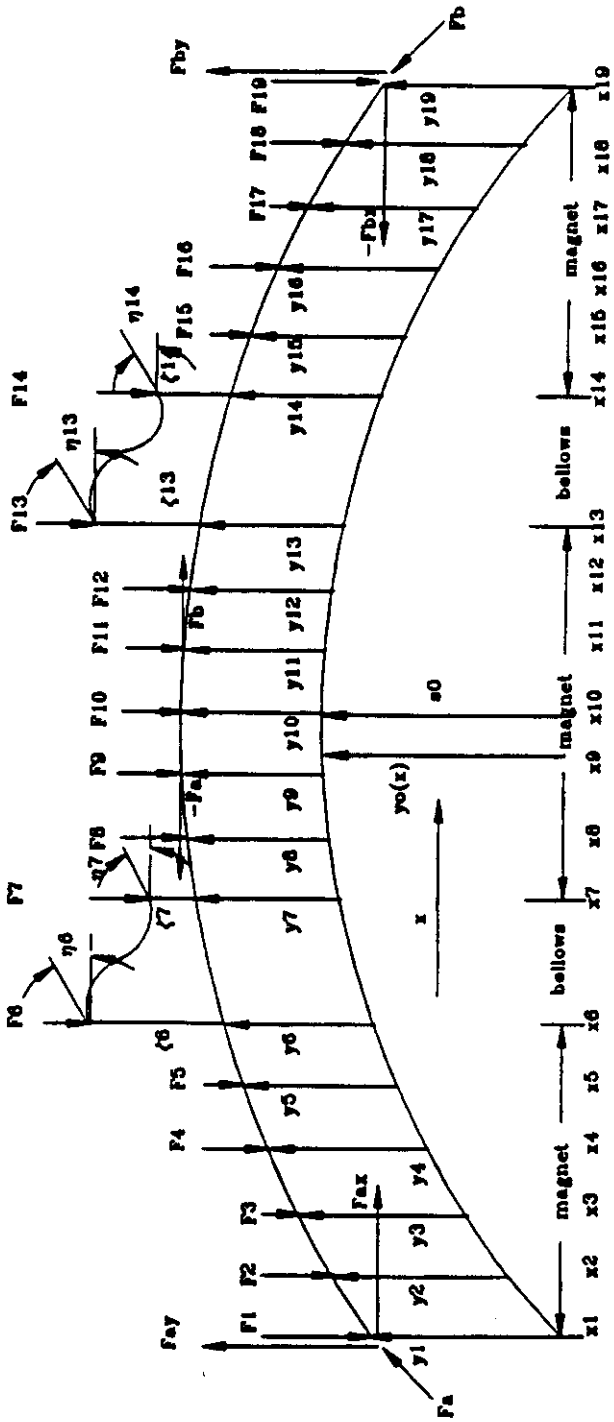
Fb
Fby
-Fbx
Fax
Fay
Fa
F1 F2 F3 F4 F5 F6 F7 F8 F9 F10 F11 F12 F13 F14 F15 F16 F17 F18 F19
y1 y2 y3 y4 y5 y6 y7 y8 y9 y10 y11 y12 y13 y14 y15 y16 y17 y18 y19
x1 x2 x3 x4 x5 x6 x7 x8 x9 x10 x11 x12 x13 x14 x15 x16 x17 x18 x19
magnet
bellows
magnet
bellows
magnet
s0
yo(x)
x
η6 η7 η13 η14
ζ6 ζ7 ζ13 ζ14

Figure 9.

small tolerances, the offsets can be due to inaccuracies of the bellows end mountings or welding procedures.

It has been shown in Section II, eqs. 4a, 4b, that the effects of internal pressure p on arbitrarily shaped or distorted cylinders or bellows can be calculated by merely applying end forces $\pm\pi D^2 p/4$ along the, however deflected, axis of the pressurized container. D, again, is the inner diameter of a cylinder or average diameter of a bellows. Force components in directions x and y, if y(x) represents the bellows axis, are at x = 0

$$F_x(0) = \frac{\pi D^2 p}{4}\,(1 - y'(0)^2) \approx \frac{\pi D^2 p}{4} = F_w$$

if $y'(0)$ is small, and

$$F_y(0) = \frac{\pi D^2 p}{4} y'(0) = F_w y'(0)$$

Replacing zero by length ℓ gives corresponding expressions at x = ℓ. If additional forces act, we obtain eqs. 4a, 4b. Adding bellows precompression force λK to F_w, we define

$$F_a = \lambda K + \frac{\pi D^2 p_a}{4} = \lambda K + F_{wa} \tag{54}$$

which is to act (approximately) in the x-direction. $\left(F_{wa} y'\right)$ is to act in the y-direction. $F_{ax} \approx F_a$ and $F_{ay} = F_{wa} y_1'(x_1)$ are shown at $x = x_1$, $y = y_1$ in Fig. 9. (Actually bellows precompression force λK acts at axially fixed location x_3, but for simplicity we shall locate it at $x = x_1$, which is unimportant for this calculation.) In order also to analyze the effect of unequal pressures at magnet ends, as could be encountered during asymmetrical magnet quenches, it is assumed, and shown at $x = x_{10}$ that force $-F_a$, acting at x_{10}, provides equilibrium (together with the relevant force in the y-direction) for F_a at $x = x_1$. From here on force $F_b = \lambda K + \frac{\pi D^2 p_b}{4} = \lambda K + F_{wb}$ is to act, having replaced pressure p_a by p_b. At

$x = x_{19}$, $-F_{bx} \approx -F_b$ must then act for equilibrium, and $F_{by} = F_{wb} y'_{18}(x_{19})$.

As mentioned above, there are no supports at $x = x_{6,7,13,14}$ where $k_{6,7,13,14} = 0$. $y_{6,7,13,14}$ indicate deflections at the bellows ends. This leaves magnet supports at the remaining locations. Each of the three magnets is shown with five supports. The actual number of supports for a given magnet can be adjusted by setting the $k_n \neq 0$ at the support locations. (Elsewhere $k_n = 0$.) Magnet supports can thus be specified by entering known values for the k_n. We can then analyze SSC dipoles (D) (five supports for magnet to cryostat), quadrupoles (Q) (three supports), RHIC dipoles (three supports), quadrupoles (two supports). Thus any combination such as DDD, DQD, etc., can be studied. The SSC dipole cryostat is to have only two supports to the floor. This will considerably decrease the system stiffness provided by the five magnet-to-cryostat supports.

We proceed to derive relevant relations for analysis. Refer to Fig. 9. The sagitta s_o of our system, compared to cord length $(x_{19} - x_1)$ is found to be very small. Therefore we can approximate the arc by a parabola which is given by

$$y_o(x) = \frac{4s_o}{x_{19}^2} x\,(x_{19} - x)$$

having called $x_1 = 0$. $4s_o/x_{19}^2$ is the curvature of the system which we shall, for our purpose, merely call approximately equal to the dipole curvature $\phi = 4s/\ell^2$, if s = dipole sagitta, ℓ = length. Therefore

$$y_o(x) = \phi x\,(x_{19} - x) \tag{54a}$$

Referring to Fig. 9, we can now write down differential equations for bending of the magnet and bellows in the 18 regions $(x_{n+1} - x_n)$. $(1 \leq n \leq 18.)$ For simple bending, where length > height or width of a bar or, as has been shown, for bellows,

$$y_n'' = -\frac{M_n}{E_n I_m}$$

Examples: for region $(x_2 - x_1)$:

$$-M_1 = F_a(\delta_1 - y_o(x) - y_1) - F_1(x - x_1) + F_{wa}(y_1'(x_1) + \phi x_{19})x \tag{55}$$

$$\delta_1 = \frac{F_1}{k_1} \quad (\textit{see eq. } 53)$$

$$F_{wa} = \pi D^2 p_a / 4$$

$E_1 \approx$ elastic modulus of magnet shell (including Poisson ratio)

I_1 = moment of inertia of magnet cross section (combination of shell and yoke laminations).

For region (x_7 - x_6): bellows:

$$\begin{aligned} -M_6 = & F_a(\delta_1 - y_o(x) - y_6) - \sum_{\nu=1}^{6} F_\nu(x - x_\nu) \\ & + F_{wa}\left(y_1'(x_1) + \phi x_{19}\right)x + \gamma_3 \\ & - F_a\left[d_{s6}\sin\left[\frac{\pi x}{\ell}\right] + d_{c6}\left[1 - \cos\left[\frac{2\pi x}{\ell}\right]\right]\right] \end{aligned} \tag{56}$$

$\gamma_3 = \frac{GI_p}{\ell_p} y_3'(x_3)$ takes into account a torque exerted by the center support of the magnet caused by distortion of the shell resulting in angle y_3' at x_3.

d_{s6} and d_{c6} determine the amount of prebend of the bellows before installation (see Section IV, eq. 41). Similarly, for d_{s13}, d_{c13} for bellows prebend in region x_{14} - x_{13}. All other d_{sn}, d_{cn} = 0.

E_6 = E (see eq. 6a)

I_6 = I (see eq. 6b)

A general equation, valid in all regions, can be written:

$$y_n'' = \frac{1}{E_n I_n}\Big[F_\alpha\left(\delta_{10} - y_o(x) + y_o(x_{10}) - y_n - d_{sn}\sin\left(\frac{\pi x}{\ell}\right) - d_{cn}\left(1-\cos\left(\frac{2\pi x}{\ell}\right)\right)\right)$$
$$-\sum_{\nu=1}^{n} F_\nu(x-x_\nu) + F_\beta(\delta_1 - y_o(x_{10}) - \delta_{10}) + v_n + F_{w\beta}\phi x_{19} x\Big] \tag{57}$$

In this equation it has been assumed that the slopes $y_n'(x_n)$ are $<\phi x_{19}$ (slopes at $x_1(=0)$ and x_{19} due to dipole curvature). v_n shall be the sum of torques that may be exerted by supports, such as γ_3

$$\begin{aligned} &for\ n=1,2, && v_n=0 \\ &3\le n\le 9, && v_n=\gamma_3 \\ &10\le n\le 16, && v_n=\gamma_3+\gamma_{10} \\ &17\le n\le 18, && v_n=\gamma_3+\gamma_{10}+\gamma_{17} \end{aligned}$$

For γ_{10}, γ_{17} replace $y_3'(x_3)$ by $y_{10}'(x_{10}), y_{17}'(x_{17})$, respectively. Furthermore,

$$\begin{aligned} &for\ 1\le n\le 9: F_\alpha = F_\beta = F_a \qquad F_{w\beta} = F_{wa} = \frac{\pi D^2 p_a}{4} \\ &10\le n\le 18: F_\alpha = F_b, F_\beta = F_a \end{aligned}$$

Equation 57 represents 18 second order differential equations, requiring determination of 36 integration constants. In addition, values of the support forces F_n must be determined. These forces are, of course, known to be equal to zero where a support spring constant $k_n = 0$, such as at $x_{6,7,13,14}$ (unless $F_{6,7,13,14} \neq 0$). For the SSC magnets, there are five supports for dipoles and three for quadrupoles, for RHIC, three and two, respectively. Therefore, at most 15 additional quantities must be found, for a total of 51.

There are two equilibrium conditions for the system; (1) Σ forces = 0, (2) Σ moments = 0.

Σ forces:

$$\sum_1^{19} F_\nu \ \frac{\pi D^2}{4}(p_a+p_b)x_{19}\phi = 0 \tag{58}$$

MAX BELLOWS LOCAL ELONGATION

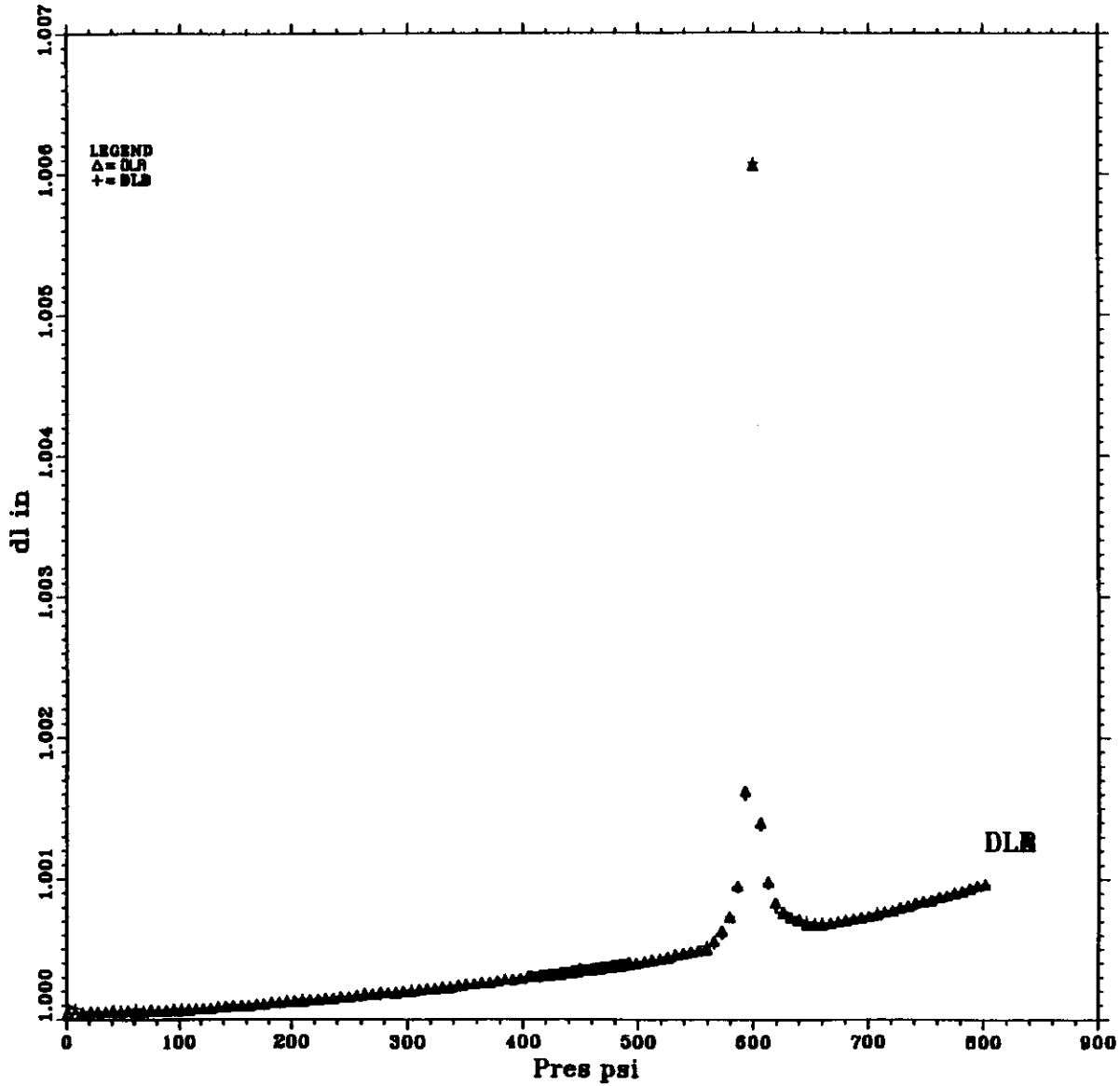

SSC ddd
zet6=0.000 in
zet7=0.000 in
zet13=0.000 in
zet14=0.000 in
et6=0.000 in
et7=0.000 in
et13=0.000 in
et14=0.000 in
ds6=0.000 in
ds13=0.000 in
f(6)= 0.0 lbs
f(13)= 0.0 lbs
K= 2759.2 lbs/in

2DUA7:<ROSSUM.BUC>FOR001.DAT;92 FIGURE D2

Table 9: Results: node location, stiffness, force at p_{op}

node	x(i) in	k(i) lbs/in	F(i) lbs
1	0.00	25000.00	87.70
2	135.69	25000.00	35.17
3	271.38	25000.00	22.61
4	407.07	25000.00	24.10
5	542.76	25000.00	27.57
6	606.38	0.00	0.00
7	615.68	0.00	0.00
8	679.30	25000.00	27.41
9	814.99	25000.00	24.90
10	950.68	25000.00	25.73
11	1086.37	25000.00	24.89
12	1222.06	25000.00	27.42
13	1285.68	0.00	0.00
14	1294.98	0.00	0.00
15	1358.60	25000.00	27.57
16	1494.29	25000.00	24.10
17	1629.98	25000.00	22.62
18	1765.67	25000.00	35.16
19	1901.36	25000.00	87.70

FIGURE D2B

plot file: 2DUA7:[ROSSUM.BUC]FOR001.DAT;185
machine: SSC mode: ddd

Table 1: Input: bellows design parameters

r_i in	D_i in	d in	β	l in	pcr psi	λ in	Eb psi
0.060	14.300	0.500	0.094	9.300	450.000	1.000	3.297E+07

Table 2: Results: bellows properties

Nb	r in	D in	A in	t in	bc in	K lbs/in	Kl lbs/in	I in^4
26	0.072	14.800	0.356	0.025	0.342	2759.212	1.048E+04	3.151E+01

Table 3: Results: maximum bellows stresses at p_{op}

σ_{mas} psi	σ_h psi	σ_{pw1} psi	σ_{pw2} psi	σ_{ps}	y_{mas} in
1.523E+05	2.778E+04	6.640E+04	6.782E+04	2.967E+04	1.472E-03

Table 4: Input: bellows misalignments

$\zeta(6)$ in	$\zeta(7)$ in	$\zeta(13)$ in	$\zeta(14)$ in	$\eta(6)$	$\eta(7)$	$\eta(13)$	$\eta(14)$
0.030	0.000	0.000	0.000	0.000	0.000	0.000	0.000

Table 5: Input: bellows initial shape

d_e6 in	d_e13 in	d_c6 in	d_c13 in
0.020	0.000	0.020	0.000

Table 6: Input: dipole properties

s in	L_D in	ovh_D in	D_m in	t_m in	Im in^4	Em psi
0.200	670.	63.6	10.5	0.188	111.	3.000E+07

Table 7: Input: quadrupole properties

L_q in	ovh_Q in	D_q in	t_q in	Iq in^4	Eq psi
210.	52.5	10.5	0.188	111.	3.000E+07

Table 8: Results: bellows maximum elongation at p_{op}

p_{op} psi	dl6 in	dl13 in
3.000E+02	5.000E+00	1.002E+00

FIGURE D3A

MAX BELLOWS LOCAL ELONGATION

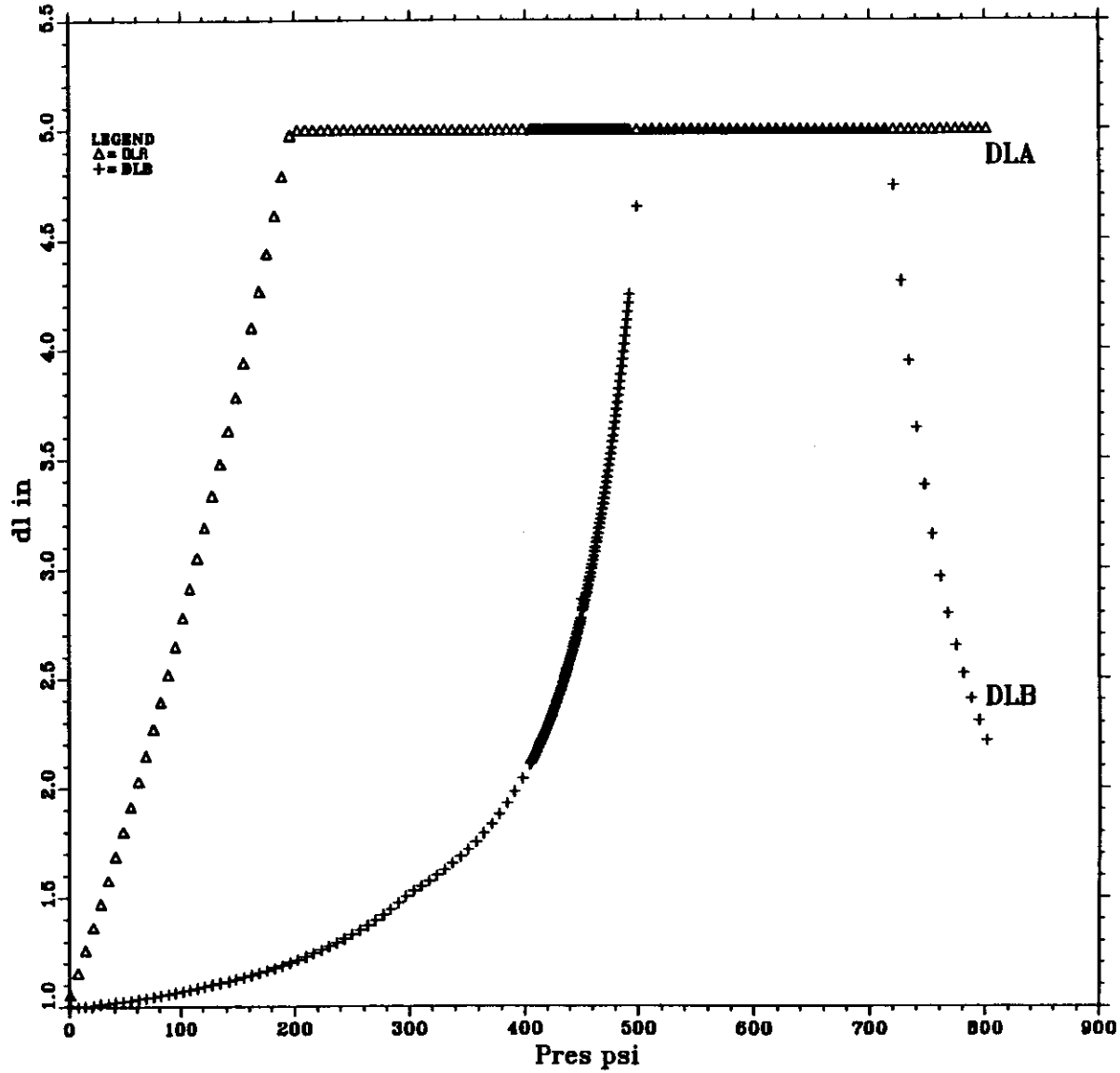

SSC dqd
zet6=0.030 in
zet7=0.000 in
zet13=0.000 in
zet14=0.000 in
et6=0.000 in
et7=0.000 in
et13=0.000 in
et14=0.000 in
ds6=0.020 in
ds13=0.000 in
f(6)=−12500.0 lbs
f(13)= 0.0 lbs
K= 2759.2 lbs/in

2DUA7:<ROSSUM.BUC>FOR001.DAT;10

FIGURE D4

Table 9: Results: node location, stiffness, force at p_{op}

node	x(i) in	k(i) lbs/in	F(i) lbs
1	0.	25000.	96.
2	136.	25000.	119.
3	271.	25000.	-580.
4	407.	25000.	-1808.
5	543.	25000.	8384.
6	606.	0.	-12500.
7	616.	0.	12500.
8	668.	25000.	-8502.
9	694.	0.	0.
10	721.	0.	0.
11	747.	0.	0.
12	773.	25000.	2067.
13	826.	0.	0.
14	835.	0.	0.
15	899.	25000.	731.
16	1034.	25000.	-193.
17	1170.	25000.	-30.
18	1306.	25000.	45.
19	1441.	25000.	69.

FIGURE D4B

FIRST BELLOWS DEFLECTION AT 300 psi

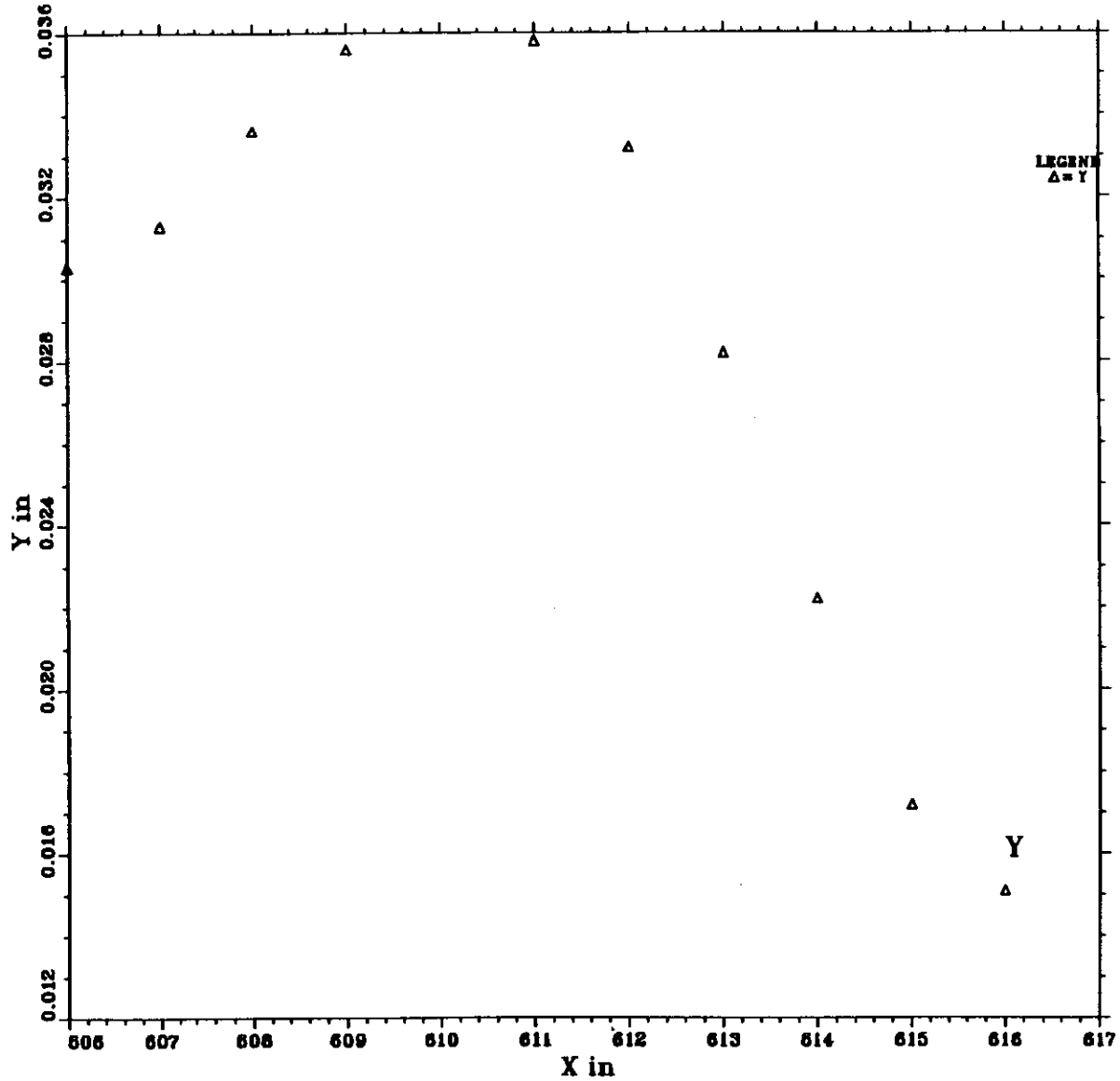

SSC ddd
zet6=0.030 in
zet7=0.000 in
zet13=0.000 in
zet14=0.000 in
et6=0.000 in
et7=0.000 in
et13=0.000 in
et14=0.000 in
ds6=0.020 in
ds13=0.000 in
f(6)= 0.0 lbs
f(13)= 0.0 lbs
K= 2759.2 lbs/in

2DUA7:<ROSSUM.BUC>FOR001.DAT;90

FIGURE D6

MAX BELLOWS LOCAL ELONGATION

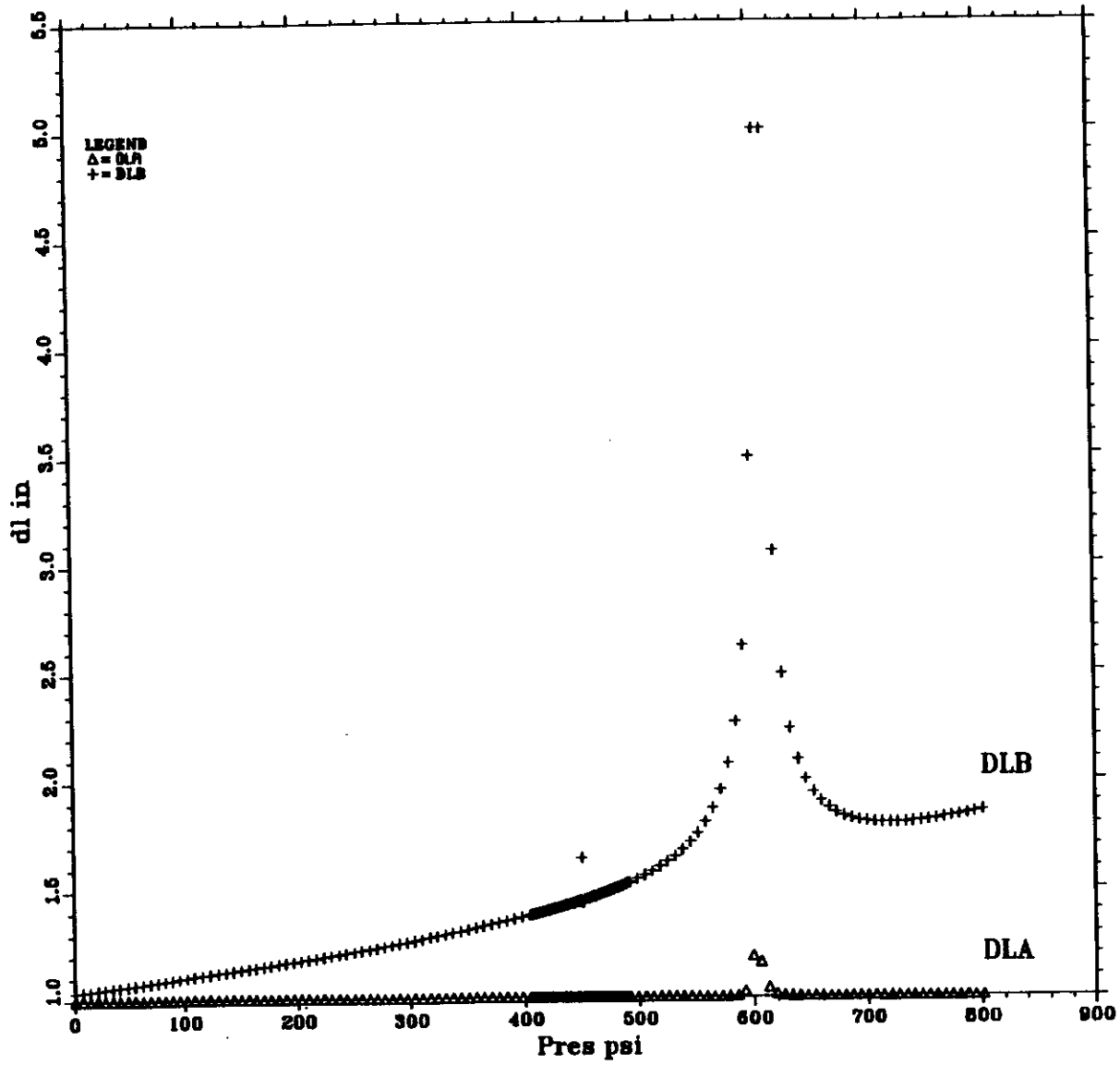

SSC ddq
zet6=0.000 in
zet7=0.000 in
zet13=0.000 in
zet14=−.030 in
et6=0.000 in
et7=0.000 in
et13=0.000 in
et14=0.000 in
ds6=0.000 in
ds13=0.020 in
f(6)= 0.0 lbs
f(13)= 0.0 lbs
K= 2759.2 lbs/in

FIGURE D8

2DUA7:<ROSSUM.BUC>FOR001.DAT;98

plot file: 2DUA7:[ROSSUM.BUC]FOR001.DAT;91
machine: RHIC mode: dqd

Table 1: Input: bellows design parameters

r_i in	D_i in	d in	β	l in	pcr psi	λ in	Eb psi
0.060	7.630	0.500	0.094	6.000	450.000	0.500	3.297E+07

Table 2: Results: bellows properties

Nb	r in	D in	Λ in	t in	bc in	K lbs/in	Kl in lbs	I in^4
17	0.072	8.130	0.352	0.024	0.346	1784.526	4.915E+03	5.137E+00

Table 3: Results: maximum bellows stresses at p_{op}

σ_{max} psi	σ_h psi	σ_{pw1} psi	σ_{pw2} psi	σ_{ps}	y_{max} in
1.066E+05	1.534E+04	6.869E+04	7.013E+04	3.071E+04	1.548E-03

Table 4: Input: bellows misalignments

$\zeta(6)$ in	$\zeta(7)$ in	$\zeta(13)$ in	$\zeta(14)$ in	$\eta(6)$	$\eta(7)$	$\eta(13)$	$\eta(14)$
0.030	0.000	0.000	0.000	0.000	0.000	0.000	0.000

Table 5: Input: bellows initial shape

d_e6 in	d_e13 in	d_e6 in	d_e13 in
0.020	0.000	0.020	0.000

Table 6: Input: dipole properties

s in	L_D in	ovh_D in	D_m in	t_m in	Im in^4	Em psi
2.00	394.	55.4	10.5	0.188	111.	3.000E+07

Table 7: Input: quadrupole properties

L_q in	ovh_Q in	D_q in	t_q in	Iq in^4	Eq psi
170.	48.0	10.5	0.188	111.	3.000E+07

Table 8: Results: bellows maximum elongation at p_{op}

p_{op} psi	dl6 in	dl13 in
3.000E+02	7.511E-01	5.139E-01

FIGURE DR1A

MAX BELLOWS LOCAL ELONGATION

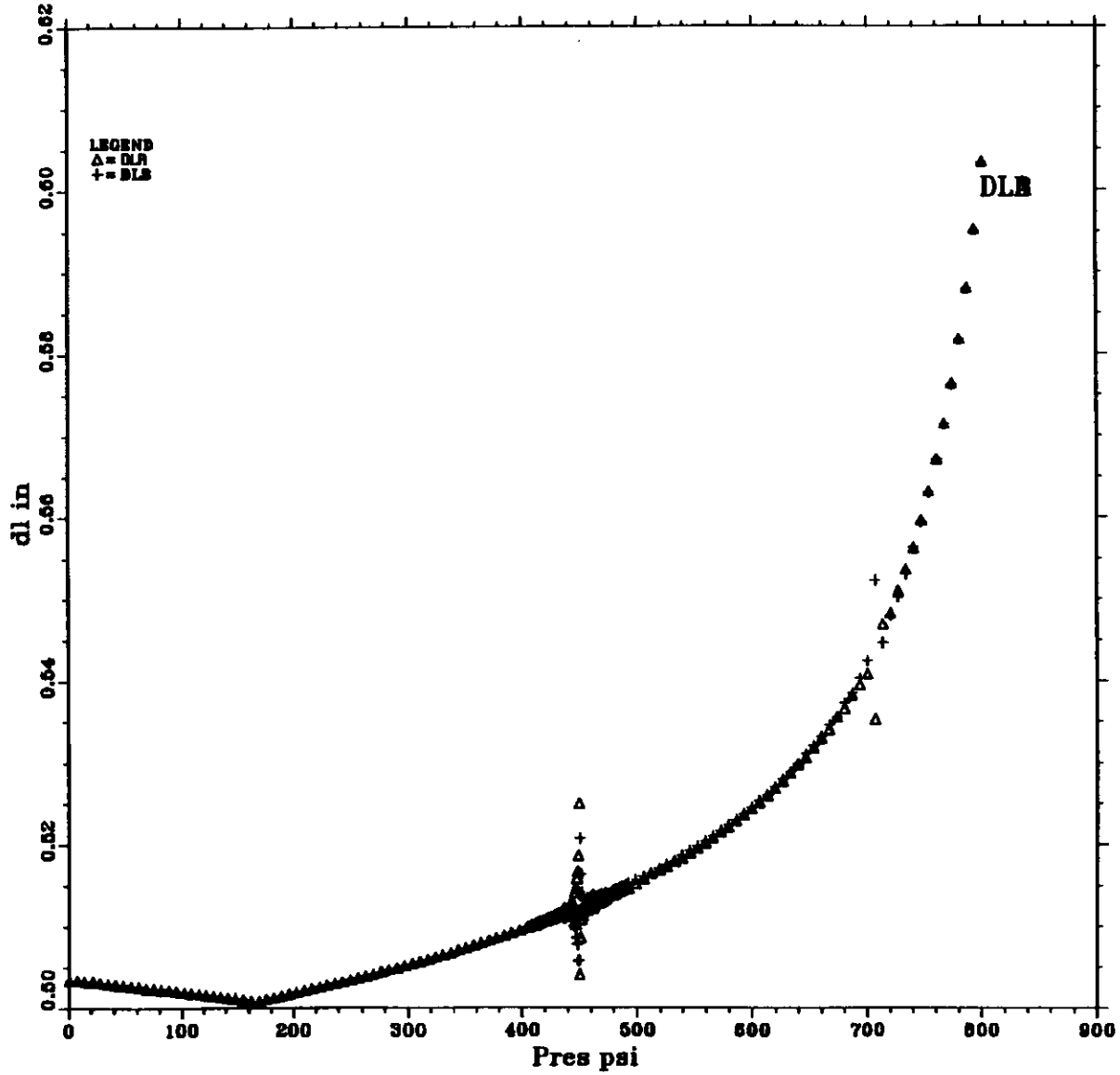

RHIC dqd
zet6=0.000 in
zet7=0.000 in
zet13=0.000 in
zet14=0.000 in
et6=0.000 in
et7=0.000 in
et13=0.000 in
et14=0.000 in
ds6=0.000 in
ds13=0.000 in
f(6)= 0.0 lbs
f(13)= 0.0 lbs
K= 1784.5 lbs/in

2DUA7:<ROSSUM.BUC>FOR001.DAT;93

FIGURE DR2

Table 9: Results: node location, stiffness, force at p_{op}

node	x(i) in	k(i) lbs/in	F(i) lbs
1	0.00	25000.00	402.98
2	70.80	0.10	0.00
3	141.60	25000.00	276.46
4	212.40	0.10	0.00
5	283.20	25000.00	205.65
6	338.60	0.00	0.00
7	344.60	0.00	0.00
8	392.60	25000.00	149.29
9	411.10	0.10	0.00
10	429.60	0.10	0.00
11	448.10	0.10	0.00
12	466.60	25000.00	149.27
13	514.60	0.00	0.00
14	520.60	0.00	0.00
15	576.00	25000.00	205.64
16	646.80	0.10	0.00
17	717.60	25000.00	276.49
18	788.40	0.10	0.00
19	859.20	25000.00	402.96

FIGURE DR2B

plot file: 2DUA7:[ROSSUM.BUC]FOR001.DAT;12
machine: RHIC mode: dqd

Table 1: Input: bellows design parameters

r_i in	D_i in	d in	β	l in	pcr psi	λ in	Eb psi
0.060	7.630	0.500	0.094	6.000	450.000	0.500	3.297E+07

Table 2: Results: bellows properties

Nb	r in	D in	Λ in	t in	bc in	K lbs/in	Kl lbs/in	I in^4
17	0.072	8.130	0.352	0.024	0.346	1784.526	4.915E+03	5.137E+00

Table 3: Results: maximum bellows stresses at p_{op}

σ_{mas} psi	σ_h psi	σ_{pw1} psi	σ_{pw2} psi	σ_{ps}	y_{mas} in
1.066E+05	1.534E+04	6.869E+04	7.013E+04	3.071E+04	1.548E-03

Table 4: Input: bellows misalignments

$\zeta(6)$ in	$\zeta(7)$ in	$\zeta(13)$ in	$\zeta(14)$ in	$\eta(6)$	$\eta(7)$	$\eta(13)$	$\eta(14)$
0.030	0.000	0.000	0.000	0.000	0.000	0.000	0.000

Table 5: Input: bellows initial shape

d_s6 in	d_s13 in	d_c6 in	d_c13 in
0.020	0.000	0.020	0.000

Table 6: Input: dipole properties

s in	L_D in	ovh_D in	D_m in	t_m in	Im in^4	Em psi
2.00	394.	55.4	10.5	0.188	111.	3.000E+07

Table 7: Input: quadrupole properties

L_q in	ovh_Q in	D_q in	t_q in	Iq in^4	Eq psi
170.	48.0	10.5	0.188	111.	3.000E+07

Table 8: Results: bellows maximum elongation at p_{op}

p_{op} psi	dl6 in	dl13 in
3.000E+02	2.165E+00	6.724E-01

FIGURE DR3A

ASSEMBLY DEFLECTIONS AT 303.5 psi

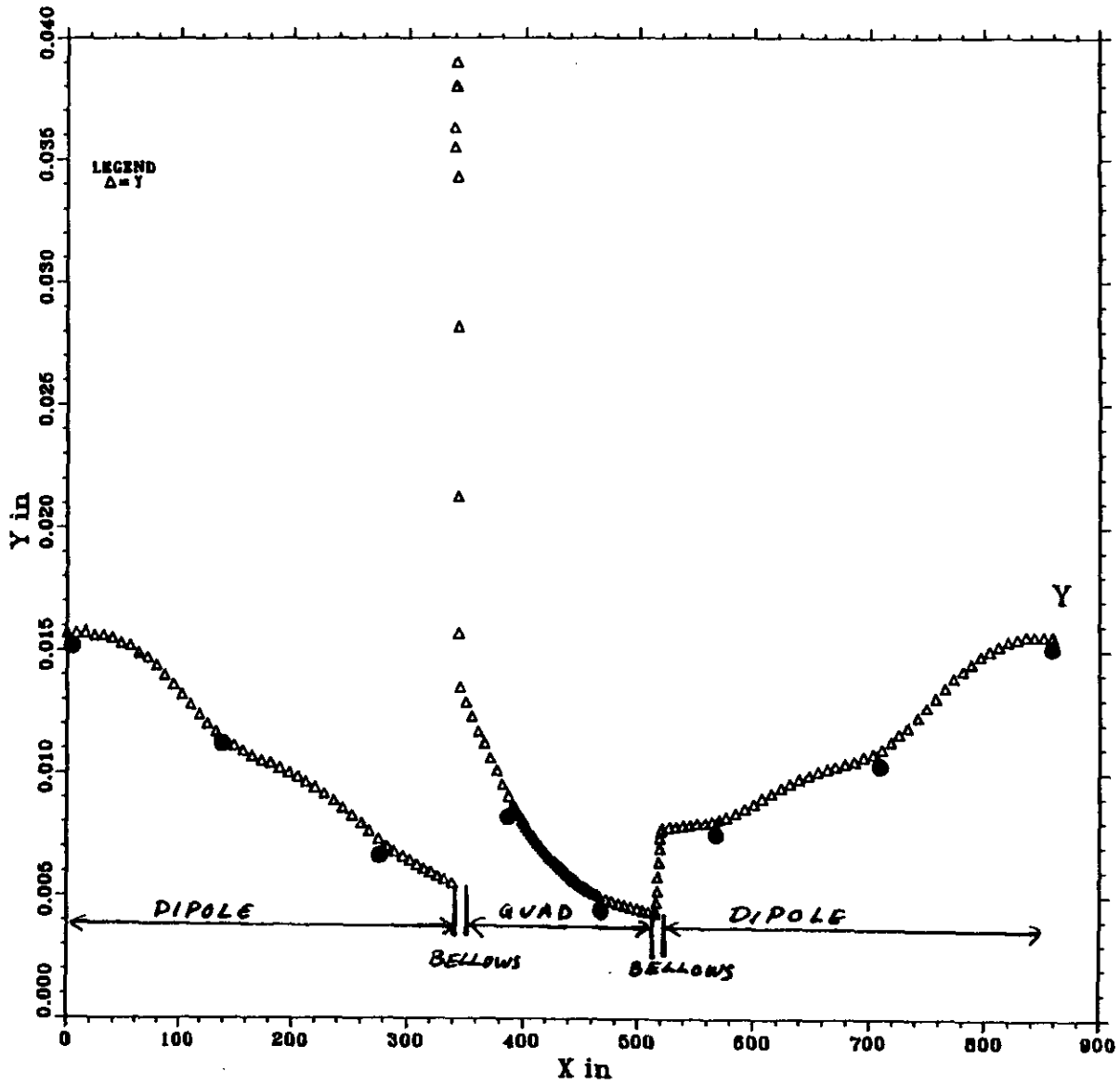

RHIC dqd
zet6=0.030 in
zet7=0.000 in
zet13=0.000 in
zet14=0.000 in
et6=0.000 in
et7=0.000 in
et13=0.000 in
et14=0.000 in
ds6=0.020 in
ds13=0.000 in
f(6)= 0.0 lbs
f(13)= 0.0 lbs
K= 1784.5 lbs/in

2DUA7:<ROSSUM.BUC>FOR001.DAT;91

FIGURE DR4

MAX BELLOWS LOCAL ELONGATION

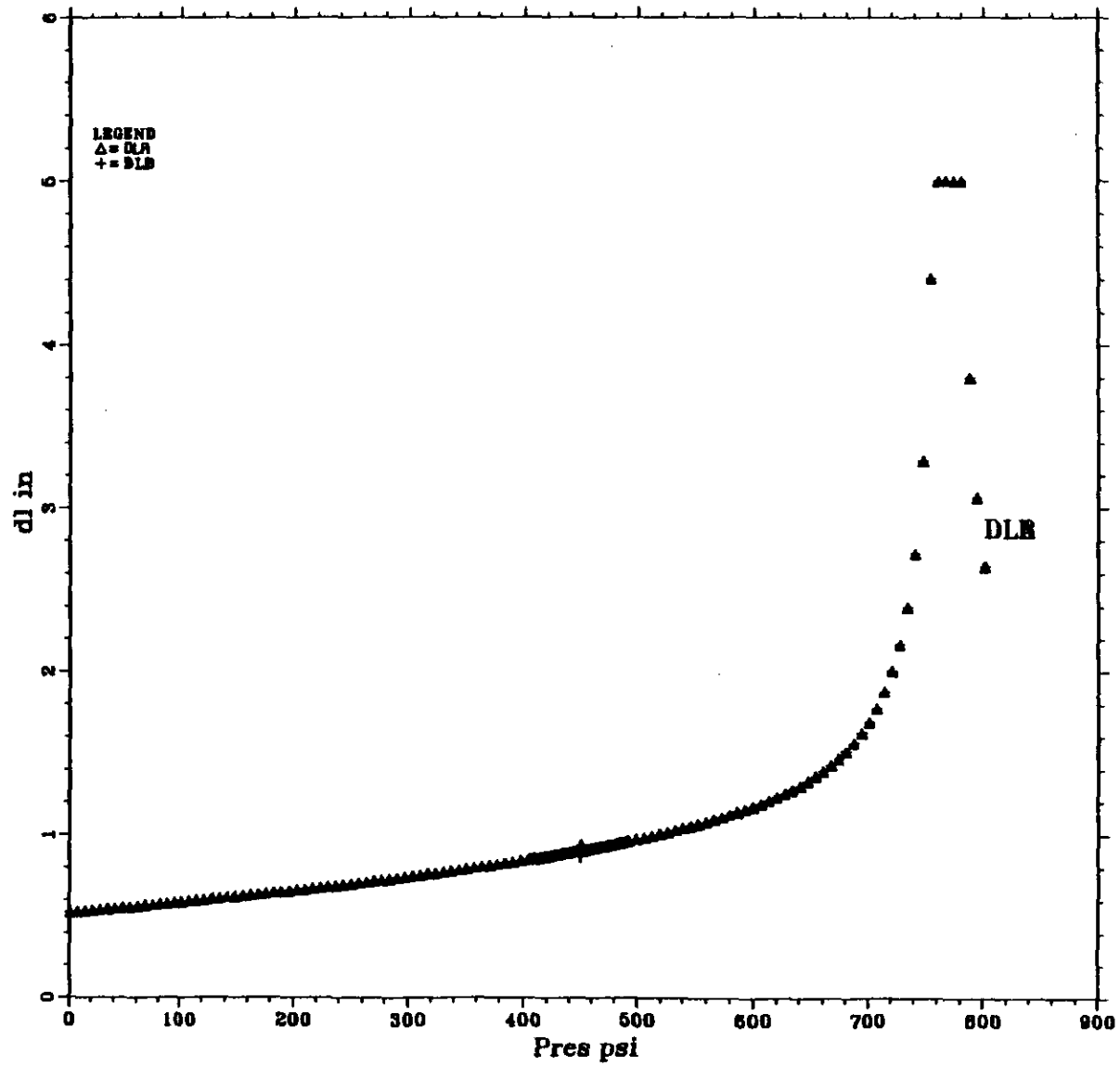

RHIC qdq
zet6=0.030 in
zet7=0.000 in
zet13=0.000 in
zet14=-.030 in
et6=0.000 in
et7=0.000 in
et13=0.000 in
et14=0.000 in
ds6=0.020 in
ds13=0.020 in
f(6)= 0.0 lbs
f(13)= 0.0 lbs
K= 1784.5 lbs/in

2DUA7:<ROSSUM.BUC>FOR001.DAT;102 FIGURE DR6

MAX BELLOWS LOCAL ELONGATION

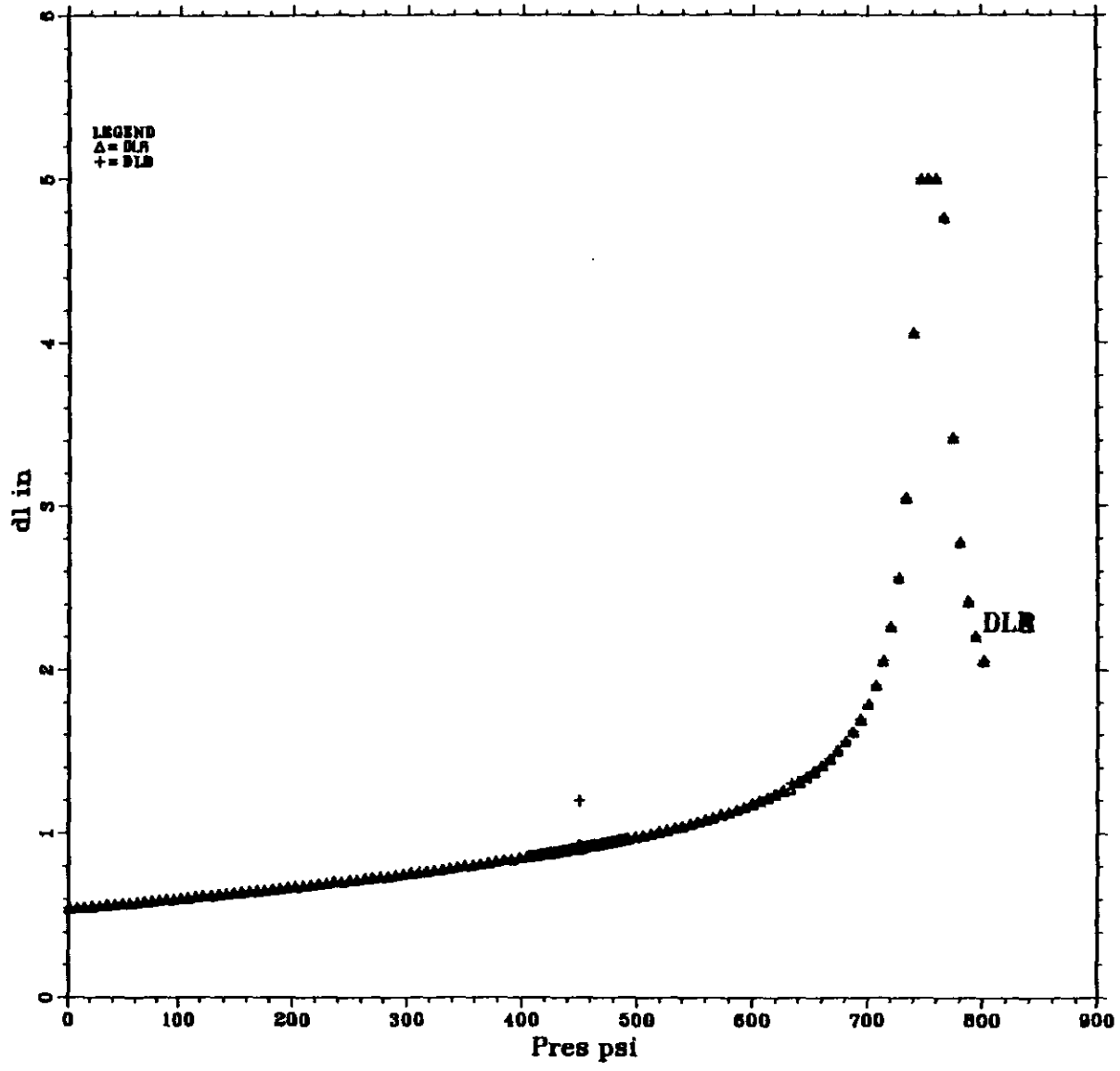

RHIC dqd
zet6=0.030 in
zet7=0.000 in
zet13=0.000 in
zet14=−.030 in
et6=0.000 in
et7=0.000 in
et13=0.000 in
et14=0.000 in
ds6=0.020 in
ds13=0.020 in
f(6)= 0.0 lbs
f(13)= 0.0 lbs
K= 2732.3 lbs/in

2DUA7:<ROSSUM.BUC>FOR001.DAT;104

FIGURE DR8

A, B of eq.64. Function pfor() opens a file to which the fortran expressions will be written, then calls dfor() described above, and also creates fortran expressions for C, D, Es, Ec and G which are needed in addition to A, B in eq.64 to obtain y.

The values for omega appearing in the solutions of the differential equations are then defined. They are needed in the subroutine COEF which are the MACSYMA generated coefficients called Q(i,j), the vector of right-hand sides is W. Q and W are copied into arrays A and B and inverted using the numerical routines LUDCMP and LUBKSB from [6]. Upon inversion of the matrix, array B contains the solutions XA, XB, F which are needed to obtain the explicit expressions for deflections, slopes and curvatures y, y', y". Additional coefficients E, G, D, which are needed for these expressions are generated by MACSYMA are given by subroutine IND. Finally the maximum local bellows elongation DL can be computed.

Subroutine PLOT produces four types of output in addition to a table of values. Option 1 plots maximum local bellows elongation versus pressure, there are two curves, one for each bellows. Option 2 plots support deflections for each support versus pressure. Option 3 gives the deflected shape of the magnet-bellows assembly at pcr and pop. Option 4 provides the deflected shape of the bellows at pcr and pop. These are written in the plot file FOR001.DAT. The Table containing all the various design parameters and summary of the output is in the file ECHO.TEX which must be further processed with the TEX program.

```
(c24) dispfun(bc1,bc2,bc3,bc4,bc5,bc6,eq);

                                          m1    m2
(e24)                bc1() := f1 + f2 - fw (--- - ---)
                                          kt1   kt2

                                   f1   f2              m1
(e25)        bc2() := m1 + m2 - fa (-- - --) + (f1 - fw (---)) l
                                   k1   k2              kt1

                                          m1
(e26)                     bc3() := cyp0() - ---
                                          kt1

                                          m2
(e27)                     bc4() := cyp1() - ---
                                          kt2

                                                  f1
(e28)             bc5() := expand(ratsimp(cy(0) - z - --))
                                                  k1

                                          f2
(e29)                      bc6() := cy(1) - --
                                          k2

                                       f1          fw m1
                            fa (yx + y0 - --) + f1 x - ----- x + m1
                                       k1           kt1
(e30)   eq() := expand(ypp = - ----------------------------------------)
                                              e i

(d30)                              done

(c31) dispfun(sol,pfor);

(e31)            sol() := sol : part(solve(leq(), lunk), 1)

(e32) pfor() := (writefile("workcoef.for"),

detrig : trigsimp(denom(rhs(part(sol, 1)))),

                    detrig
detsimp : expand(---------------), fortran(determ = subst(ls, detsimp)),
                 l k1 k2 kt1 kt2

FOR k THRU 6 DO fortran(subst(ls, s3(k))), fortran(cd = subst(ls, xd)),

fortran(cq = subst(ls, xq)), closefile())

(d32)                              done
```

FIGURE E4

```
(c13) "derivative of y w.r.t. x"$dispfun(yp,pab,hp,hep);

(c14)
(e14)            yp(i, j) := pab(i, j) + hp(i, j) + hep(i, j)

(e15) pab(i, j) := - om(i) xa(i) sin(om(i) x(j)) + om(i) xb(i) cos(om(i) x(j))

(e16)                  hp(i, j) := zc(i) + 2 zd(i) x(j)

(e17) hep(i, j) := (IF i = 6 THEN xinit : x(6)

 ELSE (IF i = 13 THEN xinit : x(13)), zes(i) pil cos(pil (x(j) - xinit))

 + zec(i) (- 2 pil) sin(2 pil (x(j) - xinit)))

(d17)                                done

(c18) "list of unknowns"$dispfun(u);

(c19)
(e19) u(i) := IF i <= 18 THEN xa(i) ELSE (IF i <= 36 THEN xb(i - 18)

 ELSE (IF i <= 41 THEN f(i - 36) ELSE (IF i <= 46 THEN f(i - 34)

 ELSE (IF i <= 51 THEN f(i - 32)))))

(d19)                                done
```

FIGURE E6

```
(c50) "torsional rigidity of supports at center of the 3 magnets"$dispfun(gam);

(c51)
(e51) gam(i) := IF i = 3 THEN gam3 ELSE (IF i = 10 THEN gam10

                                        ELSE (IF i = 17 THEN gam17 ELSE 0))

(d51)                                done

(c52) "product EI for each of the 3 magnets"$dispfun(aml);

(c53)
(e53) aml(i) := IF i <= 5 THEN am ELSE (IF i = 6 THEN al

                  ELSE (IF i <= 12 THEN aq ELSE (IF i = 13 THEN al ELSE am)))

(d53)                                done

(c54) "axial force"$dispfun(fab);

(c55)
(e55)                fab(i) := IF i <= 9 THEN fa ELSE fb

(d55)                                done

(c56) "useful functions of aml, fab"$dispfun(a,b);

(c57)
                                     fab(i)
(e57)                        a(i) := ------
                                     aml(i)

                                 sum(f(j), j, 1, i)
(e58)                   b(i) := - ------------------
                                      aml(i)

(d58)                                done

(c59) "function expressing the curvature of the magnet and derivatives"$dispfun(f0,f0p,f0pp);

(c60)
(e60)                 f0(i) := - p x(i) (x(i) - x(19))

(e61)                  f0p(i) := - (2 x(i) - x(19)) p

(e62)                       f0pp(j) := - 2 p

(d62)                                done
```


FIGURE E8

```
(c28) "boundary condition at the supports relating force to displacement"$dispfun(ceq);

(c29)
                                                f(i)
(e29) ceq(i) := IF i <= 5 THEN expand(y(i, i) - -----)
                                                sk(i)

                                                f(i + 2)
 ELSE (IF i <= 10 THEN expand(y(i + 2, i + 2) - ---------)
                                                sk(i + 2)

                                                f(i + 4)
 ELSE (IF i <= 14 THEN expand(y(i + 4, i + 4) - ---------)
                                                sk(i + 4)

                                               f(i + 4)
 ELSE (IF i = 15 THEN expand(y(i + 3, i + 4) - ---------))))
                                               sk(i + 4)


(d29)                                done

(c30) "boundary condition for continuity of deflection"$dispfun(eq);

(c31)
(e31) eq(i) := - ab(i, i + 1) + ab(i + 1, i + 1)

 + expand(ratsimp(- h(i, i + 1) + h(i + 1, i + 1))) - he(i, i + 1)

 + he(i + 1, i + 1) - zet(i + 1)


(d31)                                done

(c32) "boundary condition for continuity of slope"$dispfun(peq);

(c33)
(e33) peq(i) := - pab(i, i + 1) + pab(i + 1, i + 1)

 + expand(ratsimp(- hp(i, i + 1) + hp(i + 1, i + 1))) - hep(i, i + 1)

 + hep(i + 1, i + 1) - et(i + 1)


(d33)                                done

(c34) "moment equation"$dispfun(mom);

(c35)
                                 f(10)    f(19)
(e35) mom() := (mom : expand(fb (------ - ------ - (f0(19) - f0(10)))
                                 sk(10)   sk(19)

      f(1)    f(10)
 + fa (----- - ------ - (f0(10) - f0(1)))),
      sk(1)   sk(10)

                                                                  2
mom + sum(gam(i) - f(i) (x(19) - x(i)), i, 1, 19) + fwa p x (19))
```

FIGURE E10

TECHNICAL NOTE DISTRIBUTION

Building 902

Blake, A.
Cottingham, J. G.
Garber, M.
Ghosh, A.
Greene, A.
Gupta, R.
Herrera, J.
Kahn, S.
Kelly, E.
Morgan, G.
Muratore, J.
Ozaki, S.
Prodell, A.
Rehak, M.
Rohrer, E.P.
Sampson, W.
Shutt, R.
Thompson, P.
Wanderer, P.
Willen, E.

Building 1005S

Brown, D.
Claus, J.
Courant, E.
Dell, F.
Gavigan, M.
Lee, S.Y.
Milutinovic, J.
Parzen, G.
Rhoades-Brown, M.
Ruggiero, S.
Sondericker, J.
Tepekian, S.
Wolf, L.

Building 911

AD Library, (R. Cohen)
P. Hughes (1) plus one for ea. author

Building 460

Samios, N. P.

Building 510

Banks, M.

For SSC Papers

FNAL

Mantsch, P.
Strait, J.

SSCL

Bush, T.
Coombes, R.
Goodzeit, C.
Kelly, V.
Tompkins, J.
Library Copy

LBL

Taylor, C.

S&P in Magnet Division for all MD papers

S&P in Accelerator Physics Division for all Cryogenic Papers (and J. Briggs, R. Dagradi, H. Hildebrand, W. Kollmer

Σ moments:

$$F_b\left(\delta_{10}-y_o(x_{19})+y_o x_{10}-\delta_{19}\right)-\sum_{1}^{18} F_v(x_{19}-x_v)$$
$$+F_a\left(\delta_1-y_o(x_{10})-\delta_{10}\right)+\gamma_3+\gamma_{10}+\gamma_{17}+\frac{\pi D^2 p_a}{4}\phi x_{19}^2=0 \tag{59}$$

In addition, we need 49 boundary conditions to solve for the mentioned 51 forces and integration constants: as defined,

$$y_n(x_n)=\delta_n=\frac{F_n}{k_n}(1\le n\le 18,\ n\ne 6,7,13,14) \tag{60}$$

This results in 18 - 4 = 14 equations. One additional equation must be

$$y_{18}(x_{19})=\frac{F_{19}}{k_{19}} \tag{61}$$

Continuity (y_n to y_{n+1} "nodes") equations are

$$y_{n+1}(x_{n+1})-\zeta_{n+1}=y_n(x_{n+1}) \tag{62}$$

$$y'_{n+1}(x_{n+1})-\eta_{n+1}=y'_n(x_{n+1}) \tag{63}$$

Equations 62, 63 are valid when $1\le n\le 17$, therefore result in 2 x 17 = 34 more equations, for a total of 14 + 1 + 34 = 49, as needed. Only $\zeta_{6,7,13,14}$, $\eta_{6,7,13,14}$ will be $\ne 0$ for the system drawn in Fig. 9.

Note that, in Fig. 9, $\zeta_{7,14},\eta_{7,14}$ are drawn so that they must be entered as negative values; for instance, $y_7(x_7)-\zeta_7=y_6(x_7)$; since in Fig. 9 $y_7(x_7)<y_6(x_7)$, ζ_7 must be <0: for abrupt increases of y(x) (or $y'(x)$) with x, ζ (*or* η) > 0 and for decreases ζ (*or* η) < 0.

The solution for equation 57 is

$$y_n(x)=A_n\cos\omega_n x+B_n\sin\omega_n x+C_n x+D_n x^2$$
$$+E_{sn}\sin\left[\frac{\pi}{\ell}(x-x_n)\right]+E_{cn}\cos\left[\frac{2\pi}{\ell}(x-x_n)\right]+G_n \tag{64}$$

$$\omega_n = \left(F_\alpha / E_n I_n\right)^{1/2}$$

$$C_n = -\frac{1}{F_\alpha}\left[\sum_{\nu=1}^{n} F_\nu + F_\alpha \phi x_{19} - \phi F_{w\alpha} x_{19}\right]$$

$$D_n = \phi$$

$$E_{sn} = d_{sn}\left[\frac{\omega_n \ell}{\pi}\right]^2 \left[1 - \left[\frac{\omega_n \ell}{\pi}\right]^2\right]^{-1}$$

$$E_{cn} = -d_{cn}\left[\frac{\omega_n \ell}{2\pi}\right]^2 \left[1 - \left[\frac{\omega_n \ell}{2\pi}\right]^2\right]^{-1}$$

$$G_n = \frac{1}{F_\alpha}\left[\left(F_\alpha - F_\beta\right)\left(\delta_{10} + y_o\left(x_{10}\right)\right) + F_\beta \delta_1 + \sum_{1}^{n} F_\nu x_\nu + v_n - 2\phi E_n I_n - F_\alpha d_{cn}\right]$$

The A_n,B_n are to be determined, together with the F_n, by solving eqs. 58 to 63.

VIIa. Numerical Results: Spring Constants, Wall Stresses and Deflections

The step by step bellows design procedure summarized in IIIa was applied to obtain the following numerical results. The input parameters that one is free to choose are given in Table 1, the remaining bellows design parameters resulting from the preceding choices are shown in Table 2, stresses σ_{max}, σ_h at operating pressure p_{op} are shown in Table 3. The ratio D_i'/d must be large for the theory to apply. The first three cases correspond to bellows whose diameter is smaller than the shell of the magnet in order to reduce forces on the magnet supports. In the last two cases, where the bellows diameter is larger than that of the shell, it is assumed that the supports have been designed to carry the resulting loads.

When the bellows is internally pressurized the deflections and stresses are computed following equations in IIIb. The system of 10 boundary conditions and three equilibrium conditions (eq. 36a) is solved using techniques discussed in the section on the Numerical Method. The maximum stresses in the two circular sections of a convolution, σ_{pw1}, σ_{pw2}, and in the straight section σ_{px} corresponding to eq. 40 appear in Table 3 along with the maximum deflection of the straight section, denoted y_{max}. Plots of wall deflections w1, w2 in polar coordinates are shown in Fig. a1 for the first case of the table, corresponding stresses σ_{pw1}, σ_{pw2} appear in Fig. a2. These must be added to σ_{max} to obtain the total maximum stress. The total stress is large but admissible (for fatigue) to the manufacturers for a number of about 2000 cycles.

The wall deflection y is shown in Fig. a3 and the stress σ_{px} appears in Fig. a4. It is verified that y_{max} is less than r_i so that the convolution walls do not touch when the bellows is pressurized (Table 3).

Table 1: Input: bellows design parameters

r_i in	D_i in	d in	β	l in	pcr psi	λ in	Eb psi
0.060	7.630	0.500	0.094	6.000	450.000	0.500	3.297E+07
0.060	7.630	0.500	0.094	7.000	450.000	0.500	3.297E+07
0.060	7.630	0.500	0.094	8.000	450.000	0.500	3.297E+07
0.060	11.800	0.500	0.094	9.300	450.000	0.500	3.297E+07
0.060	14.300	0.700	0.094	9.300	450.000	1.000	3.297E+07

Table 2: Results: bellows properties

Nb	r in	D in	Λ in	t in	bc in	K lbs/in	Kl lbs/in	I in^4
17	0.072	8.130	0.352	0.024	0.346	1784.526	4.915E+03	5.137E+00
19	0.073	8.130	0.356	0.026	0.342	2095.286	4.240E+03	5.516E+00
22	0.074	8.130	0.361	0.029	0.337	2410.052	3.734E+03	6.049E+00
26	0.073	12.300	0.356	0.027	0.342	2732.325	7.169E+03	1.943E+01
23	0.075	15.000	0.401	0.031	0.533	2756.610	1.076E+04	4.080E+01

Table 3: Results: maximum bellows stresses at p_{op}

σ_{max} psi	σ_h psi	σ_{pw1} psi	σ_{pw2} psi	σ_{px}	y_{max} in
1.066E+05	1.534E+04	6.869E+04	7.013E+04	3.071E+04	1.548E-03
1.037E+05	1.484E+04	5.942E+04	6.077E+04	2.649E+04	1.246E-03
9.964E+04	1.345E+04	4.924E+04	5.047E+04	2.185E+04	9.405E-04
8.083E+04	2.157E+04	5.741E+04	5.873E+04	2.557E+04	1.184E-03
1.181E+05	1.883E+04	7.946E+04	8.090E+04	3.719E+04	2.558E-03

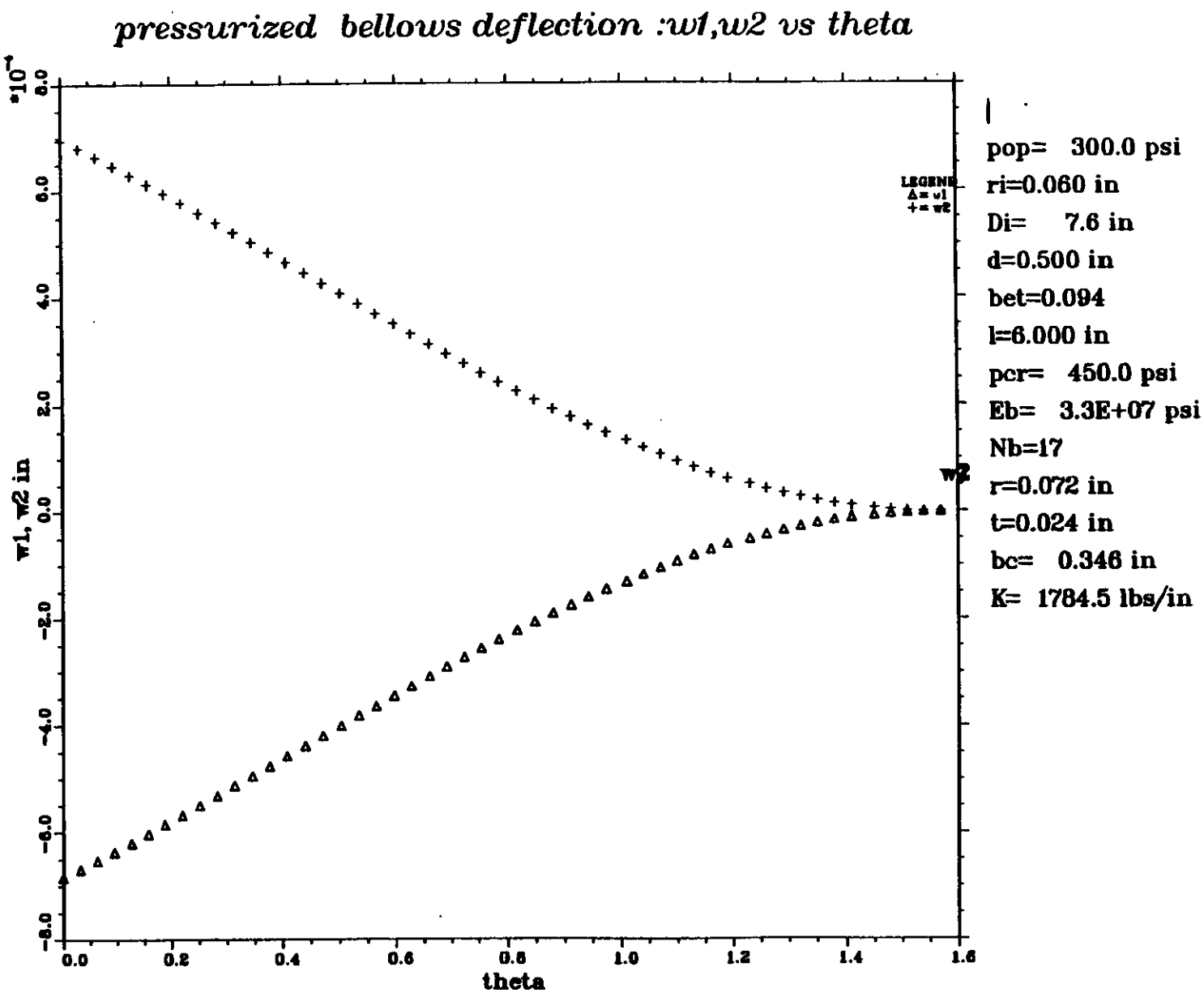

2DUA7:<ROSSUM.BUC>FOR001.DAT;80

FIGURE A1

pressurized bellows stresses: sigpw1,sigpw2 vs theta

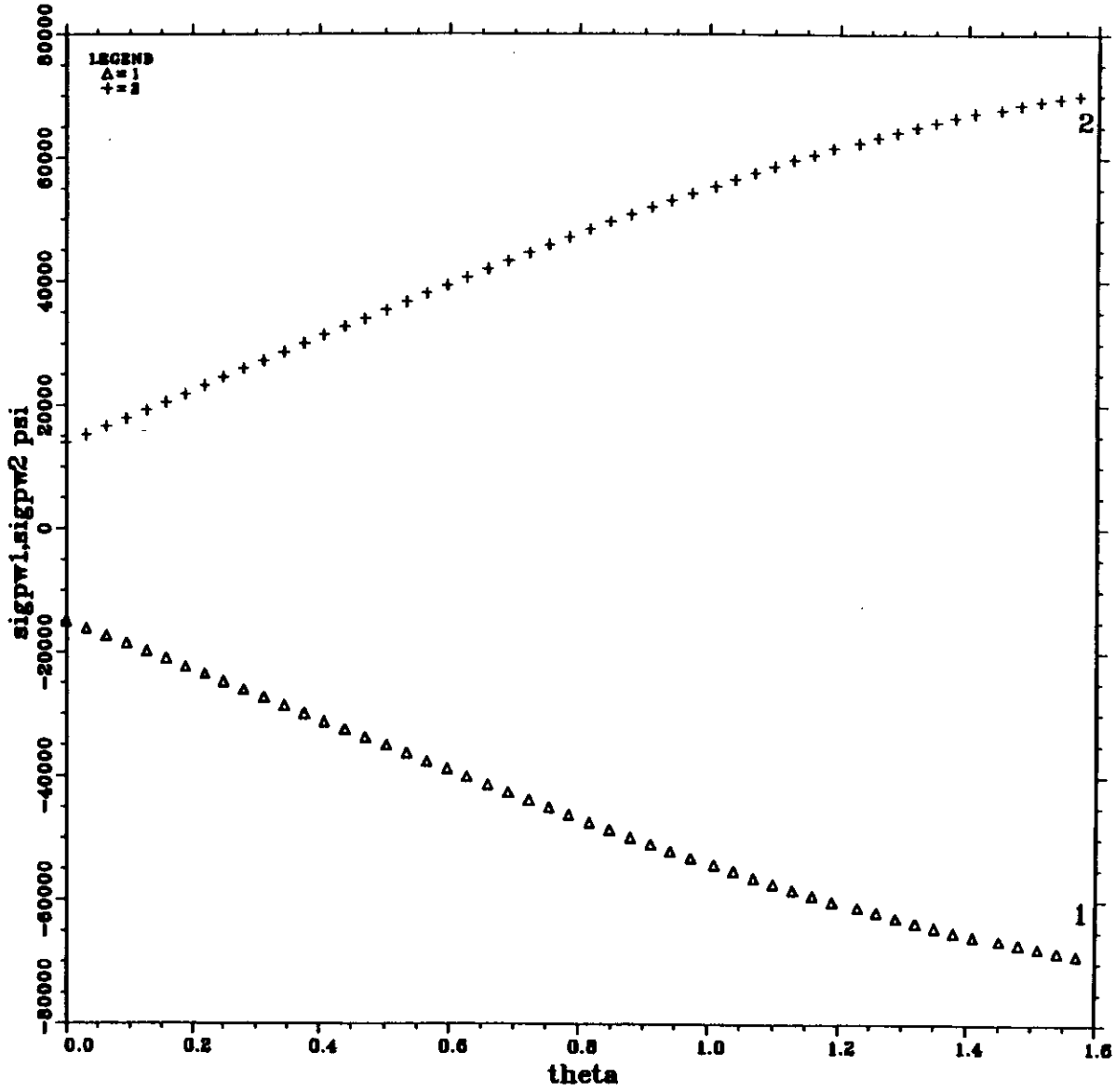

pop= 300.0 psi
ri=0.060 in
Di= 7.6 in
d=0.500 in
bet=0.094
l=6.000 in
pcr= 450.0 psi
Eb= 3.3E+07 psi
Nb=17
r=0.072 in
t=0.024 in
bc= 0.346 in
K= 1784.5 lbs/in

2DUA7:<ROSSUM.BUC>FOR001.DAT;80

FIGURE A2

pressurized bellows deflection: y vs x

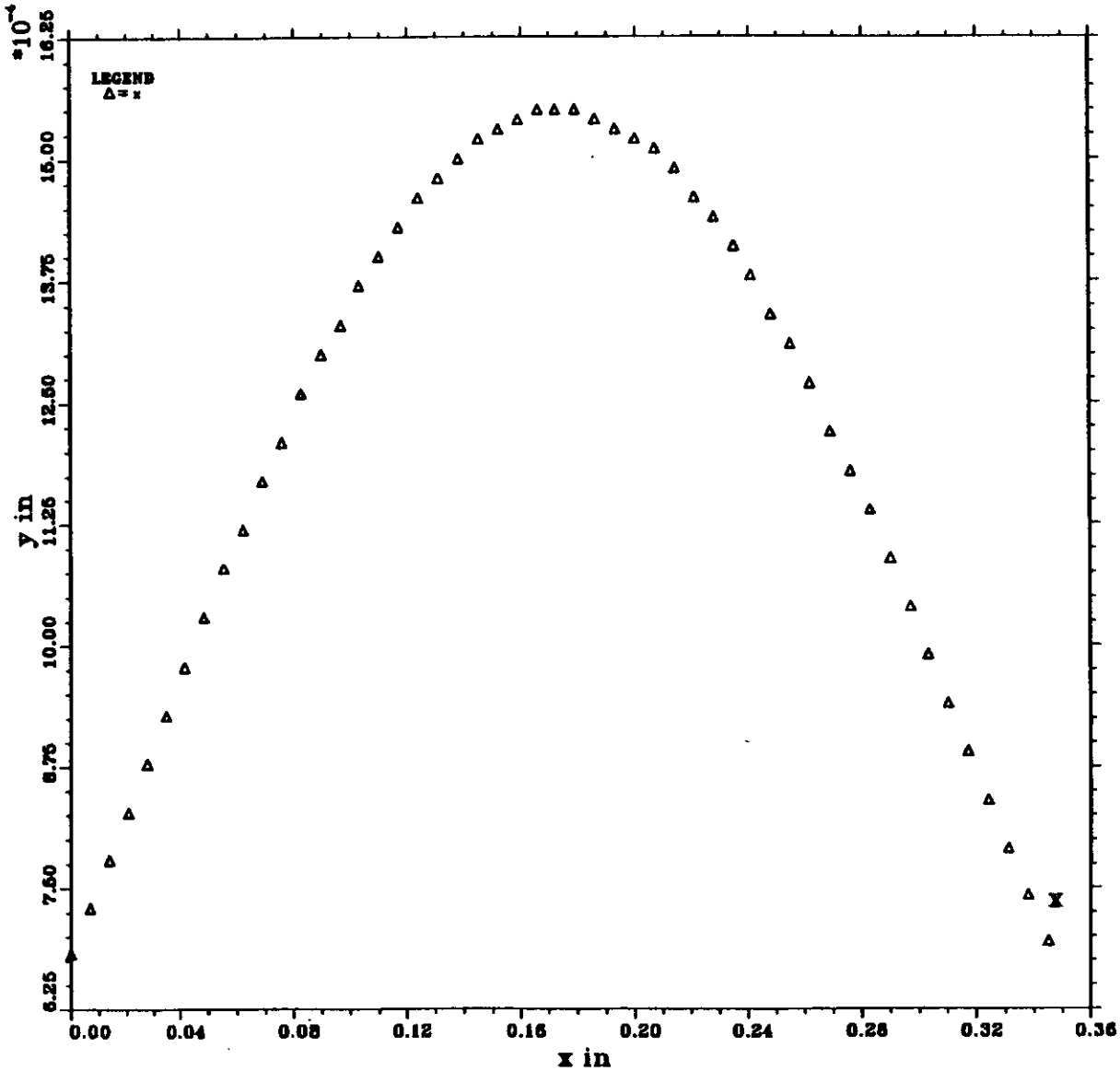

pop= 300.0 psi
ri=0.060 in
Di= 7.6 in
d=0.500 in
bet=0.094
l=6.000 in
pcr= 450.0 psi
Eb= 3.3E+07 psi
Nb=17
r=0.072 in
t=0.024 in
bc= 0.346 in
K= 1784.5 lbs/in

2DUA7:<ROSSUM.BUC>FOR001.DAT;80

FIGURE A3

pressurized bellows stresses: sigpx vs x

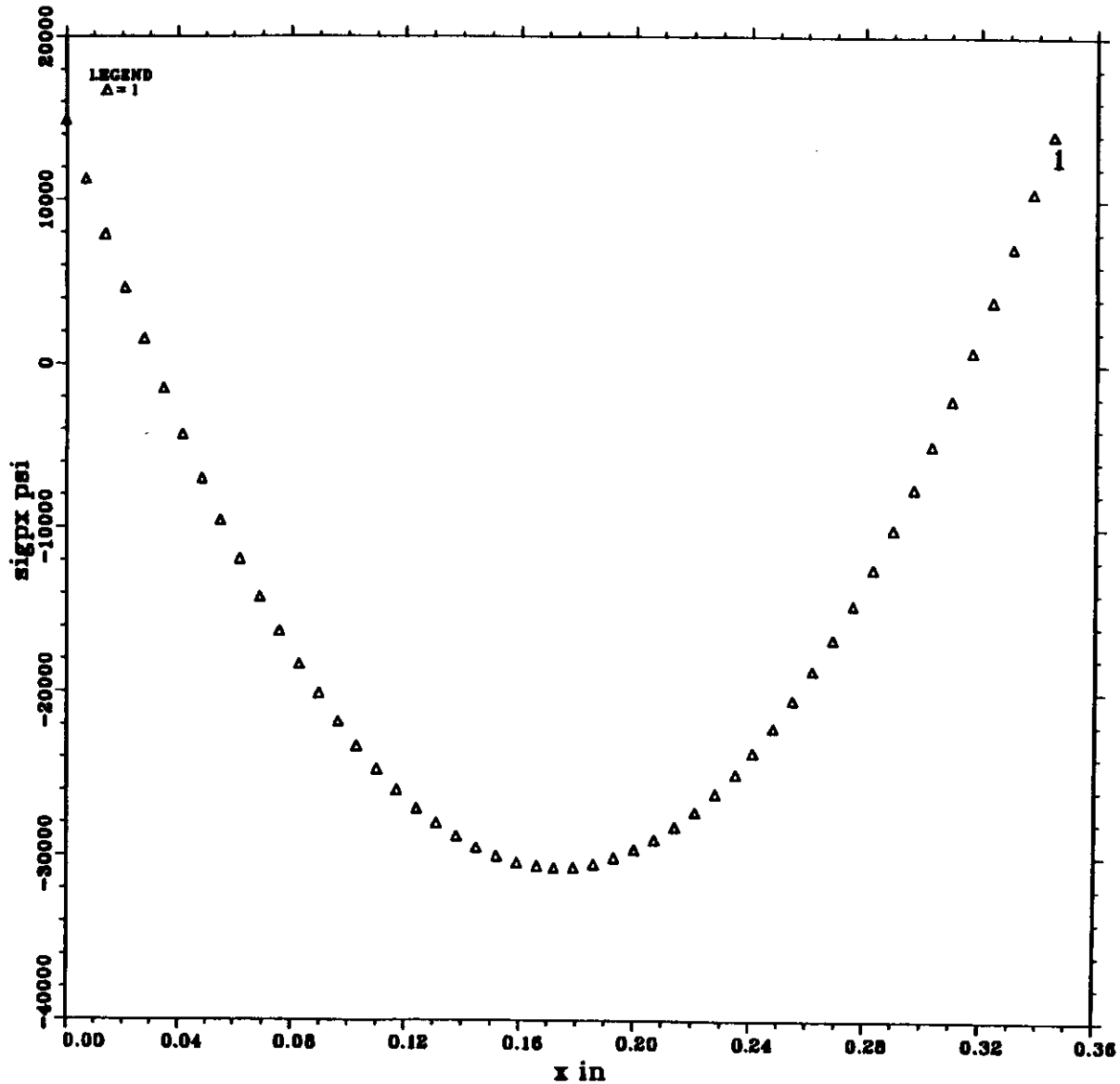

pop= 300.0 psi
ri=0.060 in
Di= 7.6 in
d=0.500 in
bet=0.094
l=6.000 in
pcr= 450.0 psi
Eb= 3.3E+07 psi
Nb=17
r=0.072 in
t=0.024 in
bc= 0.346 in
K= 1784.5 lbs/in

2DUA7:<ROSSUM.BUC>FOR001.DAT;80

FIGURE A4

VIIb. Numerical Results: Spring--Supported bellows model

In order to obtain the bellows deflection y(x) (IV, eq.47), one must solve a system of 6 equations formed by the six boundary conditions eqs.43, 44, 46a to 46d for the 6 unknowns, A, B, Mc1, Mc2, F1, F2. (See the Numerical Method section for details.)

The solution reveals that A and B have a common denominator which is the determinant of the matrix shown in Fig. e1 along with the surface determinant=0 as a function of pressure and stiffnesses. When the determinant approaches zero, y becomes unbounded or indeterminate and the bellows is unstable. The determinant is, as expected, a symmetrical expression with respect to left and right since the indices 1 and 2 can be interchanged without altering its value. It is a function of Fa (both directly and through ω, eq. 47a) and of k1, k2, k_{t1}, k_{t2}. With this expression one can find the critical buckling load of the bellows due to the support system only, that is the value of Fa (or pressure p) which will reduce the determinant to zero for given stiffnesses. For simplicity, the realistic assumptions that $k_{t1} = k_{t2}$ and k1 = k2 are used from now on. The precompression is λ = 0.

********** SSC **********

Fig. b1 shows a plot of the maximum bellows elongation defined in eq.50 as a function of pressure. The bellows was designed to have a critical load at 450 psi due to an assumed initial sine shape (prebend). According to the last case in the preceeding three tables, this determines an axial stiffness of K=2760 lb/in for a bellows of inner diameter D_i = 14.3 in and length 9.3 in, the supports have assumed stiffnesses of k_{t1} = 3.e7 lb in/radian and k1 = 7e3 lb/in. There is a peak at 600 psi and one at 1875 psi. The expected peak, for which the bellows was designed at 450 psi, is absent because y (eq.47) is indeterminate (zero appears both in the numerator and denominator). Nevertheless the bellows should be designed as having a critical load at that value since deviations could lead to large deflections. Seide [3] and Haringx [4,5] discuss and present experimental data on the stability of internally pressurized bellows. Haringx shows that a bellows with clamped ends

can fail at relatively low values for pressure. Keeping in mind that there can be a peak at $\omega\ell = \pi$, the spring model will be used here only to find the buckling load due to support details.

We show next how the analysis of the determinant alone allows one to predict the critical load due to the spring supports only. The determinant is solved first for the variable k1, the solution is plotted for several values of k_{t1} as a function of p in Fig. b2. Figure e2 shows the equation giving the value of k1 which will make the determinant go to zero for various values of k_{t1}. Asymptotic expressions where k_{t1} goes to zero or infinity appearing in Fig. e3 are plotted as curves 1 and 7 in Fig. b2. A horizontal line drawn at k1=7e3 lb/in intersects the curve of solutions with k_{t1}=3e7 lb in/radian when p is about 610 psi. (Curves are truncated at 20000 lb/in.) With k_{t1}=0, p is only somewhat larger, at about 650 psi.

An equivalent way to predict the buckling load is to solve the determinant for the variable k_{t1} as a function of k1 and p. There are two solutions since the determinant is a quadratic function of k_{t1}. The first one, denoted k_{t1a} in Fig. b3, shows that a horizontal line drawn at 3e7 lb in/radian would intersect the determinant=0 curve for k1=7e3 lb/in at 610 psi. The second root, denoted k_{t1b} in Fig. b4 shows that for all values of k1 the determinant is equal to zero at 1875 psi when k_{t1}=3e7 lb in/radian. We have thus explained the origin of the two peaks in Fig. b1: they can be traced to a given combination of support stiffnesses. Figures.b2, b3, b4 can be used to ensure that peaks due to supports remain always above the critical load for which the bellows is designed. Expressions for k1, k_{t1a}, k_{t1b} which cause the determinant to be equal to zero are shown in Fig. e2. Limits when ω=0 are given in Fig. e3 for the cases where k1=0 and k1 infinite.

We now give an example where the support peak occurs below the $\omega\ell = \pi$ peak. Figure b4 predicts that a peak could be obtained at 425 psi if k1=7000 lb/in and k_{t1}=1.e4 lb in/radian, this is verified in Fig. b5 which shows the 425 psi peak. In addition there are the peaks at 650 psi and at 1830 psi shown in Fig. b2 and/or b3.

Table 4 lists peak locations according to their origin for two values of k_{t1}. The influence of the mounting offset ς is to accelerate the rate of rise to the peaks, but not to cause them. It is a multiplying factor of the numerator of y and does not appear in the

$$\text{determinant} = fa\left(\left(\frac{1}{k2} + \frac{1}{k1}\right)\left(-o^2 \sin(l\,o) + \frac{fa\,(fa - fw)\sin(l\,o)}{kt1\,kt2}\right.\right.$$

$$\left. - fa\left(\frac{1}{kt2} + \frac{1}{kt1}\right) o \cos(l\,o)\right) + \left(\frac{1}{kt2} + \frac{1}{kt1}\right)(\sin(l\,o) - l\,o\cos(l\,o))$$

$$- \frac{fa\,l\sin(l\,o)}{kt1\,kt2} + fw\left(\frac{1}{k2\,kt2} + \frac{1}{k1\,kt1}\right) o\,(1 - \cos(l\,o)))$$

$$+ o\,(l\,o\sin(l\,o) + 2\,(\cos(l\,o) - 1))$$

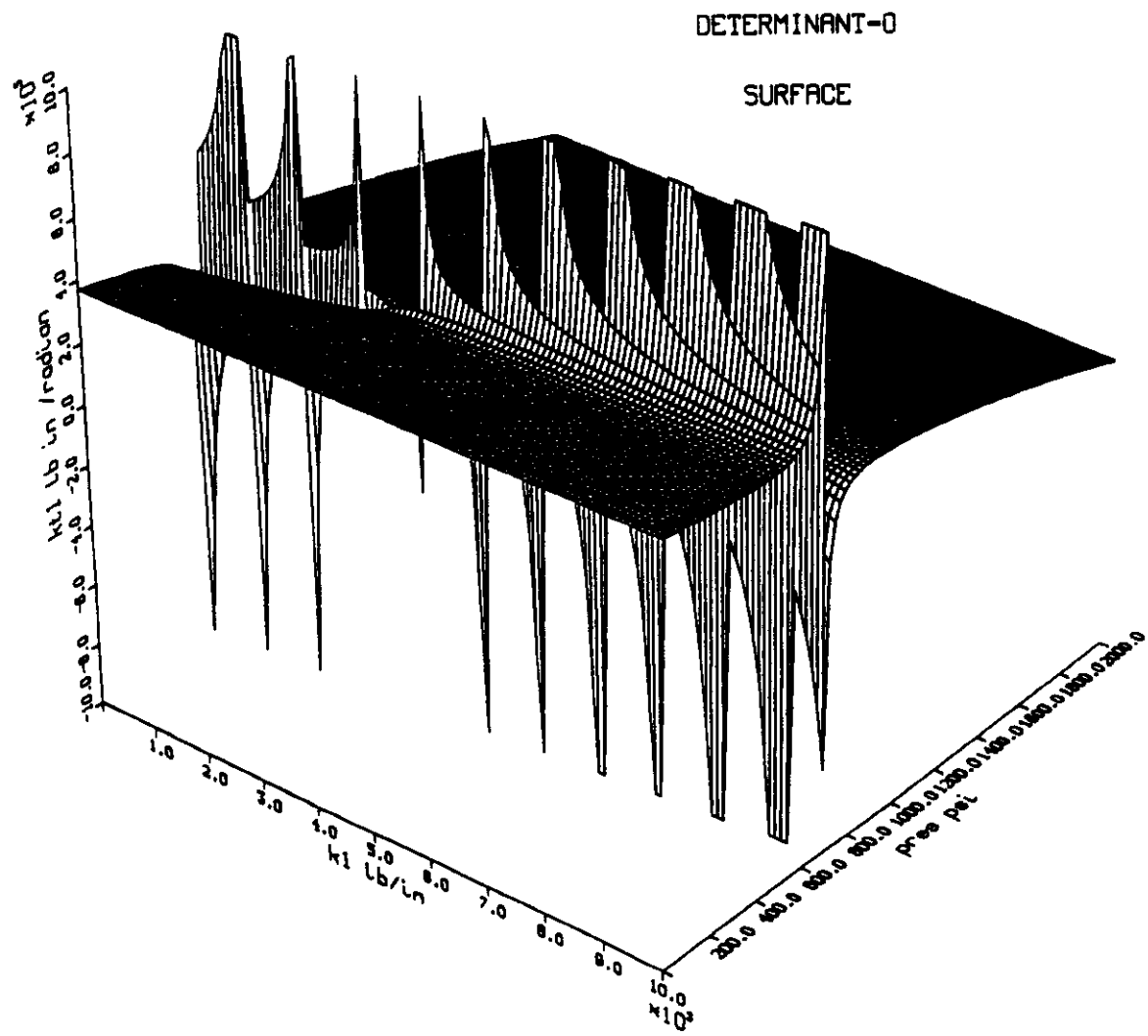

FIGURE E1

$$
\begin{aligned}
k1 = {} & - (kt1\ (- fa\ fw\ o \sin^2(l\ o) - fa\ fw\ o \cos^2(l\ o) \\
& + (fa\ fw - 2\ fa^2)\ o \cos(l\ o)) + kt2\ (2\ fa\ kt1\ o^2 \sin(l\ o) \\
& + (fa\ fw - 2\ fa^2)\ o \cos(l\ o) - fa\ fw\ o) + (2\ fa^2\ fw - 2\ fa^3) \sin(l\ o)) \\
& /(kt2\ (kt1\ (o \sin^2(l\ o) - l\ o^2 \sin(l\ o) + o \cos^2(l\ o) - 2\ o \cos(l\ o) + o) \\
& - fa \sin(l\ o) + fa\ l\ o \cos(l\ o)) + kt1\ (fa\ l\ o \cos(l\ o) - fa \sin(l\ o)) \\
& + fa^2\ l \sin(l\ o))
\end{aligned}
$$

$$
\begin{aligned}
ktla = {} & (k2\ (k1\ (2\ fa\ l\ o \cos(l\ o) - 2\ fa \sin(l\ o)) \\
& + (fa\ fw - 2\ fa^2)\ o \cos(l\ o) - fa\ fw\ o) \\
& + fa\ k1\ k2\ (2\ (\sin(l\ o) - l\ o) + (\frac{1}{k2} + \frac{1}{k1})\ o\ (fw\ (\cos(l\ o) - 1) + 2\ fa)) \\
& + k1\ ((fa\ fw - 2\ fa^2)\ o \cos(l\ o) - fa\ fw\ o)) \\
& /(k2\ (k1\ (2\ l\ o^2 \sin(l\ o) + 4\ o \cos(l\ o) - 4\ o) - 2\ fa\ o^2 \sin(l\ o)) \\
& - 2\ fa\ k1\ o^2 \sin(l\ o))
\end{aligned}
$$

$$
\begin{aligned}
ktlb = {} & - (k2\ (k1\ (2\ fa \sin(l\ o) - 2\ fa\ l\ o \cos(l\ o)) \\
& + (2\ fa^2 - fa\ fw)\ o \cos(l\ o) + fa\ fw\ o) \\
& + fa\ k1\ k2\ (2\ (\sin(l\ o) - l\ o) + (\frac{1}{k2} + \frac{1}{k1})\ o\ (fw\ (\cos(l\ o) - 1) + 2\ fa)) \\
& + k1\ ((2\ fa^2 - fa\ fw)\ o \cos(l\ o) + fa\ fw\ o)) \\
& /(k2\ (k1\ (2\ l\ o^2 \sin(l\ o) + 4\ o \cos(l\ o) - 4\ o) - 2\ fa\ o^2 \sin(l\ o)) \\
& - 2\ fa\ k1\ o^2 \sin(l\ o))
\end{aligned}
$$

FIGURE E2

limit k1, kt1=0

$$-\frac{2\,fw - 2\,fa}{l}$$

limit k1, kt1=infinity

$$\frac{2\,fa\,o\,\sin(l\,o)}{l\,o\,\sin(l\,o) + 2\cos(l\,o) - 2}$$

limit kt1a, k1=0, and with o=0

$$-\frac{(fw - fa)\cos(l\,o) - fw + fa}{o\,\sin(l\,o)}\quad,\quad\frac{fw\,l}{2}$$

limit kt1a, k1=infinity, and with o=0

$$\frac{fa\,l\cos(l\,o) - fa\,l}{l\,o\,\sin(l\,o) + 2\cos(l\,o) - 2}\quad,\quad\frac{3D^2K}{4}$$

limit kt1b, k1=0, and with o=0

$$\frac{fa\cos(l\,o) + fa}{o\,\sin(l\,o)}\quad,\quad\frac{D^2K}{4}$$

limit kt1b, k1=infinity, and with o=0

$$-\frac{2\,fa\,\sin(l\,o) - fa\,l\,o\cos(l\,o) - fa\,l\,o}{l\,o^2\,\sin(l\,o) + 2\,o\cos(l\,o) - 2\,o}\quad,\quad\frac{D^2K}{4}$$

kt1a as a function of k1 when C=%pi/l

$$kt1a = \frac{\%pi^2\,D^2\,K\,(4\,k1\,l^2 + 8\,fw\,l - \%pi^2\,D^2\,K)}{64\,k1\,l^2}$$

FIGURE E3

denominator. The influence of ς can be seen by comparing figs.b6 and b7 which differ only in that $\varsigma=0.03$ in Fig. b6 and zero in Fig. b7. The first support peak is no longer visible when $\varsigma=0$ but it could be large if ς were increased.

Table 4: Pressure (psi) values at peaks

k_{t1}	3e7 lb in/radian	1e4 lb in/radian
$\omega\ell = \pi$ peak	450	450
$\omega\ell = 2\pi$ peak	1800	1800
k1, k_{t1a} peak	610	650, 1830
k_{t1b} peak	1875	425

The effect of the sine shape of the bellows can be seen in Fig. b7 where d1=0.02; the second support peak is larger than in Fig. b1. This effect is further accentuated in Fig. b8 when d2=0.02 where there is also a peak at $\omega\ell=2\pi$ at 4 x 450 = 1800 psi which here is masked by the second support peak. In addition to ς and d1, the presence of d2 contributes to the rise of the curve even at operating pressure. The corresponding bellows deflected shape is shown in Fig. b9.

We determine next conditions for support stiffnesses such that support peaks remain always above the $\omega\ell = \pi$ peak for any pressure. A conservative value for k_{t1} is given in Fig. e3 by the limit of k_{t1a} when k1 is infinite and $\omega=0$. This value is $3D^2K/4$ for any value of k1, even infinity. A less conservative value can be obtained by using the relation between k_{t1a} and k1 given in Fig. e3 for $\omega\ell = \pi$. The root k_{t1b} is zero at $\omega\ell = \pi$ for all values of k1. Figure b3 can be used to verify that no peak will occur below $\omega\ell = \pi$ if these guidelines are followed. Figure b4 indicates that the $3D^2K/4$ value for k_{t1} is three times higher than needed in that figure to avoid low peaks. The torsional stiffness for an SSC dipole with two support posts is estimated in the next section at 1.5e7 lb in/radian which is much higher than the 4.6e5 lb in/radian obtained from the proposed limit $k_{t1}=3D^2K/4$.

Figure br1 shows a plot of the maximum bellows elongation defined in eq.50 as a function of pressure. The bellows was designed to have a critical load at 450 psi due to an assumed initial sine shape (prebend). According to the first case in the preceeding three tables this determines an axial stiffness of K=1785 lb/in for a bellows of inner diameter D_i=7.63 in and length 6 in, the supports have assumed stiffnesses of k_{t1}=3.e7 lb in/radian and k1=7e3 lb in. There is a peak at 800 psi and one at 1900 psi. The expected peak, for which the bellows was designed at 450 psi, is absent because y (eq.47) is indeterminate (zero appears both in the numerator and denominator).

Nevertheless the bellows should be designed as having a critical load at that value since deviations could lead to large deflections. Seide [3] and Haringx [4,5] discuss and present experimental data on the stability of internally pressurized bellows. Haringx shows that a bellows with clamped ends can fail at relatively low values for pressure. Keeping in mind that there can be a peak at $\omega\ell = \pi$, the spring model will be used here only to find the buckling load due to support details.

We show next how the analysis of the determinant alone allows one to predict the critical load due to the spring supports only. The determinant is solved first for the variable k1, the solution is plotted for several values of k_{t1} as a function of p in Fig. br2. Figure e2 shows the equation giving the value of k1 which will make the determinant go to zero for various values of k_{t1}. Asymptotic expressions where k_{t1} goes to zero or infinity appearing in Fig. e3 are plotted as curves 1 and 7 in Fig. br2. A horizontal line drawn at k1=7e3 lb/in intersects the curve of solutions with k_{t1}=3e7 lb in/radian when p is about 800 psi. With k_{t1}=0, p is 875 psi.

An equivalent way to predict the buckling load is to solve the determinant for the variable k_{t1} as a function of k1 and p. There are two solutions since the determinant is a quadratic function of k_{t1}. The first one, denoted k_{t1a} in Fig. br3, shows that a horizontal line drawn at 3e7 lb in/radian would intersect the determinant=0 curve for k1=7e3 lb/in at 800 psi. The second root, denoted k_{t1b} in Fig. br4 shows that for all values of k1 the determinant is equal to zero at 1900 psi when k_{t1}=3e7 lb in/radian. We have thus explained

the origin of the two peaks in Fig. br1: they can be traced to a given combination of support stiffnesses. Figures br2, br3, br4 can be used to ensure that peaks due to supports remain always above the critical load for which the bellows is designed.

Expressions for k1, k_{t1a}, k_{t1b} which cause the determinant to be equal to zero are shown in Fig. e2. Limits when $\omega=0$ are given in Fig. e3 for the cases where k1=0 and k1 infinite. We now give an example where the support peak occurs below the $\omega\ell = \pi$ peak. Figure br4 predicts that a peak could be obtained at 340 psi if k1=7000 lb/in and k_{t1}=1.e4 lb in/radian, this is verified in Fig. br5. In addition there are the peaks at 875 psi and at 1700 psi shown in Fig. br2 and/or br3. Table 5 lists peak locations according to their origin for two values of k_{t1}. The influence of the mounting offset ς is to accelerate the rate of rise to the peaks, but not to cause them. It is a multiplying factor of the numerator of y and does not appear in the denominator. The influence of ς can be seen by comparing Figs. br6 and br7 which differ only in that ς=0.03 in Fig. br6 and zero in Fig. br7. The first support peak is no longer visible when ς=0 but it could be large if ς were increased.

The effect of the sine shape of the bellows can be seen in Fig. br7 where d1=0.02; the second support peak is larger than in Fig. br1. This effect is further accentuated in Fig. br8 when d2=0.02 where there is also a peak at $\omega\ell = 2\pi$ at 4 x 450=1800 psi which here is masked by the second support peak. In addition to ς and d1, the presence of d2 contributes considerably to the rise of the curve even at operating pressure. The corresponding bellows deflected shape is shown in Fig. br9.

Finally Fig. br10 shows the maximum elongation for a bellows of large diameter, D_i=11.8 in and 9.3 in in length for the same parameter values as in Fig. br8.

Table 5: Pressure (psi) values at peaks

k_{t1}	3e7 lb in/radian	1e4 lb in/radian
$\omega\ell = \pi$ peak	450	450
$\omega\ell = 2\pi$ peak	1800	1800
k1, k_{t1a} peak	800	875, 1700
k_{t1b} peak	1900	340

We determine next conditions for support stiffnesses such that support peaks remain always above the $\omega\ell = \pi$ peak for any pressure. A conservative value for k_{t1} is given in Fig. e3 by the limit of k_{t1a} when k1 is infinite and $\omega=0$. This value is $3D^2K/4$ for any value of k1, even infinity. A less conservative value can be obtained by the relation between k_{t1a} and k1 given in Fig. e3 for $\omega\ell = \pi$. The root k_{t1b} is zero at $\omega\ell = \pi$ for all values of k1. Figure br3 can be used to verify that no peak will occur below $\omega\ell = \pi$ if these guidelines are followed. Figure br4 indicates that the $k_{t1}=3D^2K/4$ value for k_{t1} is three times higher than needed in that figure to avoid low peaks. The torsional stiffness for RHIC dipoles is estimated in the next section at 3e7 lb in/radian which is much higher than the 88500 lb in/radian obtained from the proposed limit $k_{t1}=3D^2K/4$.

VIIc Numerical Results: Bellows interactions in Magnet Systems

Magnet equivalent Stiffness

In order to relate results from the magnet bellows system to the spring-supported model it is desirable to have an approximate value for the equivalent lateral spring constant and torsional stiffness of the magnet ends.

The magnet is modeled as an axially compressed beam with five supports to which a force or moment is applied at one end. This is a classical statistically indeterminate problem solved by applying the equations derived in VI for the magnet - bellows assembly to one magnet only.

One of the major differences (of concern to us in this problem) between RHIC and SSC magnets (and also between dipoles and quadrupoles) lies in the location and number of supports which is adjusted by setting the relevant support stiffnesses to zero in the general model with five supports. Entries in Table 6 show similar stiffnesses with the exception of the last case; SSC dipoles are mounted on five supports inside the cryostat which itself is mounted on two supports to the ground. (The cryostats are interconnected by bellows.) The actual stiffness of the magnet cryostat assembly is between the two extreme cases of five supports and two supports. Tests can be made to measure the stiffness of the magnet-cryostat assembly. The lateral stiffness k, and torsional stiffness k_t are practically linear functions of the axial force equivalent to the pressure, but their increase is so small that they can be considered constant.

Table 6: Magnet stiffness

Magnet	k lb/in	k_t lb in/radian
RHIC quadrupole	6600	3.0 e7
RHIC dipole	7500	3.2e7
SSC dipole 5 support	6300	3.0 e7
SSC dipole 2 support	530	1.5e7

Magnet bellows assembly

The first example of a magnet bellows assembly is for a dipole-dipole-dipole combination with SSC dimensions. The bellows inner diameter is 14.3 in, its length is 9.3 in, and the axial stiffness which will produce a first peak at 450 psi is K=2760 lb/in, the precompression $\lambda=1$ in, the safety factor over the operating pressure of 300 psi is thus 1.5. In Fig. d1 the maximum local elongation of the two bellows is plotted versus pressure, the initial offset of the first bellows is $\varsigma_6=0.03$ in, it has an initially bent shape with ds6=0.02 and dc6=0.02 in. The upper curve made of triangles corresponds to the first bellows, the lower curve made of crosses corresponds to the second bellows. Maximum elongations are denoted in the legend dla and dlb for the first and second bellows respectively, all values are truncated at 5 in for better display of details.

Figure d1a summarizes the parameter values for the bellows, mounting offsets, magnet parameters, shows the stresses and the maximum local elongations at operating pressure. Figure d1b indicates where the supports are located, what their stiffnesses are and what forces are exerted on them, bellows are located at nodes 6, 7, 13, 14.

Peaks

There is a small peak in the curve for the first bellows at 450 psi which requires a fine mesh to be detected. It reveals the indeterminacy at $\omega\ell = \pi$ discussed in the spring-supported model. The rate of rise to this $\omega\ell = \pi$ peak is controlled by ς, ds6 and dc6 which are also equal to 0.02 in. There is a rising trend in the curve as it proceeds toward the $\omega\ell = 2\pi$ peak at 1800 psi.

The curve corresponding to the first bellows (which has the mounting offset) shows a large rise to the first support peak at 600 psi. The second bellows has a smaller peak at the same location but does not seem to rise below that. This indicates very little, if any, interaction between bellows. Going back to Fig. b2, a peak at about 600 psi for large k_t would occur at k1=6000 lb/in. This number agrees with the 6300 lb/in computed above in the section on magnet equivalent stiffness.

Mounting and shape of bellows

Figure d2 shows the ideal case where there are no mounting offsets and where the bellows are almost straight. Accompanying tables are shown in figs.d2a, d2b. Comparison with Fig. d1 shows that as with the spring-supported model, $\varsigma_{6,7,13,14}$, $\eta_{6,7,13,14}$ and ds6,13, dc6,13 increase the rate of rise to the support peak. The effect of an initial angle η is similar to the effect of ς, for instance replacing $\varsigma_6=0.03$ by $\eta_6=0.004$ would leave Fig. d1 unchanged. If both bellows were mounted in the same manner and had the same initial shapes, then the lower curve of Fig. d1 would coincide with the upper one. In the spring-supported model (Fig. b6) there was no visible support peak when $\varsigma=0$, but there is one here because the assembly was assumed to have an initial average parabolic shape due to the magnets' sagitta.

Bellows interaction

Figure d3 corresponds to the case where lateral forces ($f(7)=-f(6)=12500\ p/p_{op}$ if $p \le p_{op}$ and $f(7)=-f(6)=12500$ lbs if $p \ge p_{op}$) are applied to the first bellows according to Fig. 9 in order to simulate failure in a dipole-dipole-dipole assembly. The upper bellows curve has exceeded the 5 in cutoff limit while the lower bellows curve remains flat denoting no interaction between adjacent bellows at operating pressure. A more pronounced interaction effect is visible in Fig. d4 for the dipole-quadrupole-dipole assembly where the second bellows shows a maximum elongation of 0.5 in above the initial precompression of 1 in. Complete failure of one bellows does not cause adjacent bellows to fail.

Deflected shape of assembly and bellows

Figure d4 shows the deflected shape of the assembly corresponding to Fig. d1 at operating pressure. In order to better see the effect of the internal pressure on the system, only the departure y of the assembly from the initial shape has been plotted. The total final shape is the superposition of the initial parabolic shape, the sine and cosine bellows shapes if they apply, and y. The Table in Fig. d1b can be used to identify bellows and dipole locations. The 0.03 in offset marks the end of the first dipole and the beginning of the first bellows. The offset can also be seen in the bellows deflected shape in Fig. d5, and in Fig. d6.

Additional cases

A possible alternate configuration is shown in Fig. d6 with a dipole-quadrupole-dipole assembly. Both bellows are mounted with offsets and prebent shapes in order to maintain symmetry with respect to the center of the assembly and, as expected, both curves coincide.

The dipole-dipole-quadrupole configuration where the second bellows only is mounted with the usual offset and bent shape is shown in Fig. d7. The second bellows curve is higher than the first one because it is the one with the offset.

********** RHIC **********

Magnet bellows assembly

The first example of a magnet bellows assembly is for a dipole-quadrupole-dipole combination with RHIC dimensions. The bellows inner diameter is 7.63 in, its length is 6 in, and the axial stiffness which will produce a first peak at 450 psi is K=1785 lb/in, the precompression $\lambda=0.5$ in, the safety factor over the operating pressure of 300 psi is thus 1.5. In Fig. dr1 the maximum local elongation of the two bellows is plotted versus pressure, the initial offset of the first bellows is $\varsigma_6=0.03$ in, it has an initially bent shape with ds6=0.02 and dc6=0.02 in. The upper curve made of triangles corresponds to the first bellows, the lower curve made of crosses corresponds to the second bellows. Maximum elongations are denoted in the legend dla and dlb for the first and second bellows respectively, all values are truncated at 5 in for better display of details.

Figure dr1a summarizes the parameter values for the bellows, mounting offsets, magnet parameters, shows the stresses and the maximum local elongations at operating pressure. Figure dr1b indicates where the supports are located, what their stiffnesses are and what forces are exerted on them, bellows are located at nodes 6, 7, 13, 14.

Peaks

There is a small peak in the curve for the first bellows at 450 psi which requires a fine mesh to be detected. It reveals the indeterminacy at $\omega\ell = \pi$ discussed in the spring-supported model. The rate of rise to this $\omega\ell = \pi$ peak is controlled by ς, ds6 and dc6

which are also equal to 0.02 in. There is a rising trend in the curve as it proceeds toward the $\omega\ell = 2\pi$ peak at 1800 psi.

The curve corresponding to the first bellows (which has the mounting offset) shows a large support peak at 700 psi. The second bellows has a smaller peak at the same location but does not seem to rise below that. This indicates very little, if any, interaction between bellows. Going back to Fig. br2, a peak at about 700 psi for large k_t would occur at k1=5000 lb/in.

Mounting and shape of bellows

Figure dr2 shows the ideal case where there are no mounting offsets and where the bellows are almost straight. Accompanying tables are shown in figs.dr2a, dr2b. Comparison with Fig. dr1 shows that as with the spring-supported model, $\varsigma_{6,7,13,14}$, $\eta_{6,7,13,14}$ and ds6,13, dc6,13 increase the rate of rise to the support peak. The effect of the initial angle η is similar to the effect of ς, for instance replacing $\varsigma_6=0.03$ by $\eta_6=0.004$ would leave Fig. dr1 unchanged. If both bellows were mounted in the same manner and had the same initial shapes, then the lower curve of Fig. dr1 would coincide with the upper one. In the spring-supported model (Fig. br6) there was no visible support peak when $\varsigma=0$, but there is one here because the assembly was assumed to have an initial average parabolic shape due to the magnets' sagitta.

Bellows interaction

Figure dr3 corresponds to the case where lateral forces ($f(7)=-f(6)=3000\ p/p_{op}$ if $p \le p_{op}$ and $f(7)=-f(6)=3000$ lbs if $p \ge p_{op}$) are applied to the first bellows according to Fig. 9 in order to simulate failure in a dipole-quadrupole-dipole assembly. The interaction effect on the second bellows is small since the second bellows shows a maximum elongation of 0.17 in above the initial 0.5 in precompression. Complete failure of one bellows does not cause adjacent bellows to fail.

Deflected shape of assembly and bellows

Figure dr4 shows the deflected shape of the assembly corresponding to Fig. dr1 at operating pressure. In order to better see the effect of the internal pressure on the system, only the departure y of the assembly from the initial shape has been plotted. The total final

shape is the superposition of the initial parabolic shape, the sine and cosine bellows shapes if they apply, and y. The Table in Fig. dr1b can be used to identify bellows and dipole locations. The 0.03 in offset marks the end of the first dipole and the beginning of the first bellows. The offset can also be seen in the bellows deflected shape in Fig. dr4, and in Fig. dr5.

Additional cases

A possible alternate configuration is shown in Fig. dr6 with a quadrupole-dipole-quadrupole assembly. Both bellows are mounted with identical offsets and prebent shapes in order to maintain symmetry with respect to the center of the assembly and as expected both curves coincide.

Double peaks

In Fig. dr7 bellows with diameter $D_i = 11.8$ and length $l = 9.3$ in have been used with a dipole-quadrupole-dipole configuration. The first bellows only is mounted with an offset $\varsigma_6 = .03$ in and $ds6 = dc6 = 0.02$ in. This choice of bellows parameters accentuates the fact that in general there are two peaks due to supports where there was one in the spring support model. (Close observation of Fig. dr1 reveals that there are really two peaks which are slightly offset at 700 psi.) Indeed mounting only one bellows with an offset introduces an asymmetry in the problem. In Fig. dr7 the first bellows becomes unstable first at 630 psi, then the second bellows becomes unstable at 760 psi. A peak in one curve always coincides with a lesser peak in the other revealing some interaction between bellows when they become unstable due to the support system. When the asymmetry is removed by letting $\varsigma_{14} = -\varsigma_6$ and using bellows with identical prebent shapes the two peaks now merge at 740 psi in Fig. dr8.

********** SSC and RHIC **********

The two types of instabilities which can occur, the Euler-type of buckling and that due to the support system have been identified. The support peak (or peaks) should always be above the $\omega\ell = \pi$ peak, this is controlled mostly by ensuring a large value for the torsional stiffness of the bellows supports. Interaction between bellows affects only support peaks which are kept well above the 450 psi ($\omega\ell = \pi$).

VIII. Numerical Method

Most of the algebra required for this problem was performed using the symbolic manipulation code MACSYMA. This code has proved to be of invaluable help both numerically and analytically. Some of MACSYMA's capabilities and limitations are illustrated in the following four cases.

Convolution wall stresses and deflections

The numerical part of the internally pressurized bellows problem rests on the inversion of a 10X10 matrix which is performed analytically here using MACSYMA. Eq.(36a) in IIIb describes the linear system of 10 equations and unknowns which are solved. These very long expressions are translated into FORTRAN and written into a file for further processing (graphics, parametric study) using conventional fortran code. In this example where results are so lengthy, the availability of an analytical solution offers marginal improvement over a numerical matrix inversion.

Spring supported bellows model

The numerical part of this problem is reduced to finding the six unknowns A, B, Mc1, Mc2, F1, F2 using the six boundary conditions eqs.43, 44, 46a to 46d.

Results are now of manageable size and can lend themselves to analytical investigation in addition to the usual procedure of translation into FORTRAN. The list of boundary conditions and eq.47 appear in Fig. e4, function sol() solves the system, function pfor() opens a file in which it writes the appropriate FORTRAN statements. pfor() also rearranges the determinant of the system to produce the expression already seen in Fig. e1. In the section on Numerical Results it was shown how this determinant was solved for k1 and k_{t1} and how this allowed us to predict critical loads. In this respect MACSYMA was critical to the comprehension of the problem.

Bellows interactions in magnet systems

The numerical part of the problem in chapter VI is reduced to solving a system of 51 equations (eqs.58 to 63) and 51 unknowns which is written using matrix notation as: $X[Q]=W$. Inverting analytically the matrix with MACSYMA was not attempted due to its size, instead MACSYMA was used to find the coefficients of [Q] which is almost impossible

to do by hand due to the massive amount of algebra involved. Given the list of 51 unknowns and 51 equations, MACSYMA gathers all the coefficients of the unknowns and collects the terms forming W. The result is translated into fortran and electronically transferred to a numerical computer code where the matrix inversion is performed numerically. A discussion of the code is included in the appendix.

Magnet lateral spring constant

The lateral spring stiffness of one magnet is obtained by slightly modifying the code for the previous problem since deflection, boundary conditions and equilibrium equations are the same. Equations describing the first magnet only are kept: the number of supports is reduced from 19 to 6 and functions describing bellows are omitted. A force or moment is applied at the end of the magnet and the corresponding deflection or slope is computed, thus giving lateral stiffness and torsional stiffnesses. This last example shows how the same MACSYMA code can be adapted to two different problems with similar equations. One of the drawbacks of MACSYMA is that results are presented in a form which is often not the most concise. A considerable amount of effort must be exerted to reduce expressions to their most advantageous representation.

REFERENCES

Existing work on stability of internally pressurized bellows

The most recent reference, ref. [3], contains an extensive historical review and discussion of work related to internally pressurized bellows. It investigates the stability of a cantilevered bellows with a movable end which is permitted only to rotate about a fixed point on the longitudinal axis of the beam. This case is not applicable to the present problem.

The other two references, [4], [5] show that buckling can occur in internally pressurized bellows at a relatively low pressure even when the ends are clamped rather than simply supported. The bellows stiffness is computed based on corrugations of rectangular shape.

Roark [7] contains additional references than [3--5] and a discussion of internally pressurized bellows.

References

[1] S. Timoshenko and J. Gere, Theory of Elastic Stability, Mc Graw--Hill, 2nd edition, p.143

[2] S. Timoshenko and J. Gere, Theory of Elastic Stability, Mc Graw--Hill, 2nd edition, p.279

[3] P. Seide, "The effect of Pressure on the Bending Characteristics of an Actuator System, Journal of Applied Mechanics," Sept. 1960, pp429--437.

[4] J.A. Haringx, "Instability of Thin Walled Cylinders Subjected to Internal Pressure," Philips Research Reports, vol. 7,1952, pp.112--118.

[5] J.A. Haringx, "Instability of Bellows Subjected to Internal Pressure", Philips Research Reports, vol. 7, 1952, pp.189--196.

[6] W. Press, B. Flannery, S. Teukolsky, W. Vetterling, Numerical Recipes, Cambridge University Press.

[7] W. Young, "Roark's Formulas for Stress and Strain", 6th ed., MacGraw--Hill, 1989.

[8] A. Laupa and N.A. Weil, "Analysis of U-shaped Expansion Joints", Journal of Applied Mechanics, March 1962, p.112.

Spring-supported Bellows model:max elong vs pres

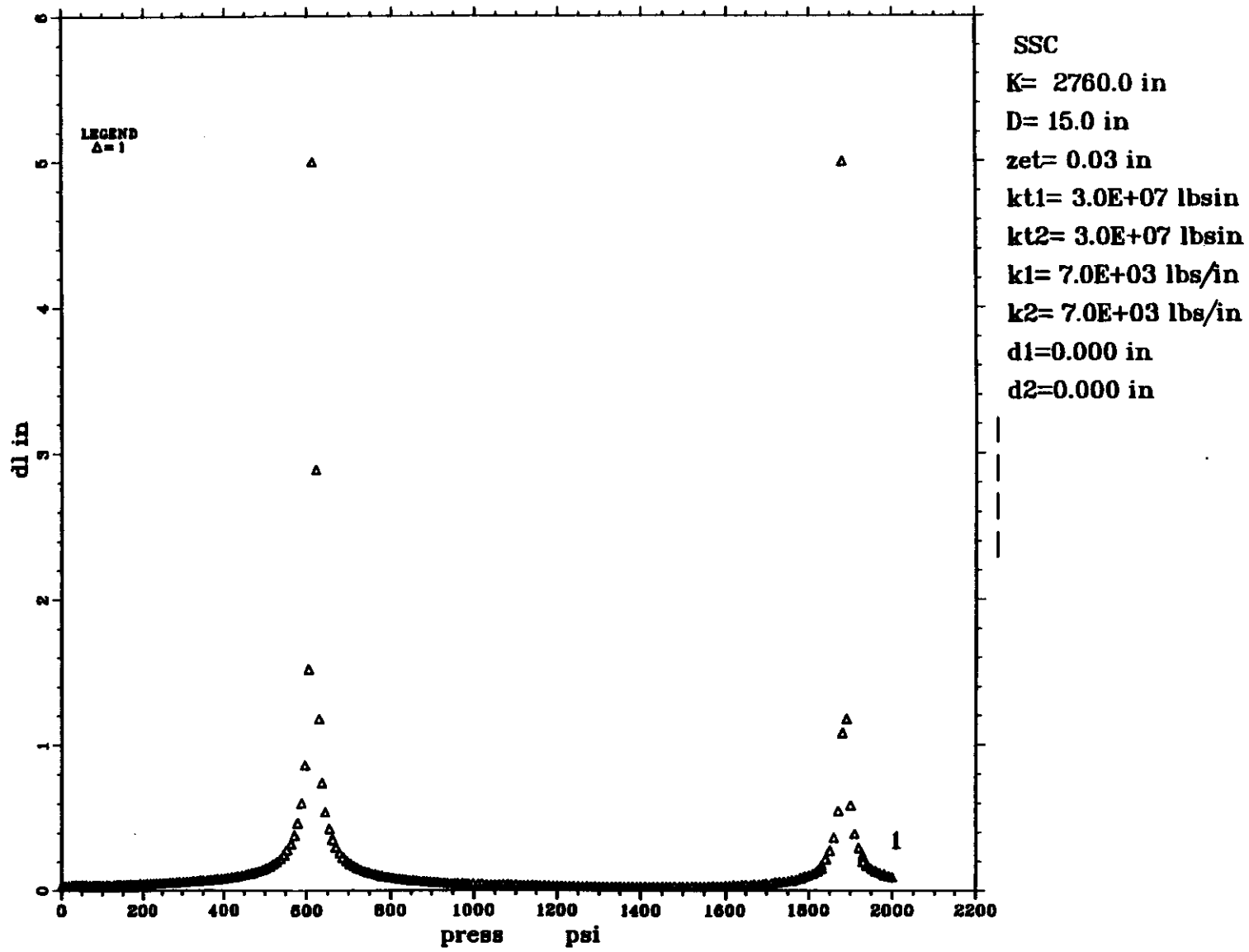

2DUA7:<ROSSUM.BUC>FOR001.DAT;81

FIGURE B1

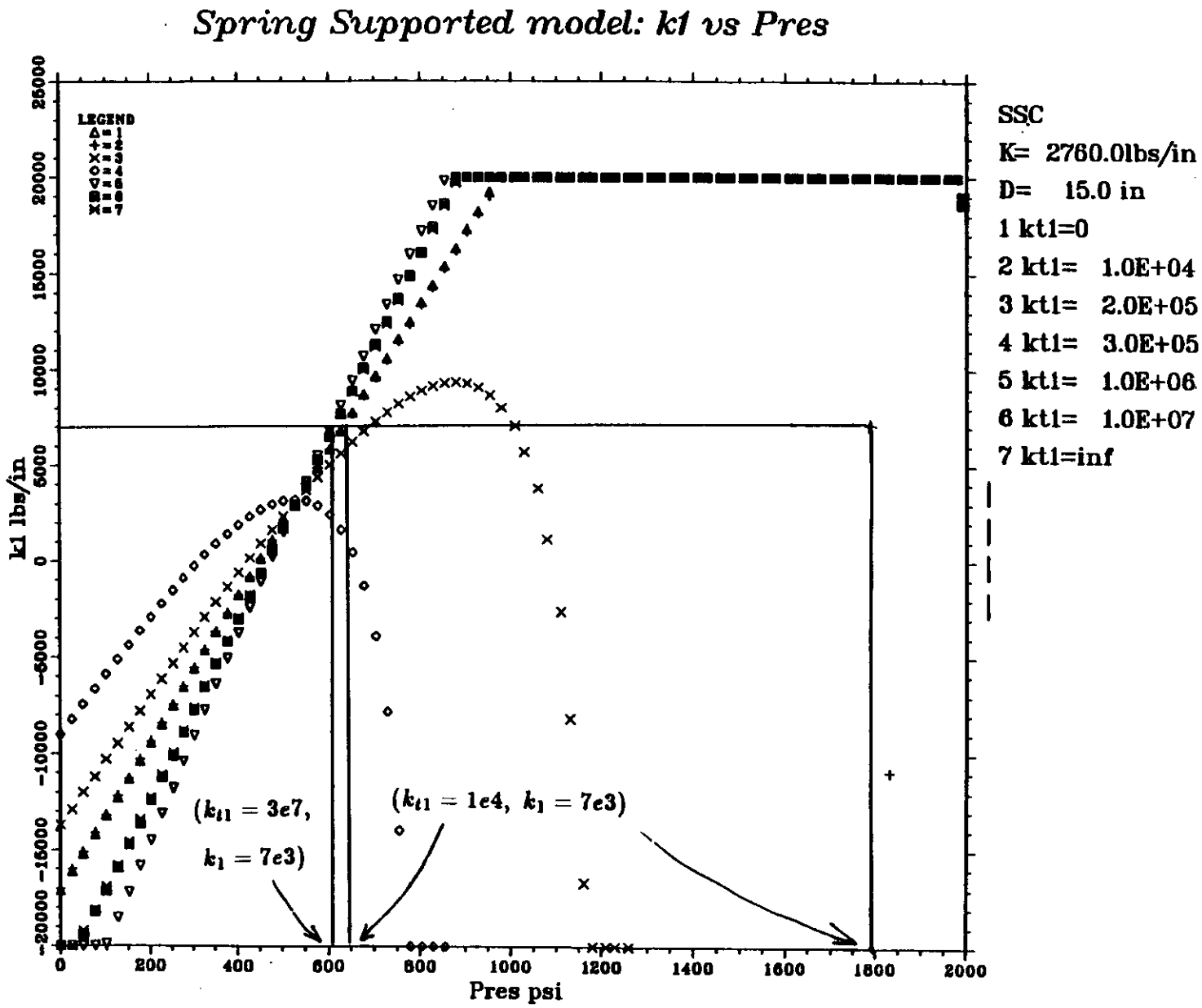

2DUA7:<ROSSUM.BUC>FOR001.DAT;77

FIGURE B2

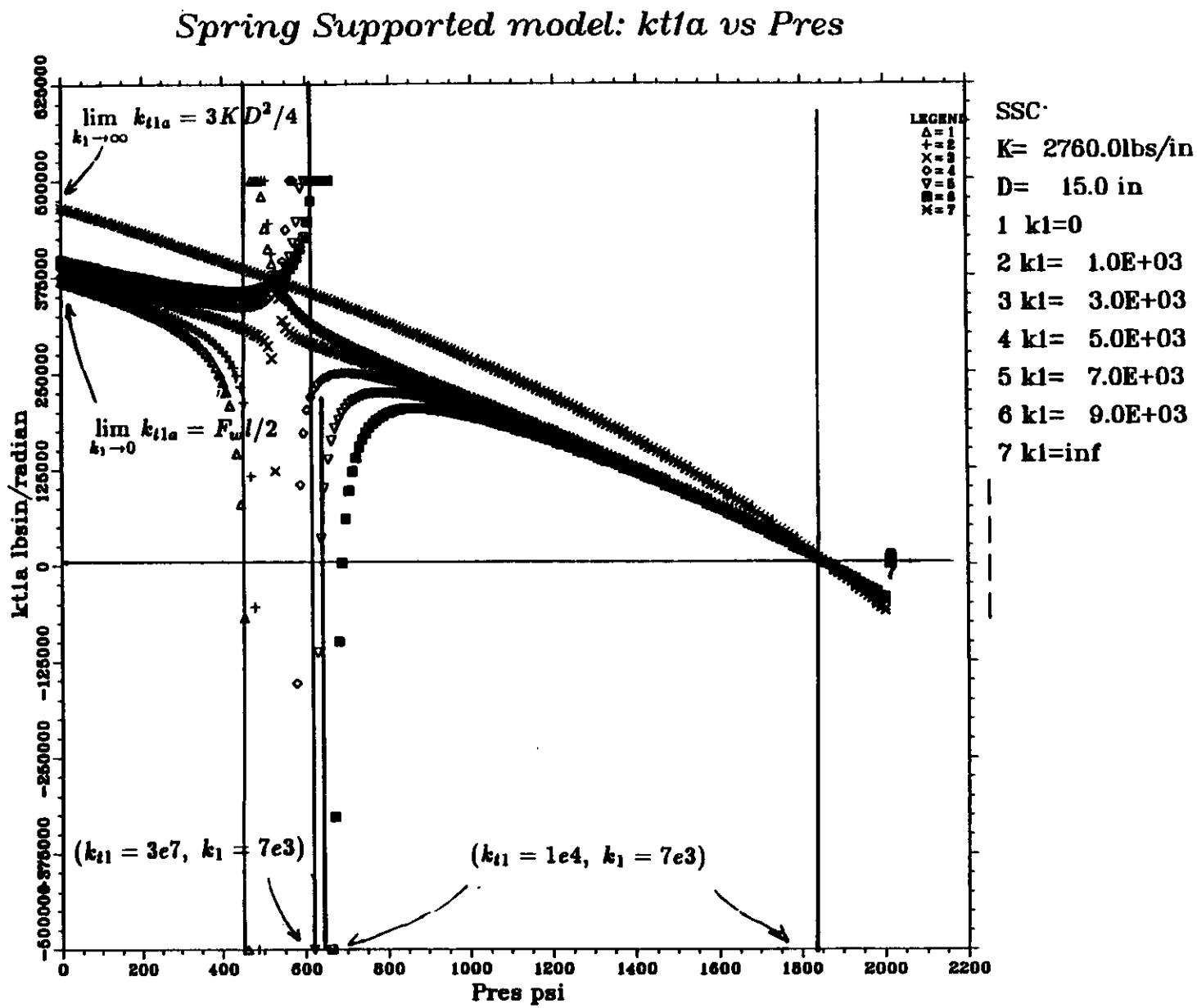

2DUA7:<ROSSUM.BUC>FOR001.DAT;152 FIGURE B3

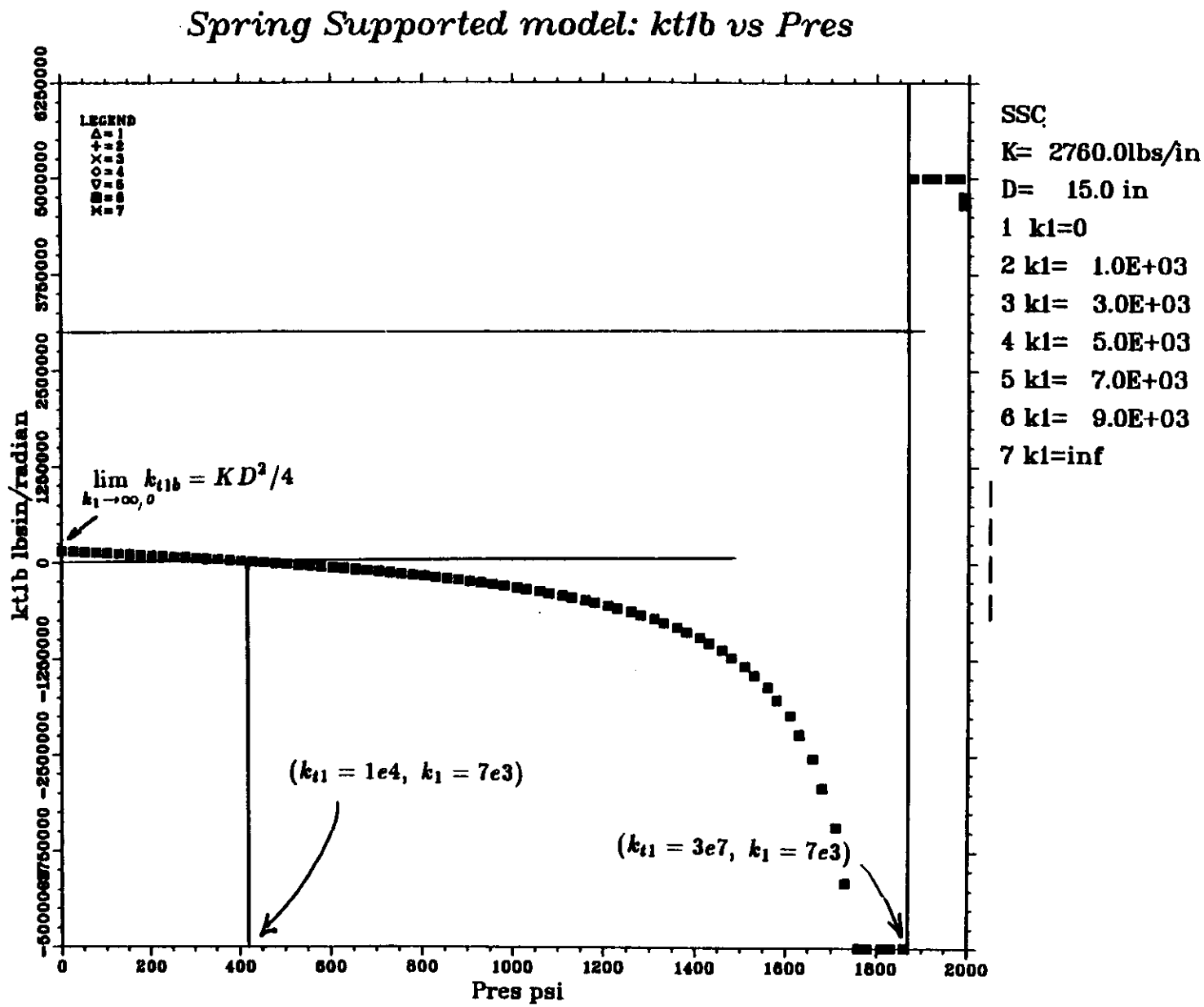

2DUA7:<ROSSUM.BUC>FOR001.DAT;77

FIGURE B4

Spring–supported Bellows model:max elong vs pres

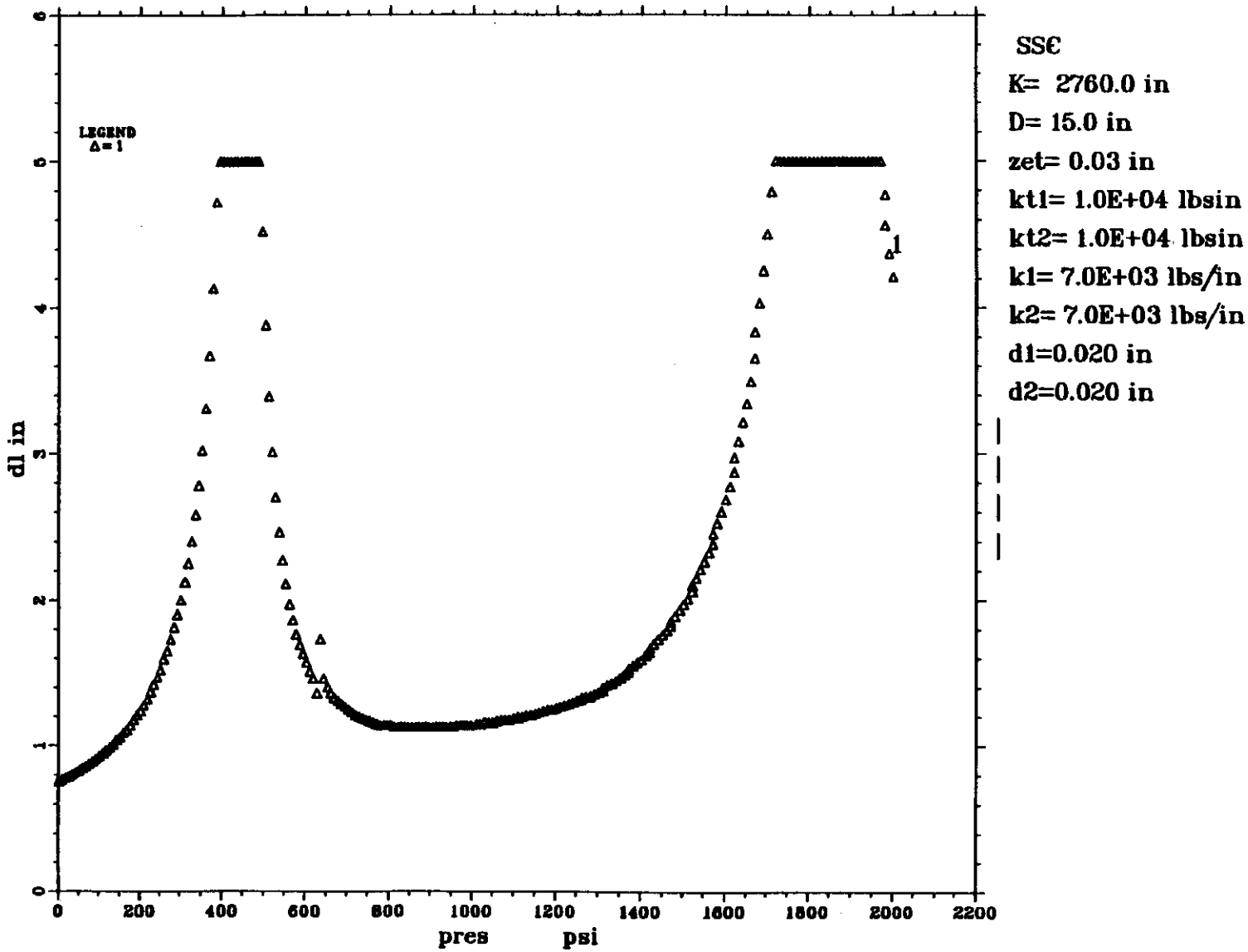

2DUA7:<ROSSUM.BUC>FOR001.DAT;75 FIGURE B5

Spring-supported Bellows model:max elong vs pres

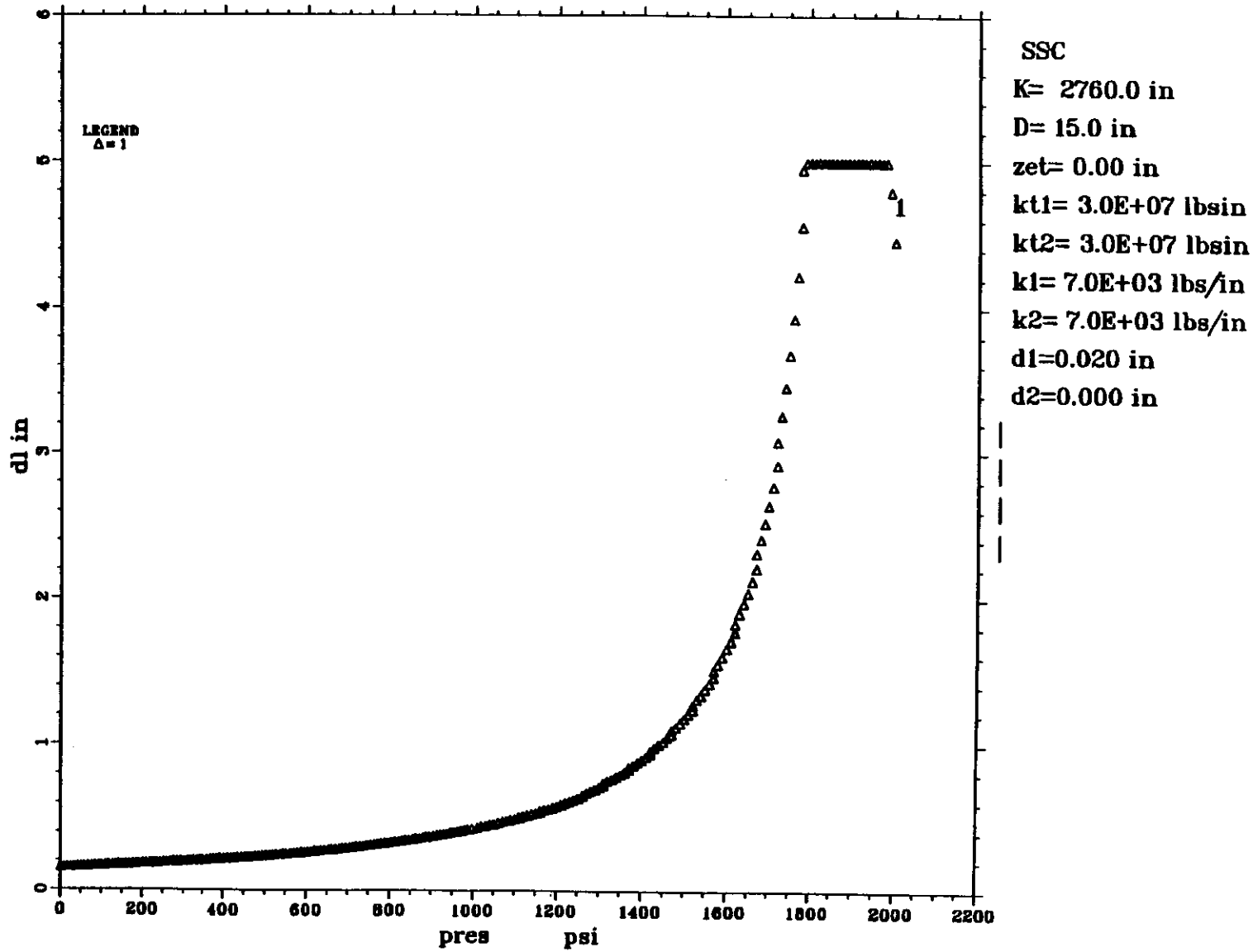

2DUA7:<ROSSUM.BUC>FOR001.DAT;85 FIGURE B6

Spring-supported Bellows model:max elong vs pres

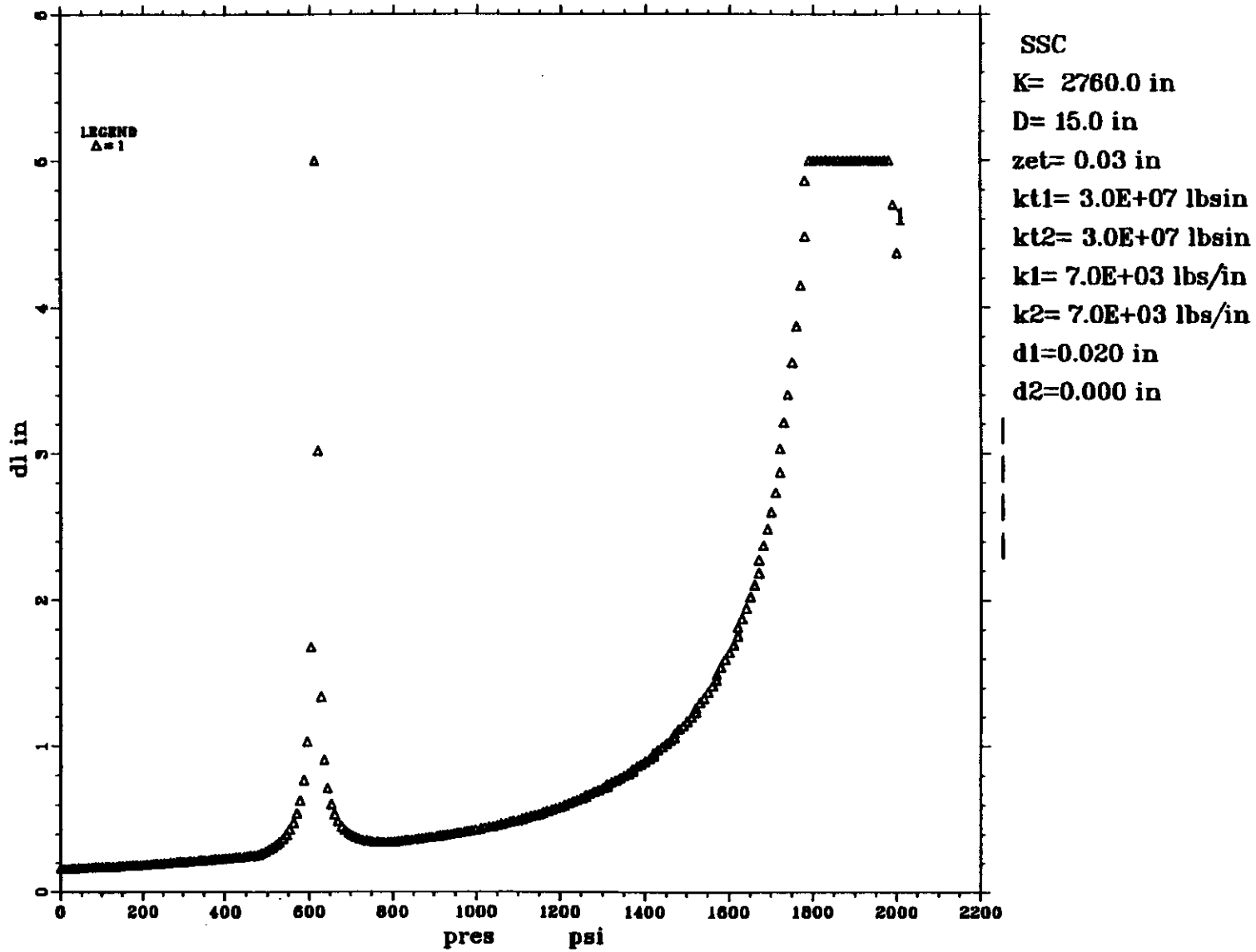

2DUA7:<ROSSUM.BUC>FOR001.DAT;83 FIGURE B7

Spring-supported Bellows model:max elong vs pres

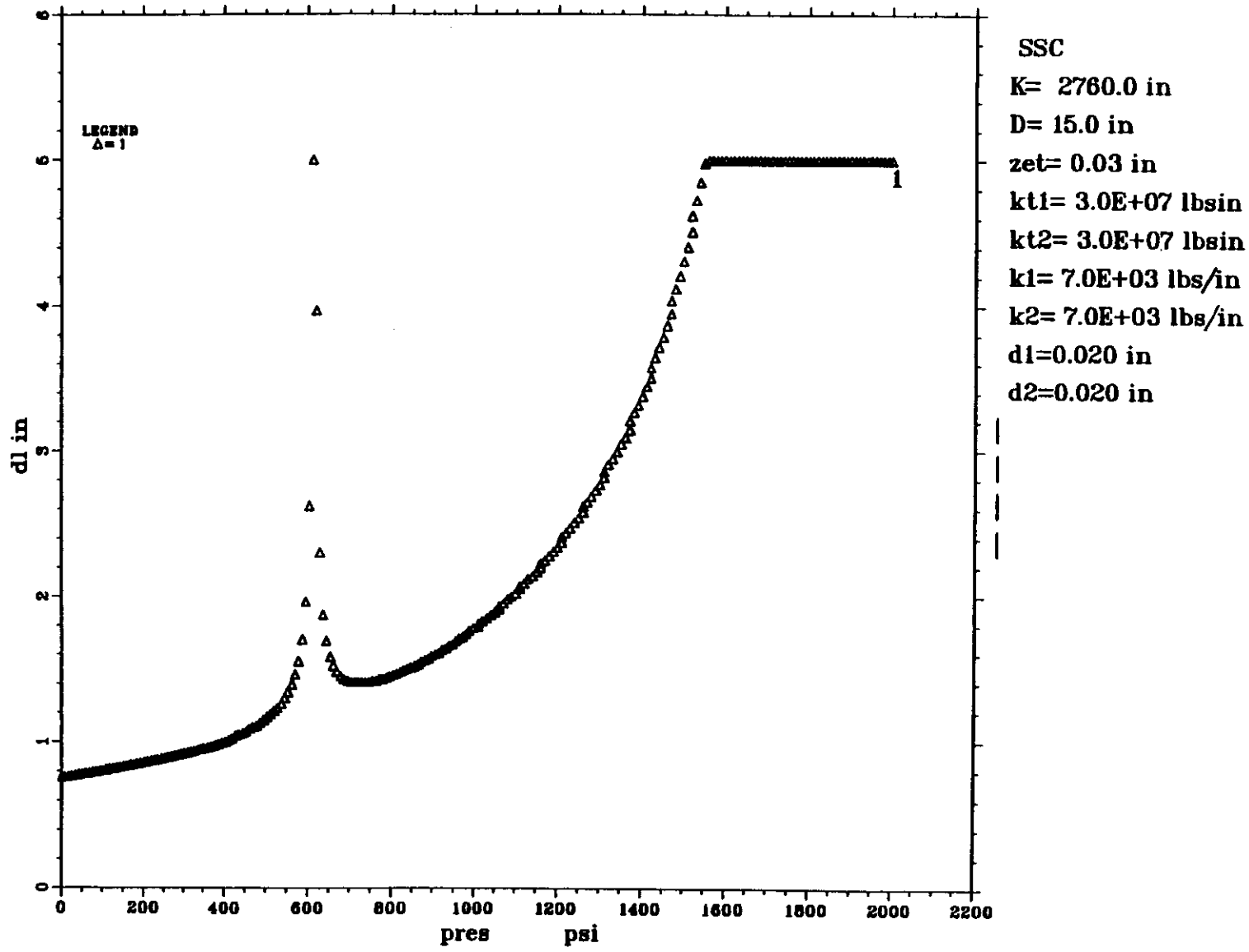

2DUA7:<ROSSUM.BUC>FOR001.DAT;87

FIGURE B8

Spring–supported Bellows model:y vs x at 300 psi

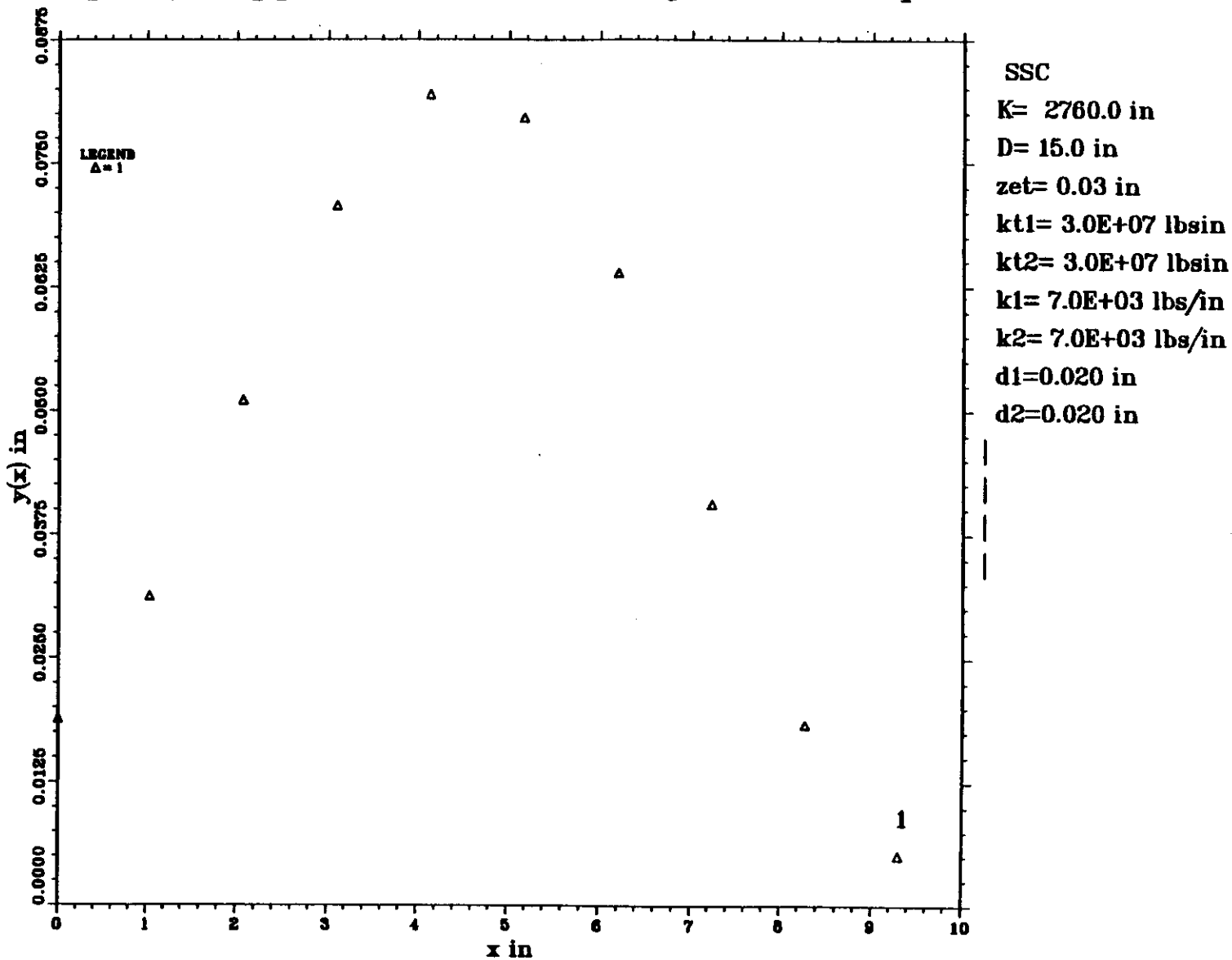

2DUA7:<ROSSUM.BUC>FOR001.DAT;87

FIGURE B9

Spring-supported Bellows model:max elong vs pres

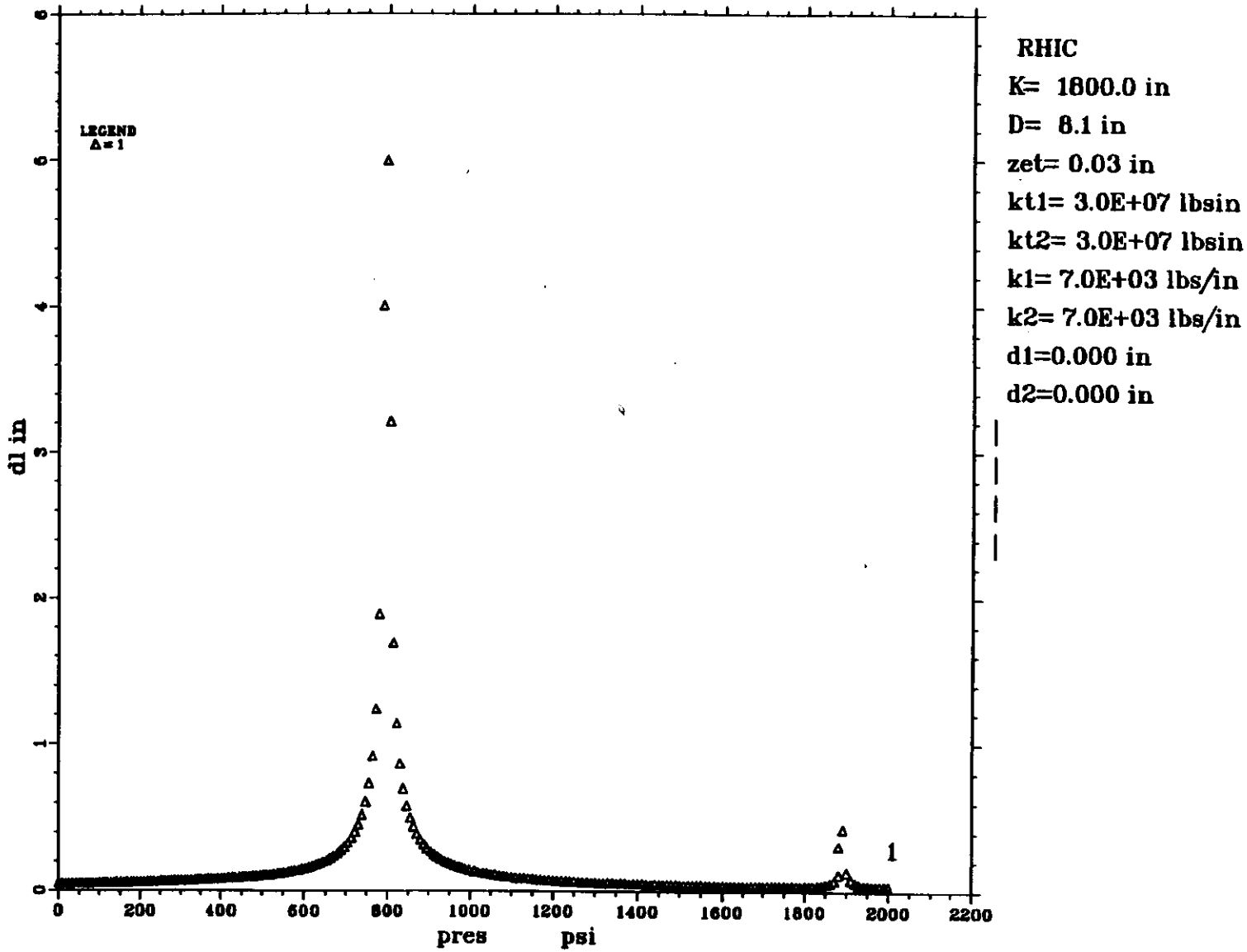

2DUA7:<ROSSUM.BUC>FOR001.DAT;82

FIGURE BR1

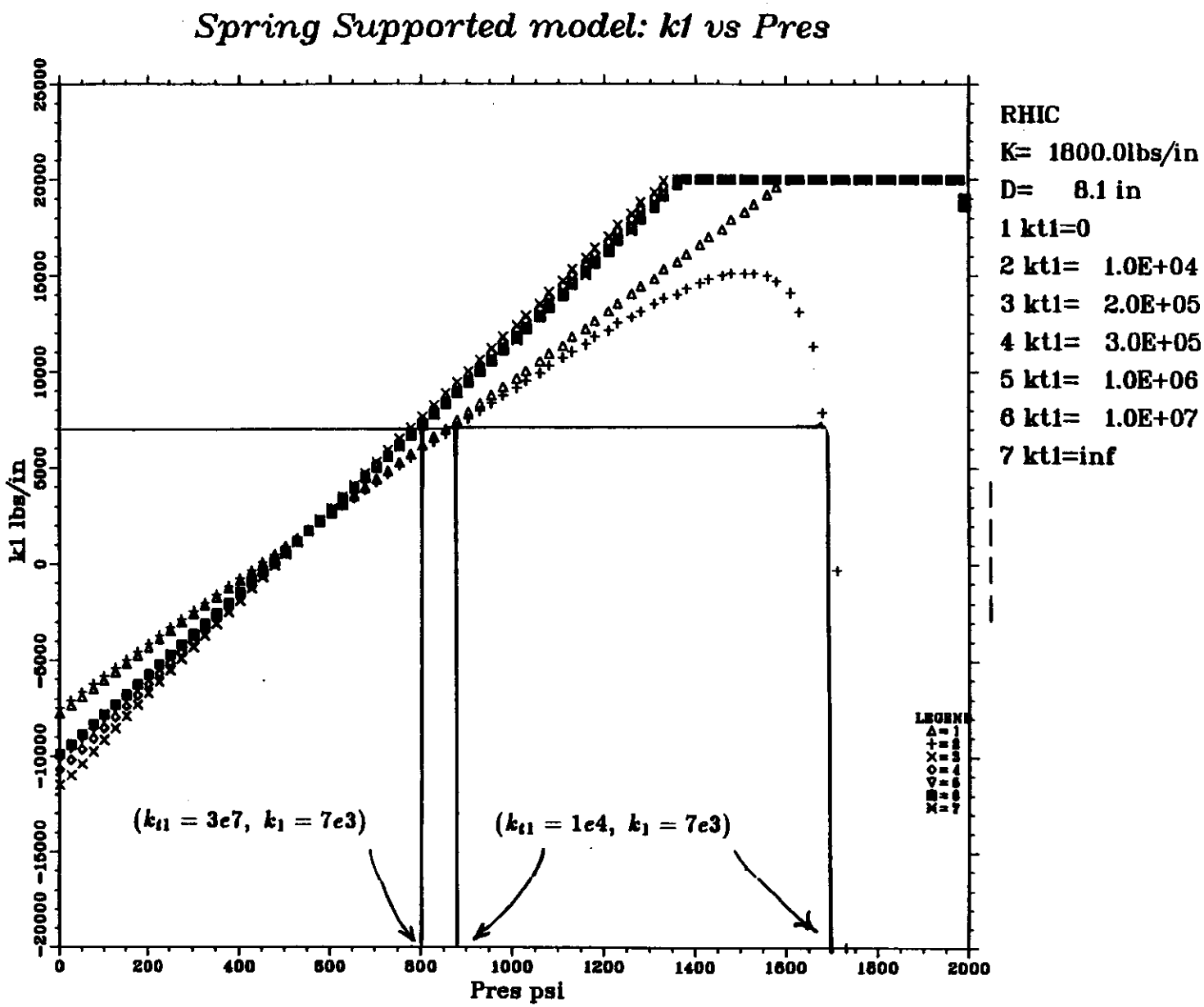

2DUA7:<ROSSUM.BUC>FOR001.DAT;76 FIGURE BR2

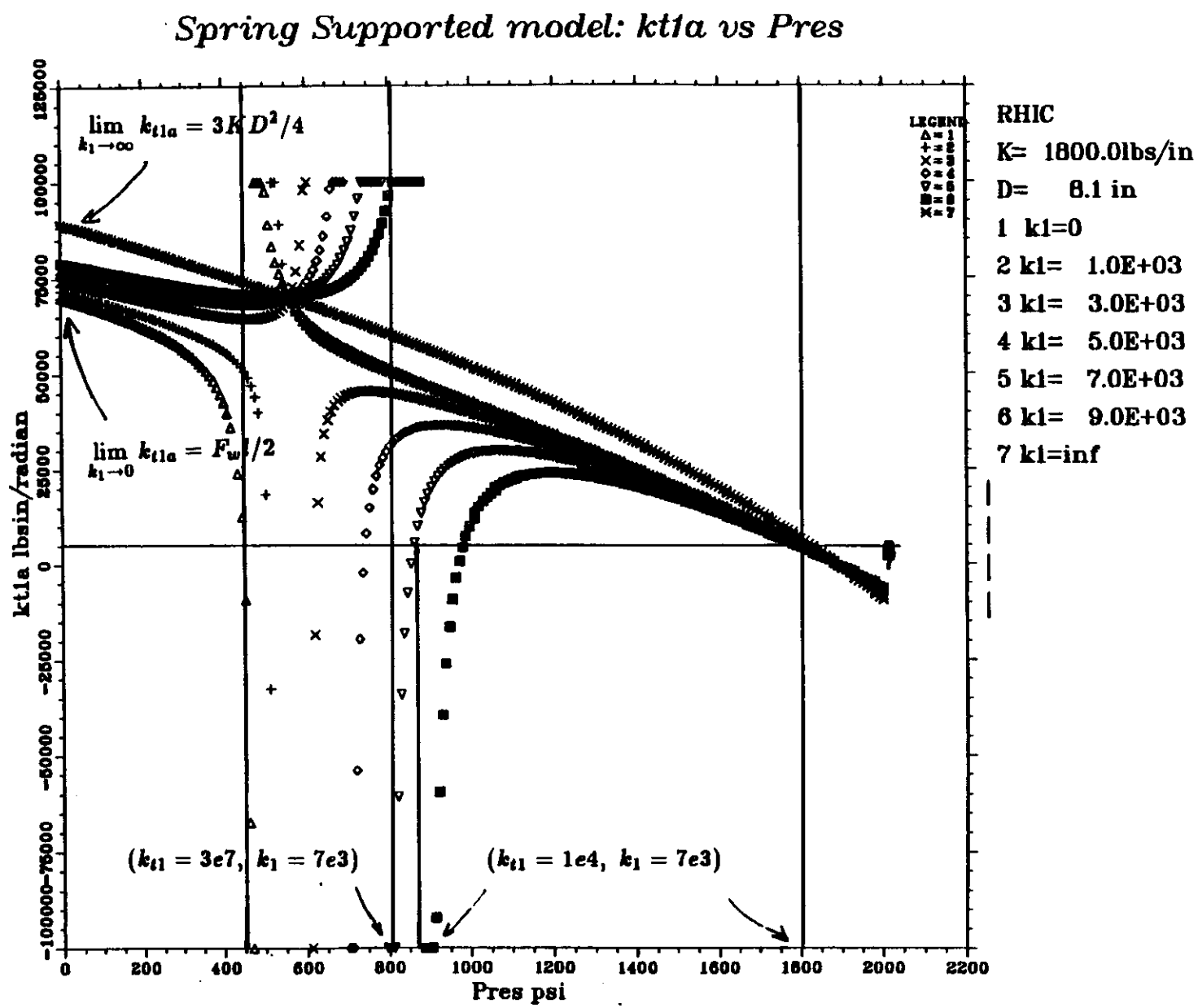

2DUA7:<ROSSUM.BUC>FOR001.DAT;149 FIGURE BR3

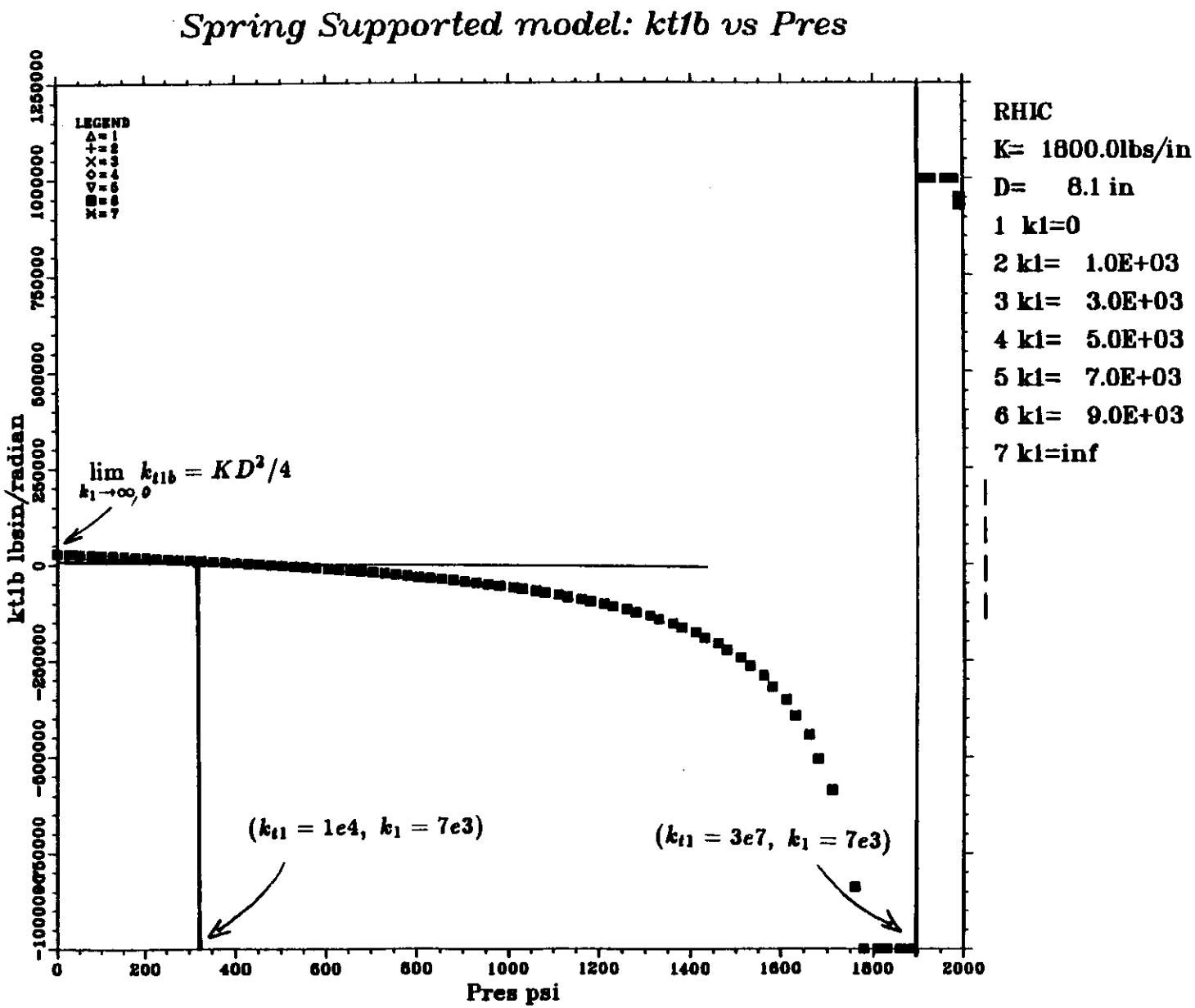

2DUA7:<ROSSUM.BUC>FOR001.DAT;108 FIGURE BR4

Spring-supported Bellows model:max elong vs pres

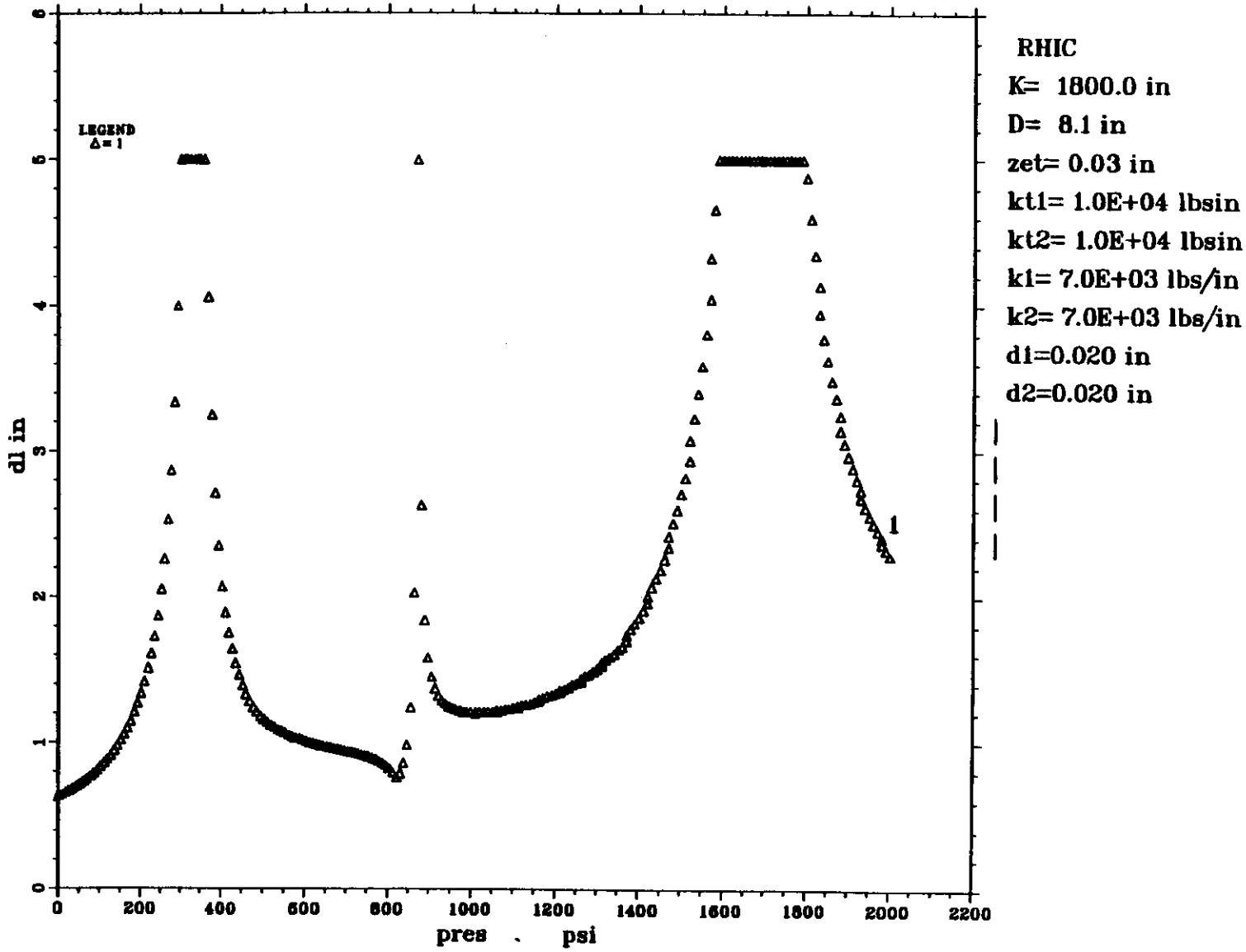

2DUA7:<ROSSUM.BUC>FOR001.DAT;79 FIGURE BR5

Spring–supported Bellows model:max elong vs pres

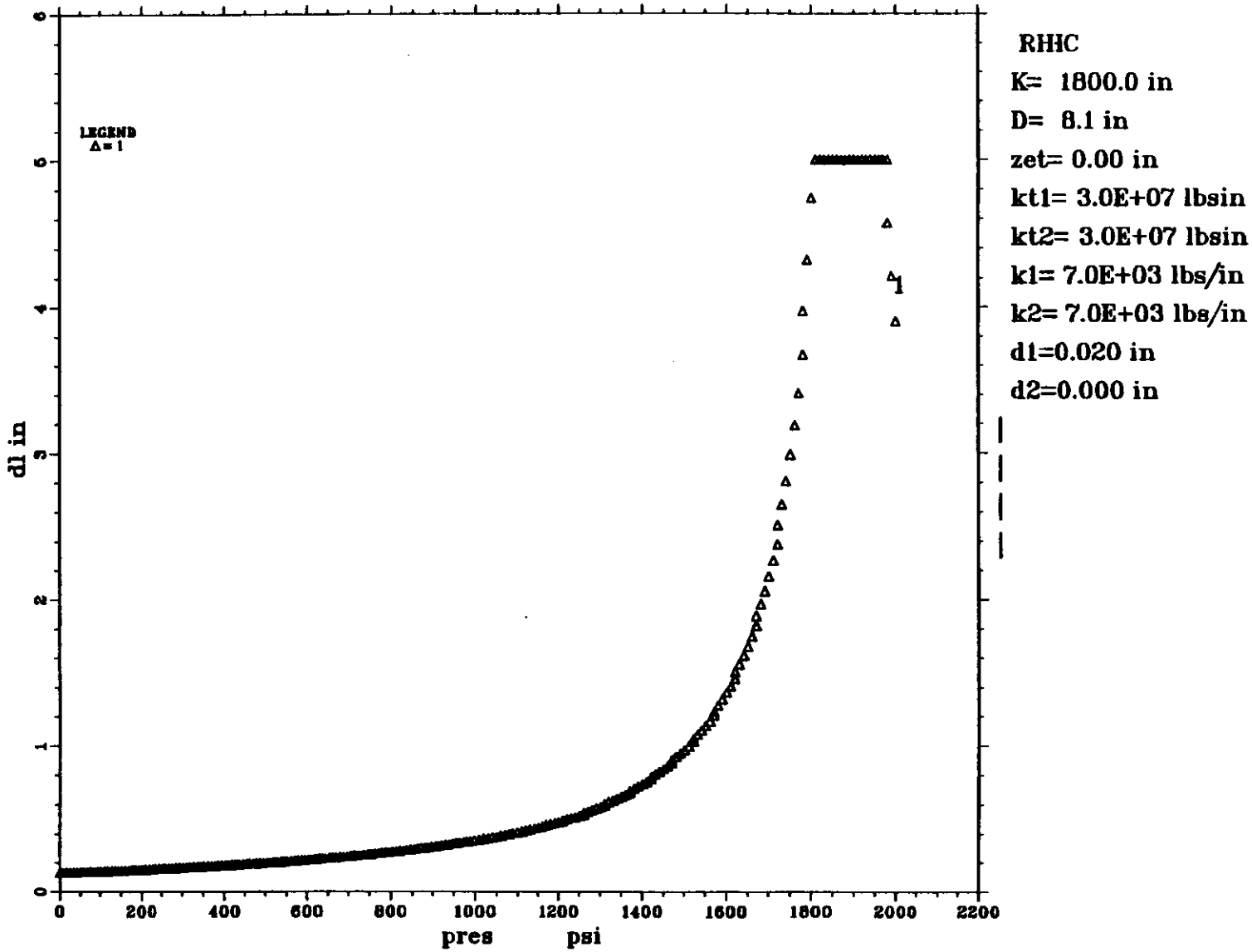

2DUA7:<ROSSUM.BUC>FOR001.DAT;86 FIGURE BR6

Spring-supported Bellows model:max elong vs pres

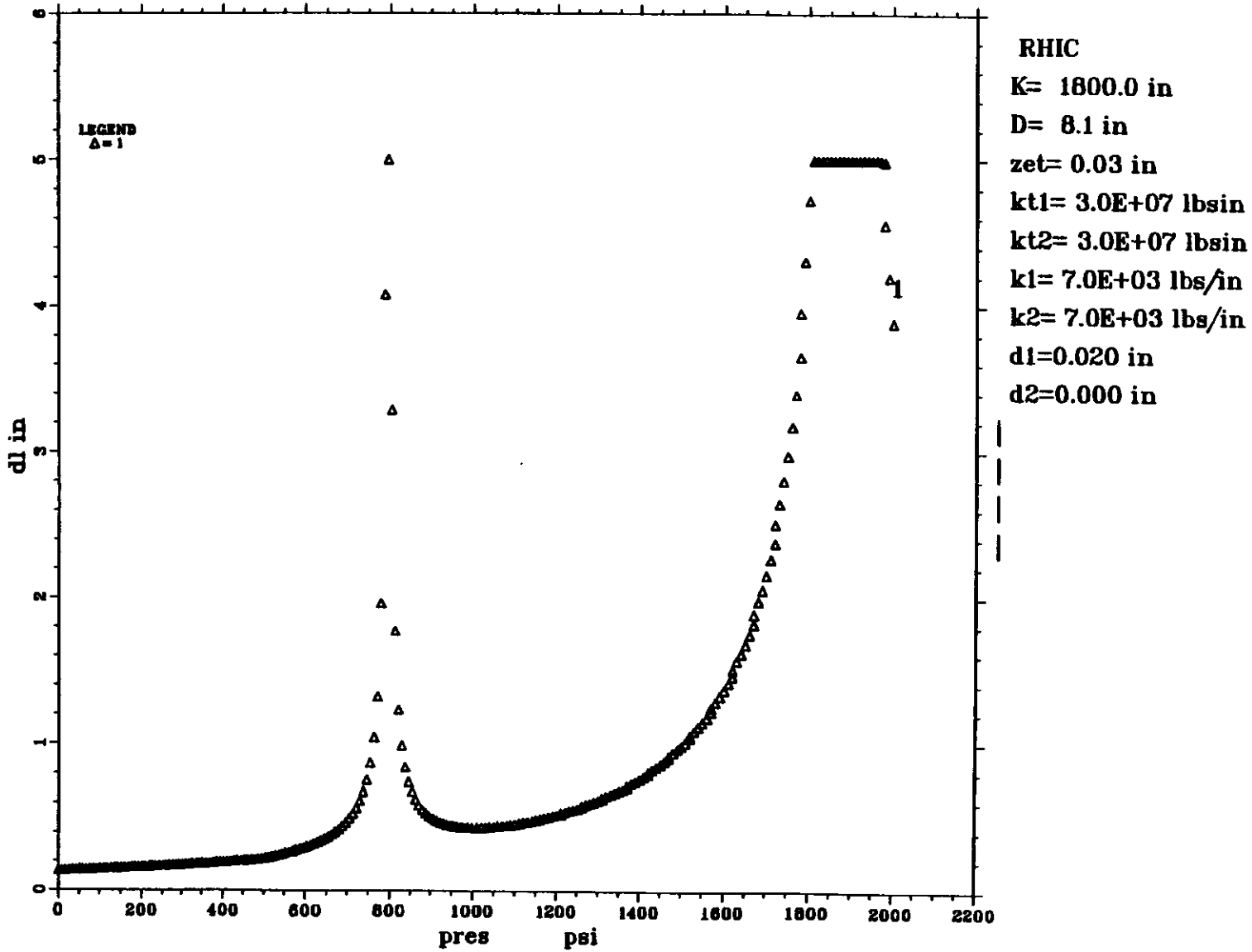

2DUA7:<ROSSUM.BUC>FOR001.DAT;84 FIGURE BR7

Spring–supported Bellows model:max elong vs pres

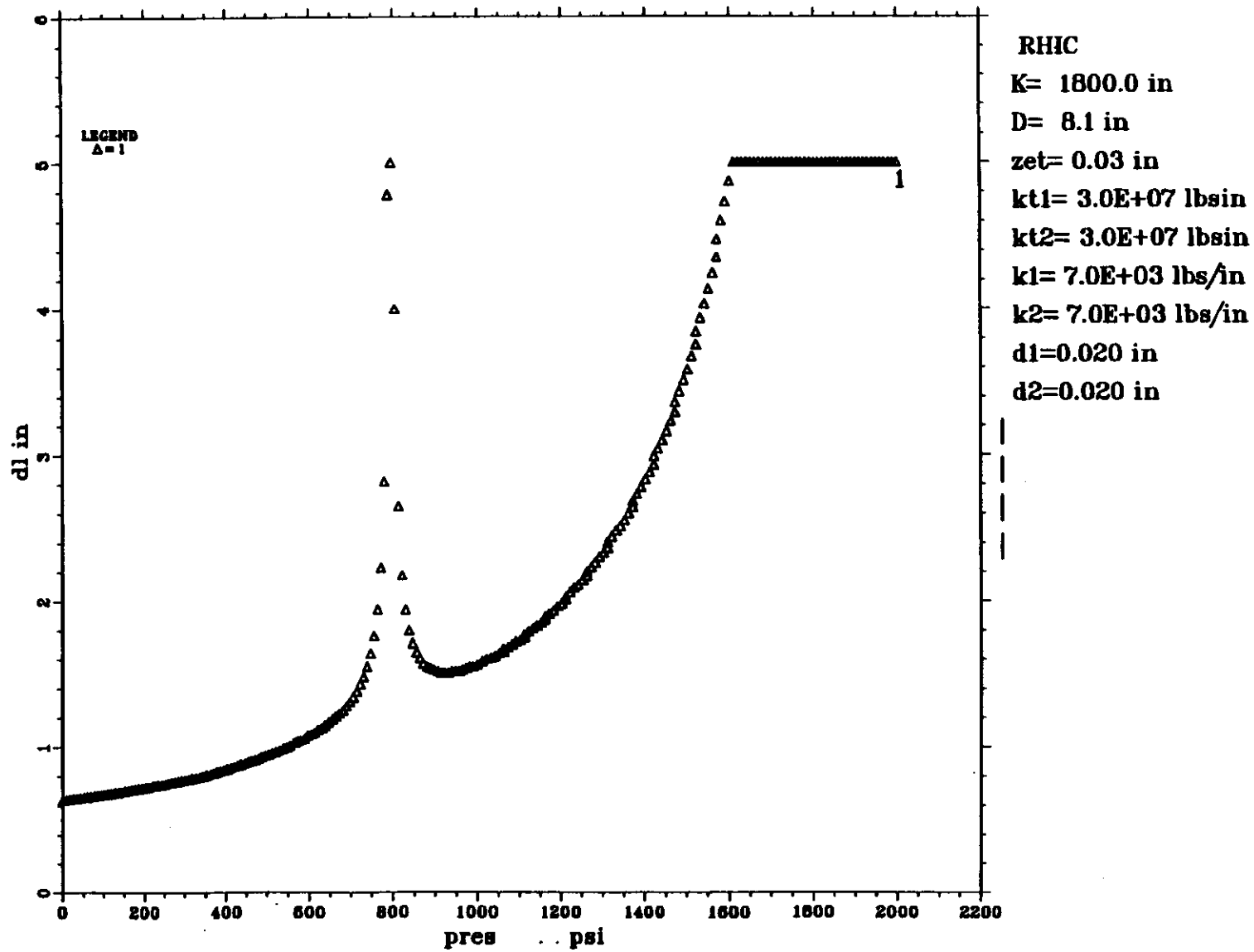

2DUA7:<ROSSUM.BUC>FOR001.DAT;66

FIGURE BR8

Spring-supported Bellows model:y vs x at 300 psi

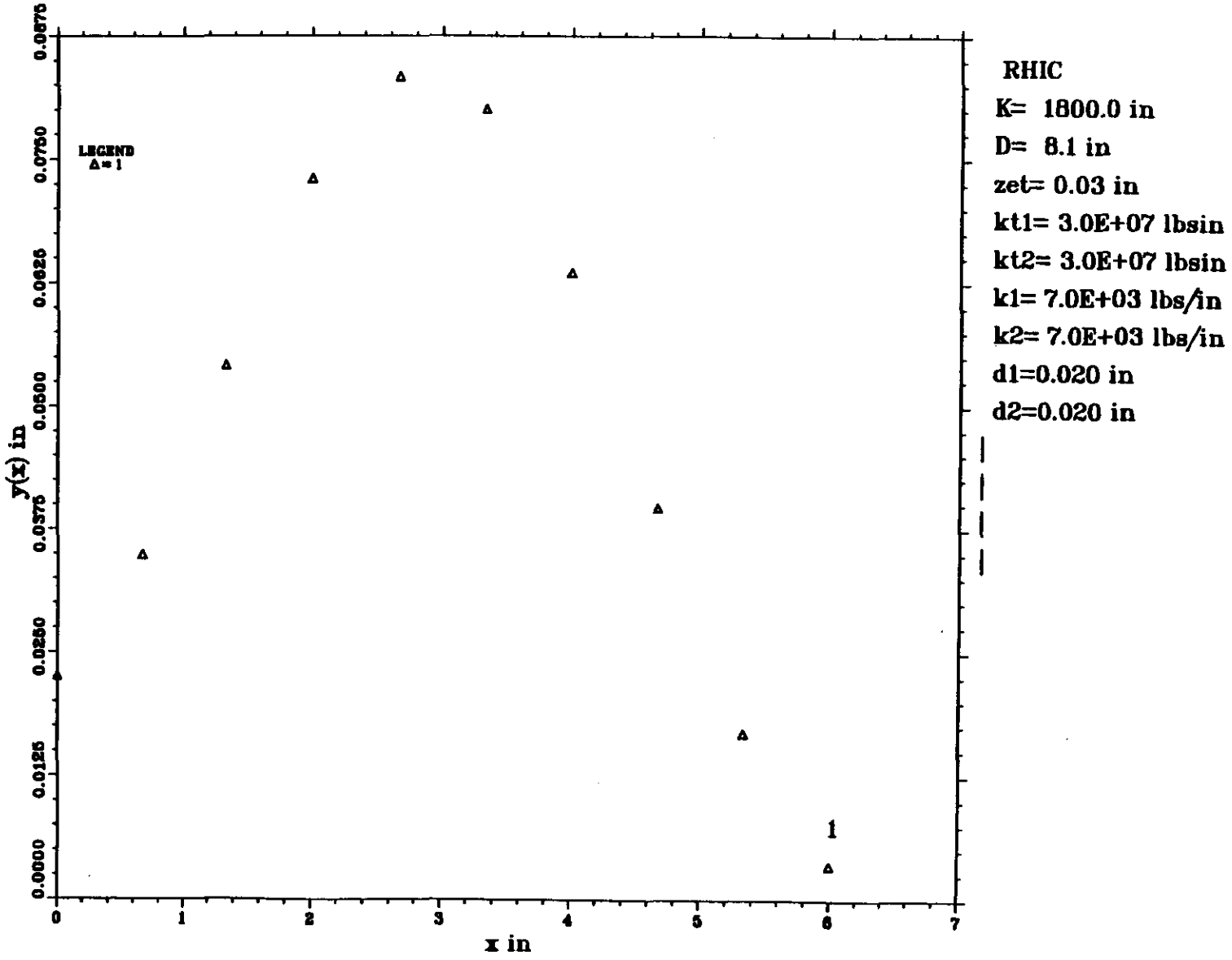

2DUA7:<ROSSUM.BUC>FOR001.DAT;88 FIGURE BR9

Spring-supported Bellows model:max elong vs pres

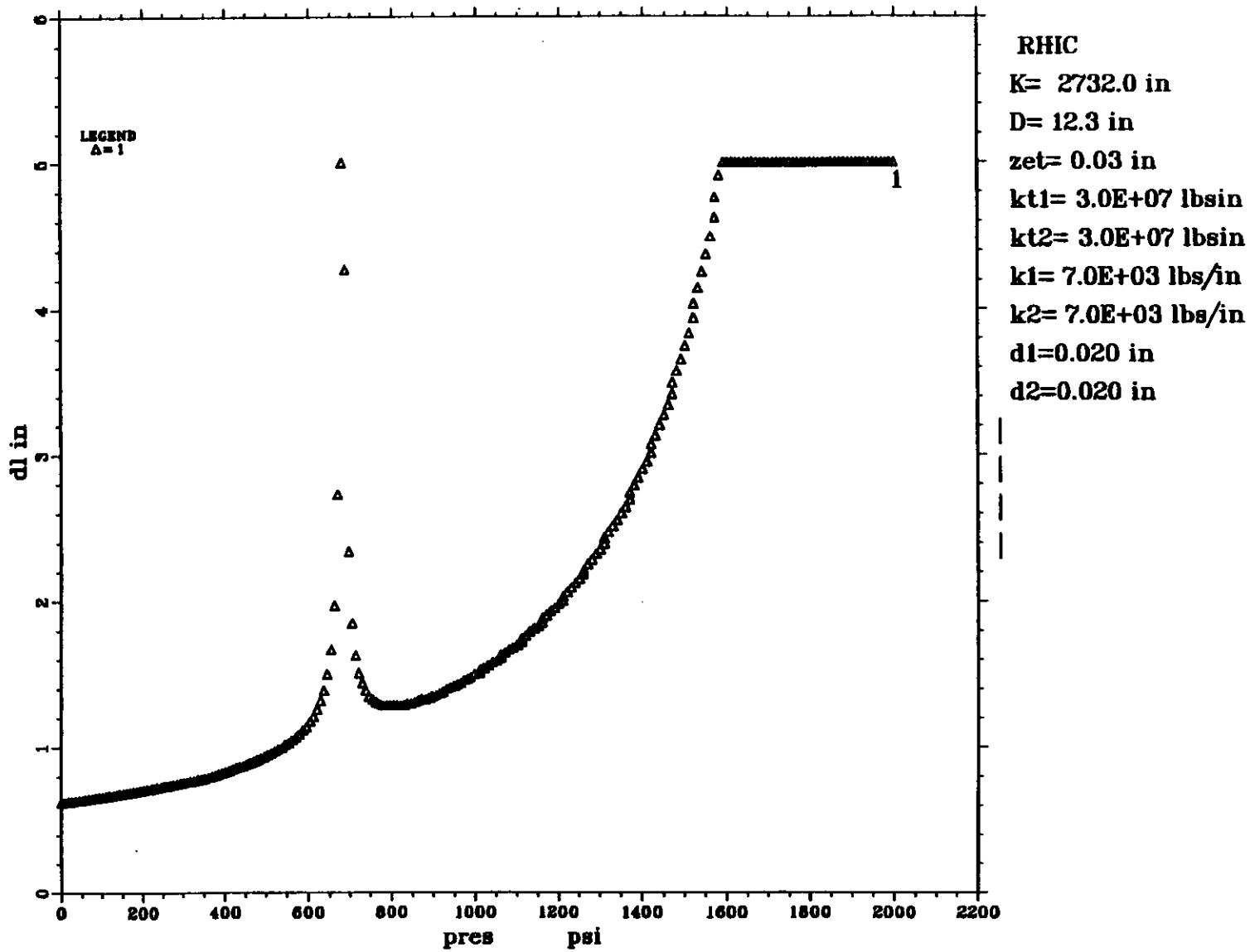

2DUA7:<ROSSUM.BUC>FOR001.DAT;69 FIGURE BR10

MAX BELLOWS LOCAL ELONGATION

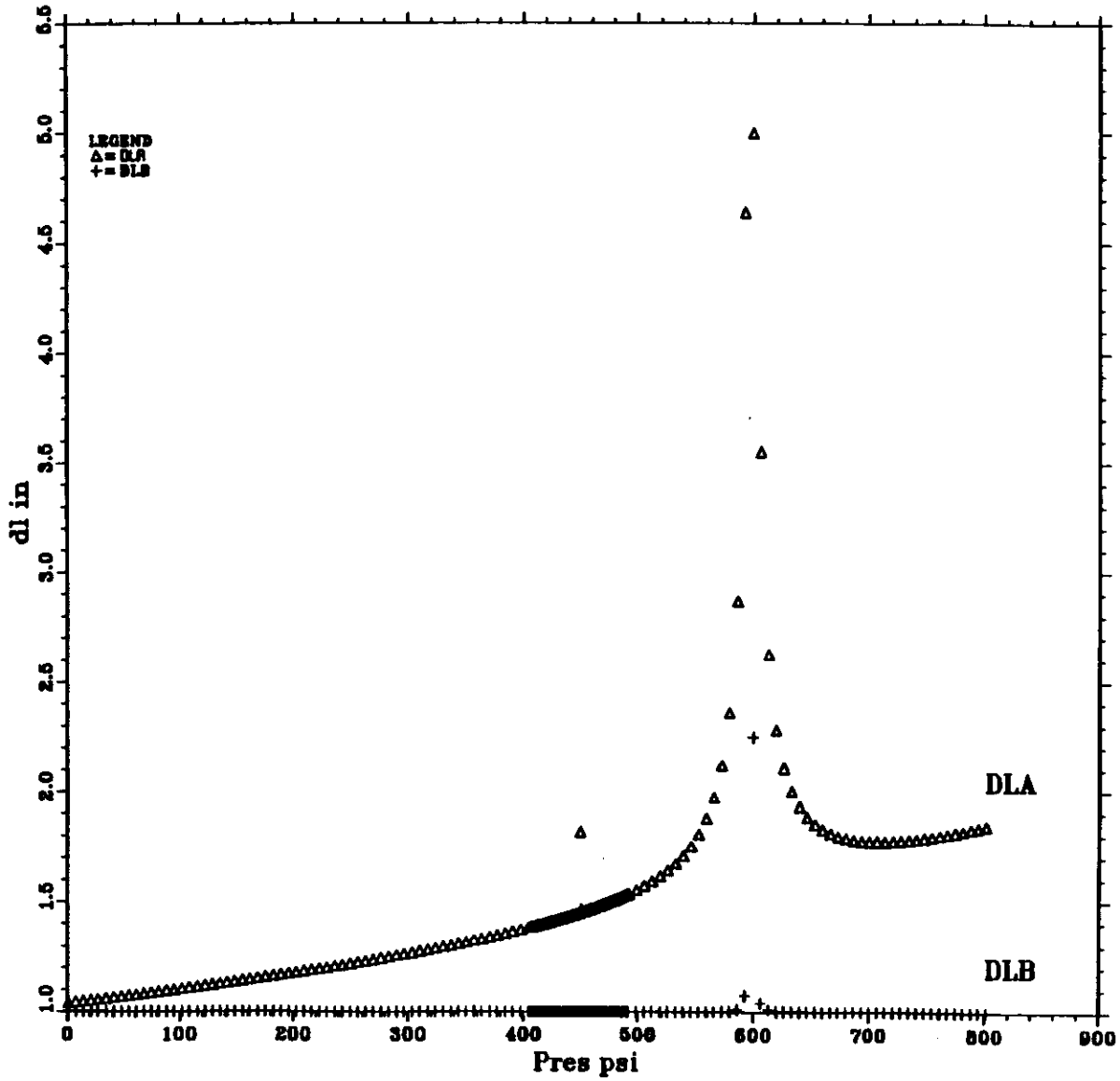

SSC ddd
zet6=0.030 in
zet7=0.000 in
zet13=0.000 in
zet14=0.000 in
et6=0.000 in
et7=0.000 in
et13=0.000 in
et14=0.000 in
ds6=0.020 in
ds13=0.000 in
f(6)= 0.0 lbs
f(13)= 0.0 lbs
K= 2759.2 lbs/in

FIGURE D1

2DUA7:<ROSSUM.BUC>FOR001.DAT;90

plot file: 2DUA7:[ROSSUM.BUC]FOR001.DAT;90
machine: SSC mode: ddd

Table 1: Input: bellows design parameters

r_i in	D_i in	d in	β	l in	pcr psi	λ in	Eb psi
0.060	14.300	0.500	0.094	9.300	450.000	1.000	3.297E+07

Table 2: Results: bellows properties

Nb	r in	D in	A in	t in	bc in	K lbs/in	Kl lbs/in	I in^4
26	0.072	14.800	0.356	0.025	0.342	2759.212	1.048E+04	3.151E+01

Table 3: Results: maximum bellows stresses at p_{op}

σ_{max} psi	σ_h psi	σ_{pu1} psi	σ_{pu2} psi	σ_{pe}	y_{max} in
1.523E+05	2.778E+04	6.640E+04	6.782E+04	2.967E+04	1.472E-03

Table 4: Input: bellows misalignments

$\zeta(6)$ in	$\zeta(7)$ in	$\zeta(13)$ in	$\zeta(14)$ in	$\eta(6)$	$\eta(7)$	$\eta(13)$	$\eta(14)$
0.030	0.000	0.000	0.000	0.000	0.000	0.000	0.000

Table 5: Input: bellows initial shape

d_s6 in	d_s13 in	d_e6 in	d_e13 in
0.020	0.000	0.020	0.000

Table 6: Input: dipole properties

s in	L_D in	ovh_D in	D_m in	t_m in	Im in^4	Em psi
0.200	670.	63.6	10.5	0.188	111.	3.000E+07

Table 7: Input: quadrupole properties

L_q in	ovh_Q in	D_q in	t_q in	Iq in^4	Eq psi
210.	52.5	10.5	0.188	111.	3.000E+07

Table 8: Results: bellows maximum elongation at p_{op}

p_{op} psi	dl6 in	dl13 in
3.000E+02	1.262E+00	1.000E+00

FIGURE D1A

Table 9: Results: node location, stiffness, force at p_{op}

node	x(i) in	k(i) lbs/in	F(i) lbs
1	0.00	25000.00	87.54
2	135.69	25000.00	35.69
3	271.38	25000.00	24.72
4	407.07	25000.00	17.59
5	542.76	25000.00	-12.71
6	606.38	0.00	0.00
7	615.68	0.00	0.00
8	679.30	25000.00	115.28
9	814.99	25000.00	-13.68
10	950.68	25000.00	18.37
11	1086.37	25000.00	26.95
12	1222.06	25000.00	27.80
13	1285.68	0.00	0.00
14	1294.98	0.00	0.00
15	1358.60	25000.00	27.45
16	1494.29	25000.00	24.13
17	1629.98	25000.00	22.63
18	1765.67	25000.00	35.16
19	1901.36	25000.00	87.70

FIGURE D1B

MAX BELLOWS LOCAL ELONGATION

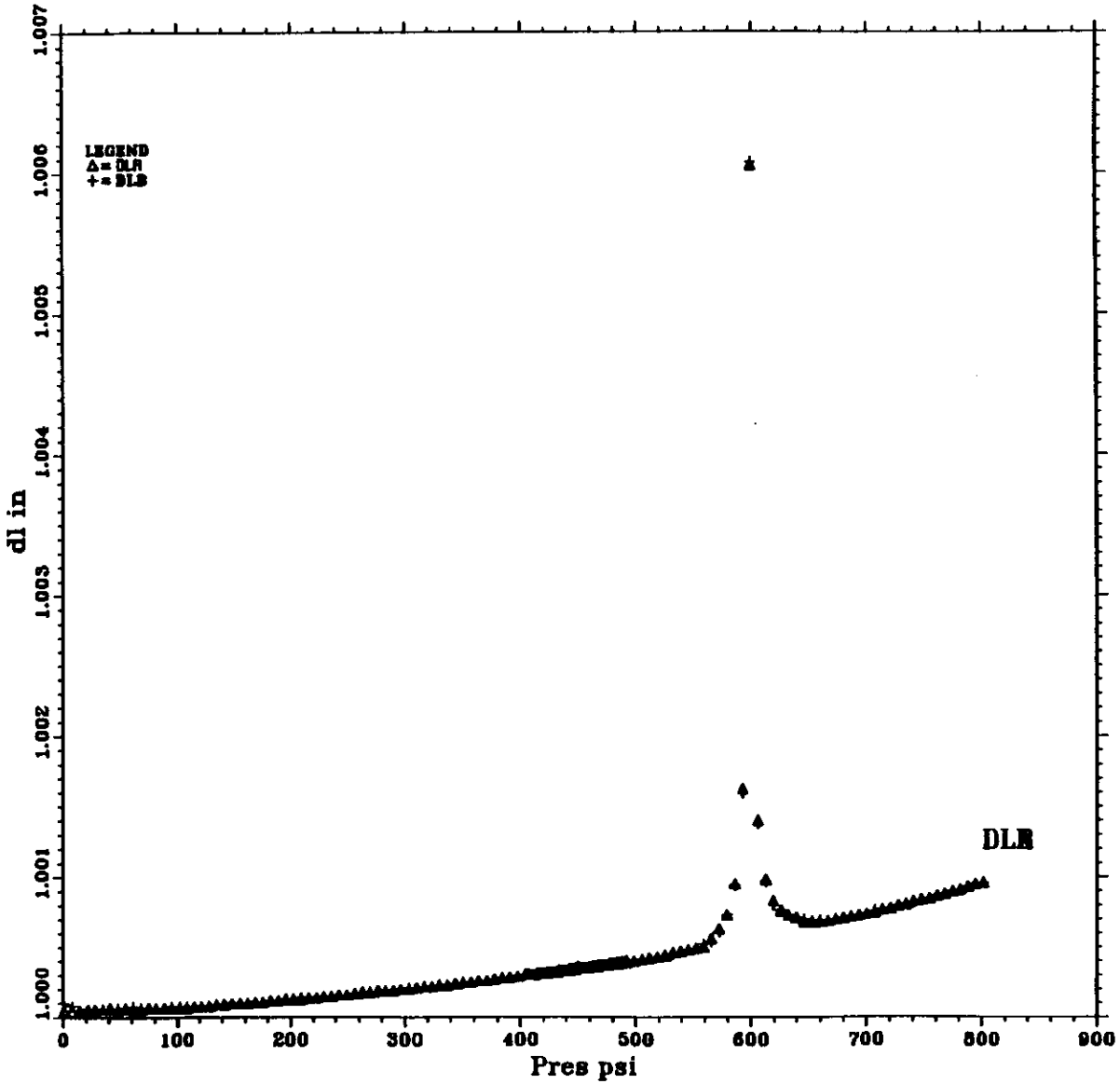

SSC ddd
zet6=0.000 in
zet7=0.000 in
zet13=0.000 in
zet14=0.000 in
et6=0.000 in
et7=0.000 in
et13=0.000 in
et14=0.000 in
ds6=0.000 in
ds13=0.000 in
f(6)= 0.0 lbs
f(13)= 0.0 lbs
K= 2759.2 lbs/in

2DUA7:<ROSSUM.BUC>FOR001.DAT;92 FIGURE D2

plot file: 2DUA7:[ROSSUM.BUC]FOR001.DAT;92
machine: SSC mode: ddd

Table 1: Input: bellows design parameters

r_i in	D_i in	d in	β	l in	pcr psi	λ in	Eb psi
0.060	14.300	0.500	0.094	9.300	450.000	1.000	3.297E+07

Table 2: Results: bellows properties

Nb	r in	D in	Λ in	t in	bc in	K lbs/in	Kl lbs/in	I in^4
26	0.072	14.800	0.356	0.025	0.342	2759.212	1.048E+04	3.151E+01

Table 3: Results: maximum bellows stresses at p_{op}

σ_{max} psi	σ_h psi	σ_{pw1} psi	σ_{pw2} psi	σ_{ps}	y_{max} in
1.523E+05	2.778E+04	6.640E+04	6.782E+04	2.967E+04	1.472E-03

Table 4: Input: bellows misalignments

$\zeta(6)$ in	$\zeta(7)$ in	$\zeta(13)$ in	$\zeta(14)$ in	$\eta(6)$	$\eta(7)$	$\eta(13)$	$\eta(14)$
0.000	0.000	0.000	0.000	0.000	0.000	0.000	0.000

Table 5: Input: bellows initial shape

d_s6 in	d_s13 in	d_e6 in	d_e13 in
0.000	0.000	0.000	0.000

Table 6: Input: dipole properties

s in	L_D in	ovh_D in	D_m in	t_m in	Im in^4	Em psi
0.200	670.	63.6	10.5	0.188	111.	3.000E+07

Table 7: Input: quadrupole properties

L_q in	ovh_Q in	D_q in	t_q in	Iq in^4	Eq psi
210.	52.5	10.5	0.188	111.	3.000E+07

Table 8: Results: bellows maximum elongation at p_{op}

p_{op} psi	dl6 in	dl13 in
3.000E+02	1.000E+00	1.000E+00

FIGURE D2A

Table 9: Results: node location, stiffness, force at p_{op}

node	x(i) in	k(i) lbs/in	F(i) lbs
1	0.00	25000.00	87.70
2	135.69	25000.00	35.17
3	271.38	25000.00	22.61
4	407.07	25000.00	24.10
5	542.76	25000.00	27.57
6	606.38	0.00	0.00
7	615.68	0.00	0.00
8	679.30	25000.00	27.41
9	814.99	25000.00	24.90
10	950.68	25000.00	25.73
11	1086.37	25000.00	24.89
12	1222.06	25000.00	27.42
13	1285.68	0.00	0.00
14	1294.98	0.00	0.00
15	1358.60	25000.00	27.57
16	1494.29	25000.00	24.10
17	1629.98	25000.00	22.62
18	1765.67	25000.00	35.16
19	1901.36	25000.00	87.70

FIGURE D2B

MAX BELLOWS LOCAL ELONGATION

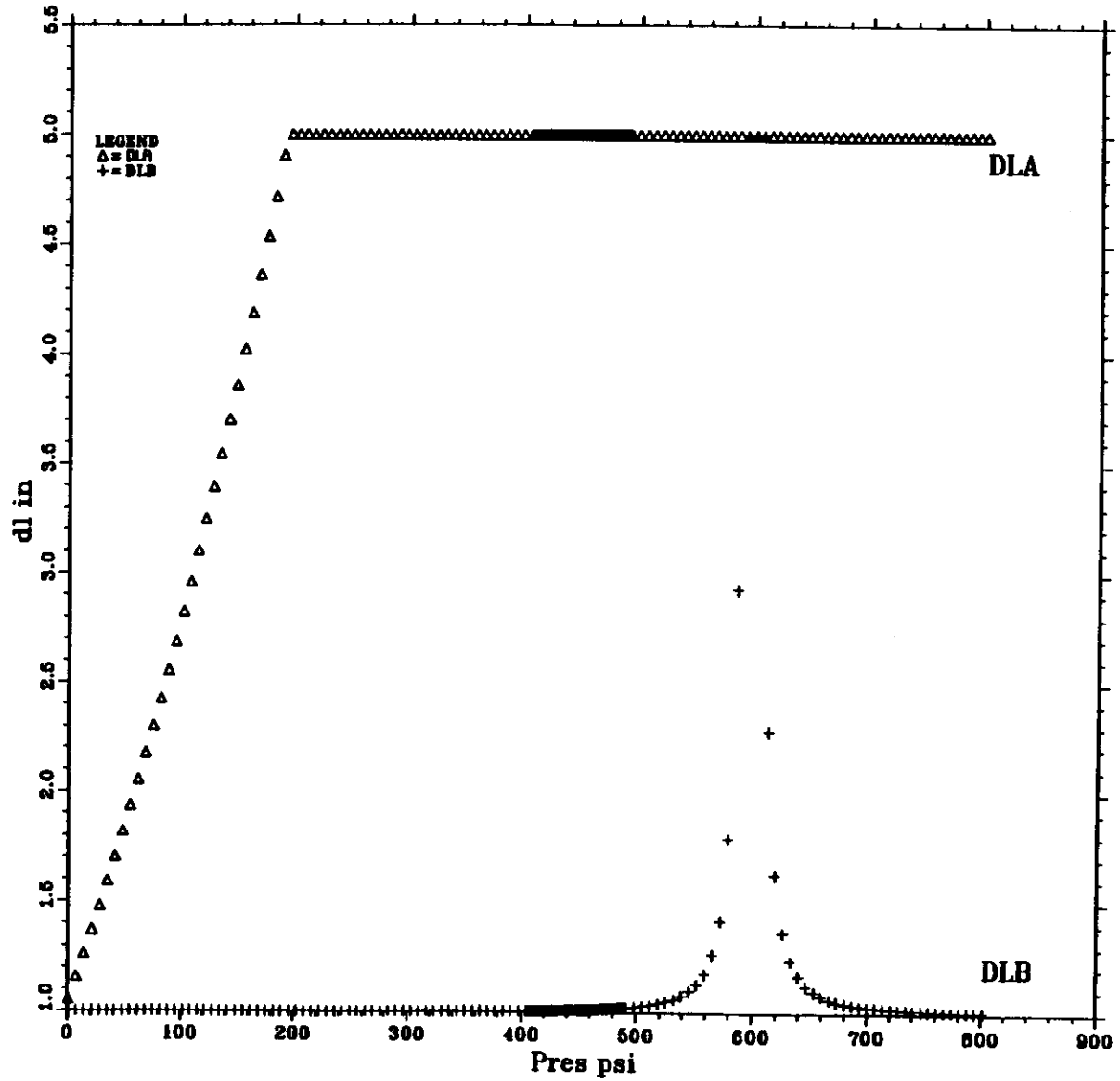

SSC ddd
zet6=0.030 in
zet7=0.000 in
zet13=0.000 in
zet14=0.000 in
et6=0.000 in
et7=0.000 in
et13=0.000 in
et14=0.000 in
ds6=0.020 in
ds13=0.000 in
f(6)=-12500.0 lbs
f(13)= 0.0 lbs
K= 2759.2 lbs/in

2DUA7:<ROSSUM.BUC>FOR001.DAT;185

FIGURE D3

plot file: 2DUA7:[ROSSUM.BUC]FOR001.DAT;185
machine: SSC mode: ddd

Table 1: Input: bellows design parameters

r_i in	D_i in	d in	β	l in	pcr psi	λ in	Eb psi
0.060	14.300	0.500	0.094	9.300	450.000	1.000	3.297E+07

Table 2: Results: bellows properties

Nb	r in	D in	A in	t in	bc in	K lbs/in	Kl lbs/in	I in^4
26	0.072	14.800	0.356	0.025	0.342	2759.212	1.048E+04	3.151E+01

Table 3: Results: maximum bellows stresses at p_{op}

σ_{max} psi	σ_h psi	σ_{pw1} psi	σ_{pw2} psi	σ_{ps}	y_{max} in
1.523E+05	2.778E+04	6.640E+04	6.782E+04	2.967E+04	1.472E-03

Table 4: Input: bellows misalignments

$\zeta(6)$ in	$\zeta(7)$ in	$\zeta(13)$ in	$\zeta(14)$ in	$\eta(6)$	$\eta(7)$	$\eta(13)$	$\eta(14)$
0.030	0.000	0.000	0.000	0.000	0.000	0.000	0.000

Table 5: Input: bellows initial shape

d_s6 in	d_s13 in	d_c6 in	d_c13 in
0.020	0.000	0.020	0.000

Table 6: Input: dipole properties

s in	L_D in	ovh_D in	D_m in	t_m in	Im in^4	Em psi
0.200	670.	63.6	10.5	0.188	111.	3.000E+07

Table 7: Input: quadrupole properties

L_q in	ovh_Q in	D_q in	t_q in	Iq in^4	Eq psi
210.	52.5	10.5	0.188	111.	3.000E+07

Table 8: Results: bellows maximum elongation at p_{op}

p_{op} psi	dl6 in	dl13 in
3.000E+02	5.000E+00	1.002E+00

FIGURE D3A

Table 9: Results: node location, stiffness, force at p_{op}

node	x(i) in	k(i) lbs/in	F(i) lbs
1	0.	25000.	112.
2	136.	25000.	114.
3	271.	25000.	-549.
4	407.	25000.	-1681.
5	543.	25000.	7975.
6	606.	0.	-12500.
7	616.	0.	12500.
8	679.	25000.	-7870.
9	815.	25000.	1685.
10	951.	25000.	594.
11	1086.	25000.	-51.
12	1222.	25000.	-3.
13	1286.	0.	0.
14	1295.	0.	0.
15	1359.	25000.	33.
16	1494.	25000.	23.
17	1630.	25000.	23.
18	1766.	25000.	35.
19	1901.	25000.	84.

FIGURE D3B

MAX BELLOWS LOCAL ELONGATION

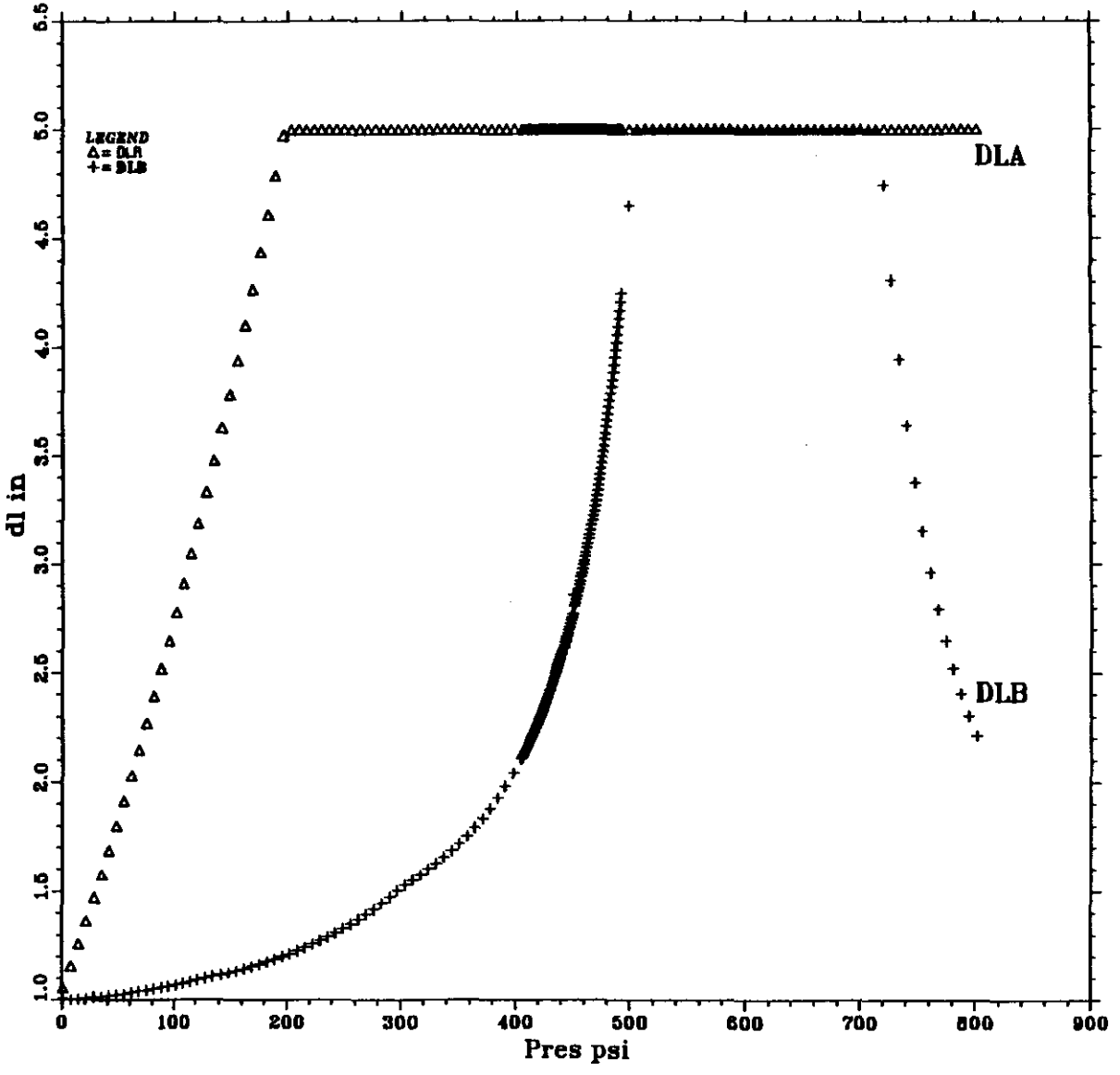

SSC dqd
zet6=0.030 in
zet7=0.000 in
zet13=0.000 in
zet14=0.000 in
et6=0.000 in
et7=0.000 in
et13=0.000 in
et14=0.000 in
ds6=0.020 in
ds13=0.000 in
f(6)=-12500.0 lbs
f(13)= 0.0 lbs
K= 2759.2 lbs/in

2DUA7:<ROSSUM.BUC>FOR001.DAT;10

FIGURE D4

plot file: 2DUA7:[ROSSUM.BUC]FOR001.DAT;10
machine: SSC mode: dqd

Table 1: Input: bellows design parameters

r_i in	D_i in	d in	β	l in	pcr psi	λ in	Eb psi
0.060	14.300	0.500	0.094	9.300	450.000	1.000	3.297E+07

Table 2: Results: bellows properties

Nb	r in	D in	Λ in	t in	bc in	K lbs/in	Kl lbs/in	I in^4
26	0.072	14.800	0.356	0.025	0.342	2759.212	1.048E+04	3.151E+01

Table 3: Results: maximum bellows stresses at p_{op}

σ_{max} psi	σ_h psi	σ_{pw1} psi	σ_{pw2} psi	σ_{ps}	y_{max} in
1.523E+05	2.778E+04	6.640E+04	6.782E+04	2.967E+04	1.472E-03

Table 4: Input: bellows misalignments

$\zeta(6)$ in	$\zeta(7)$ in	$\zeta(13)$ in	$\zeta(14)$ in	$\eta(6)$	$\eta(7)$	$\eta(13)$	$\eta(14)$
0.030	0.000	0.000	0.000	0.000	0.000	0.000	0.000

Table 5: Input: bellows initial shape

d_s6 in	d_s13 in	d_c6 in	d_c13 in
0.020	0.000	0.020	0.000

Table 6: Input: dipole properties

s in	L_D in	ovh_D in	D_m in	t_m in	Im in^4	Em psi
0.200	670.	63.6	10.5	0.188	111.	3.000E+07

Table 7: Input: quadrupole properties

L_q in	ovh_Q in	D_q in	t_q in	Iq in^4	Eq psi
210.	52.5	10.5	0.188	111.	3.000E+07

Table 8: Results: bellows maximum elongation at p_{op}

p_{op} psi	dl6 in	dl13 in
3.000E+02	5.000E+00	1.502E+00

FIGURE D4A

Table 9: Results: node location, stiffness, force at p_{op}

node	x(i) in	k(i) lbs/in	F(i) lbs
1	0.	25000.	96.
2	136.	25000.	119.
3	271.	25000.	-580.
4	407.	25000.	-1808.
5	543.	25000.	8384.
6	606.	0.	-12500.
7	616.	0.	12500.
8	668.	25000.	-8502.
9	694.	0.	0.
10	721.	0.	0.
11	747.	0.	0.
12	773.	25000.	2067.
13	826.	0.	0.
14	835.	0.	0.
15	899.	25000.	731.
16	1034.	25000.	-193.
17	1170.	25000.	-30.
18	1306.	25000.	45.
19	1441.	25000.	69.

FIGURE D4B

ASSEMBLY DEFLECTIONS AT 303.5 psi

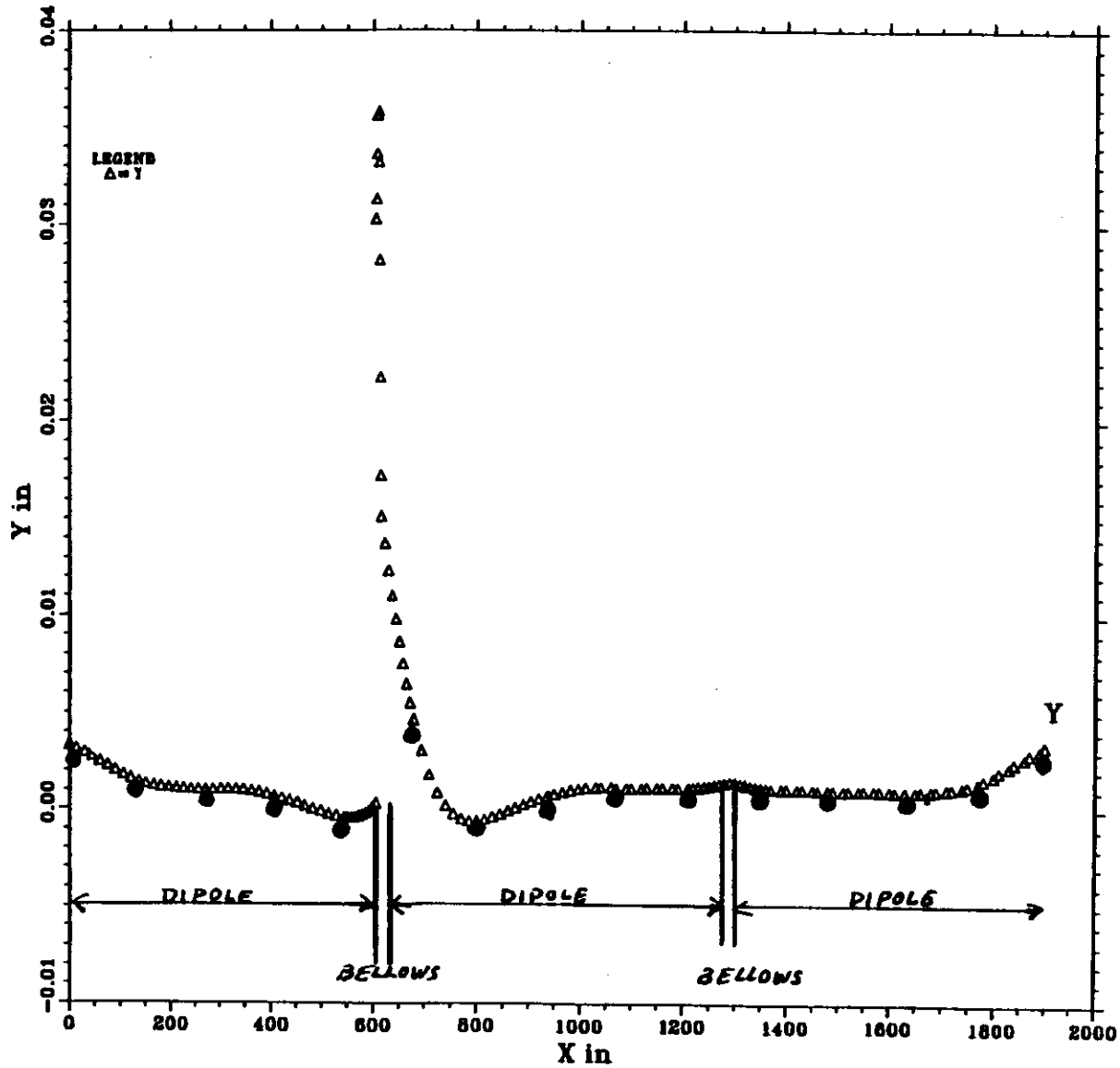

SSC ddd
zet6=0.030 in
zet7=0.000 in
zet13=0.000 in
zet14=0.000 in
et6=0.000 in
et7=0.000 in
et13=0.000 in
et14=0.000 in
ds6=0.020 in
ds13=0.000 in
f(6)= 0.0 lbs
f(13)= 0.0 lbs
K= 2759.2 lbs/in

FIGURE D5

2DUA7:<ROSSUM.BUC>FOR001.DAT;90

FIRST BELLOWS DEFLECTION AT 300 psi

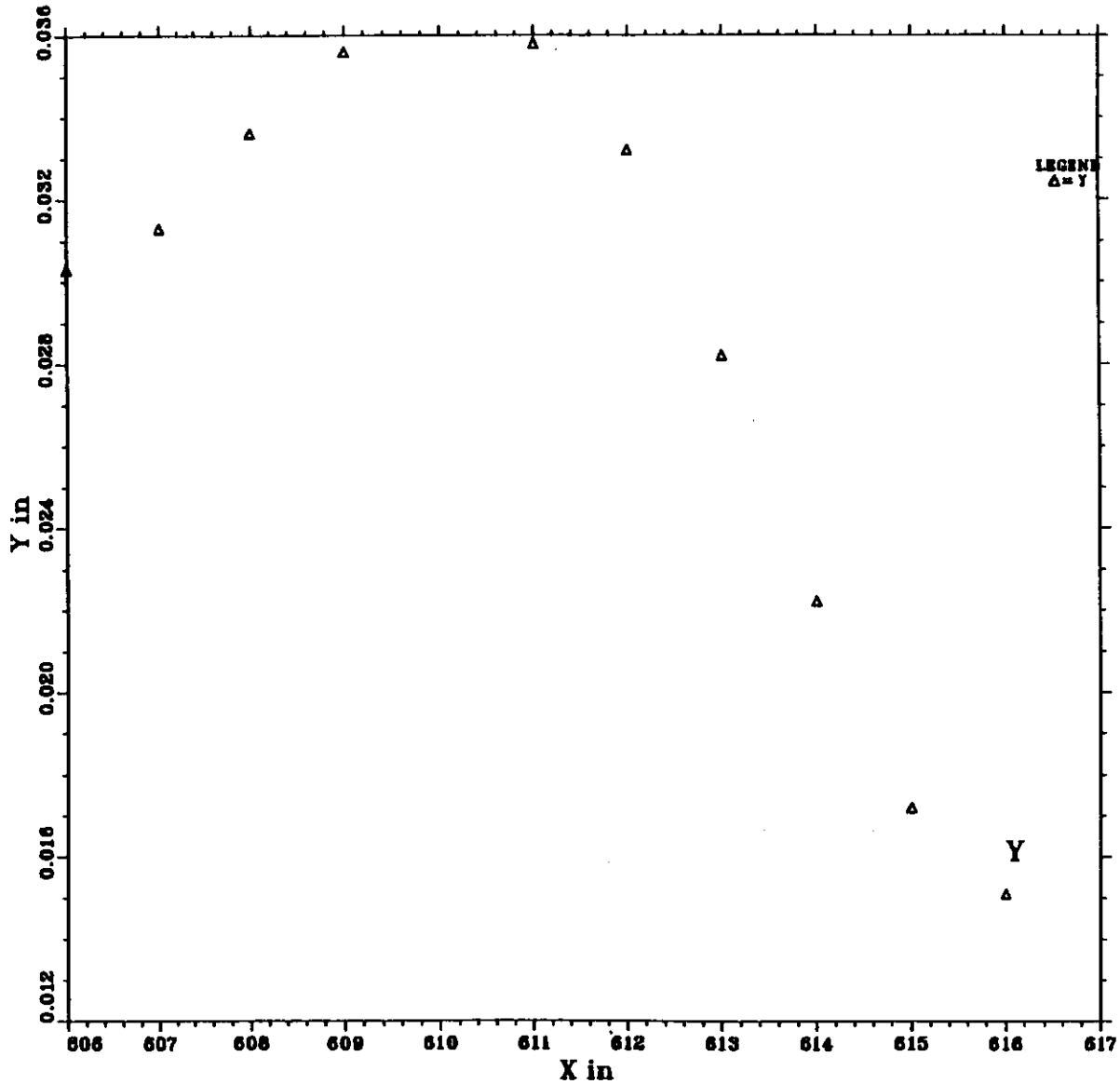

SSC ddd
zet6=0.030 in
zet7=0.000 in
zet13=0.000 in
zet14=0.000 in
et6=0.000 in
et7=0.000 in
et13=0.000 in
et14=0.000 in
ds6=0.020 in
ds13=0.000 in
f(6)= 0.0 lbs
f(13)= 0.0 lbs
K= 2759.2 lbs/in

2DUA7:<ROSSUM.BUC>FOR001.DAT;90

FIGURE D6

MAX BELLOWS LOCAL ELONGATION

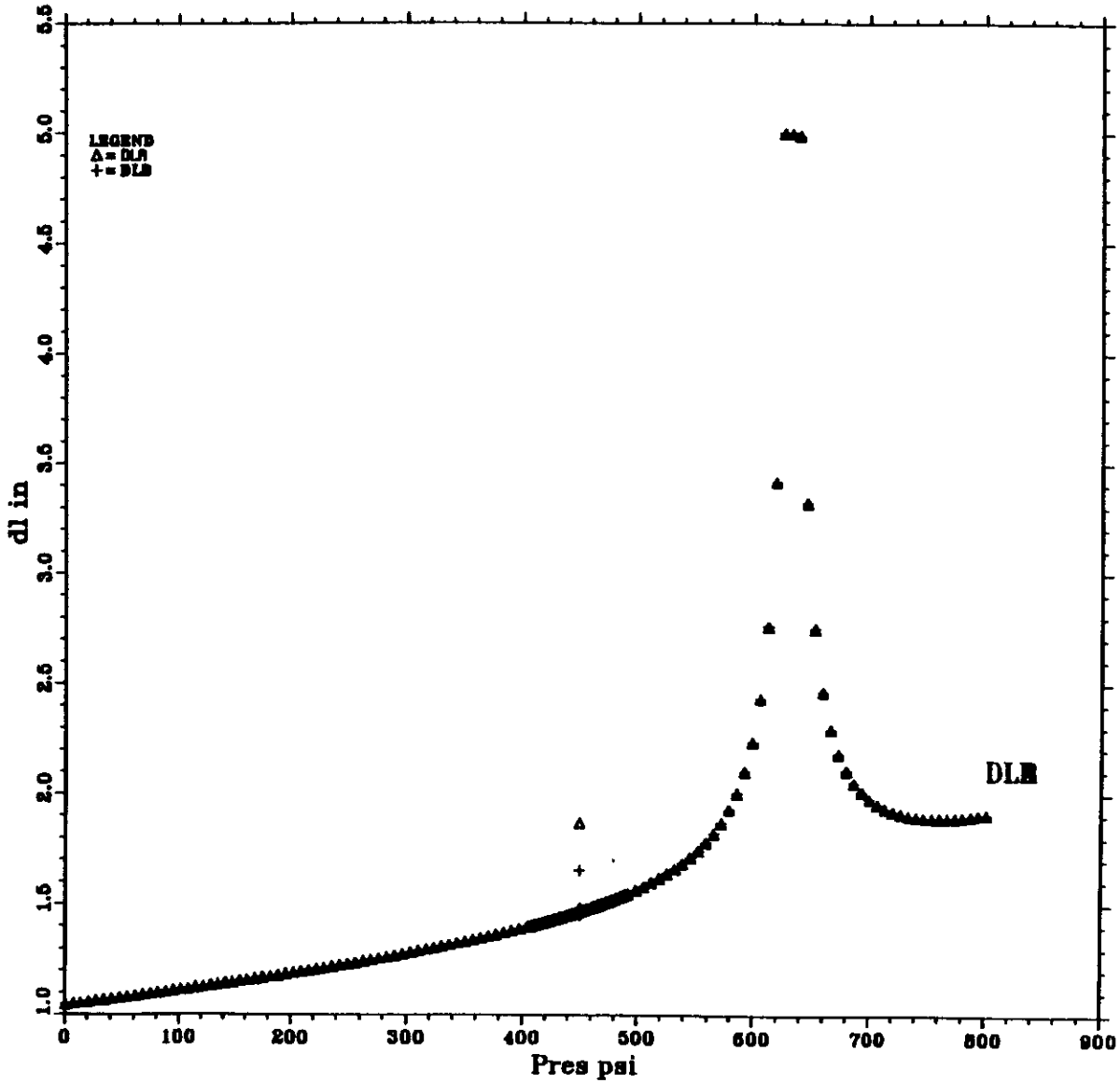

SSC dqd
zet6=0.030 in
zet7=0.000 in
zet13=0.000 in
zet14=-.030 in
et6=0.000 in
et7=0.000 in
et13=0.000 in
et14=0.000 in
ds6=0.020 in
ds13=0.020 in
f(6)= 0.0 lbs
f(13)= 0.0 lbs
K= 2759.2 lbs/in

2DUA7:<ROSSUM.BUC>FOR001.DAT;97

FIGURE D7

MAX BELLOWS LOCAL ELONGATION

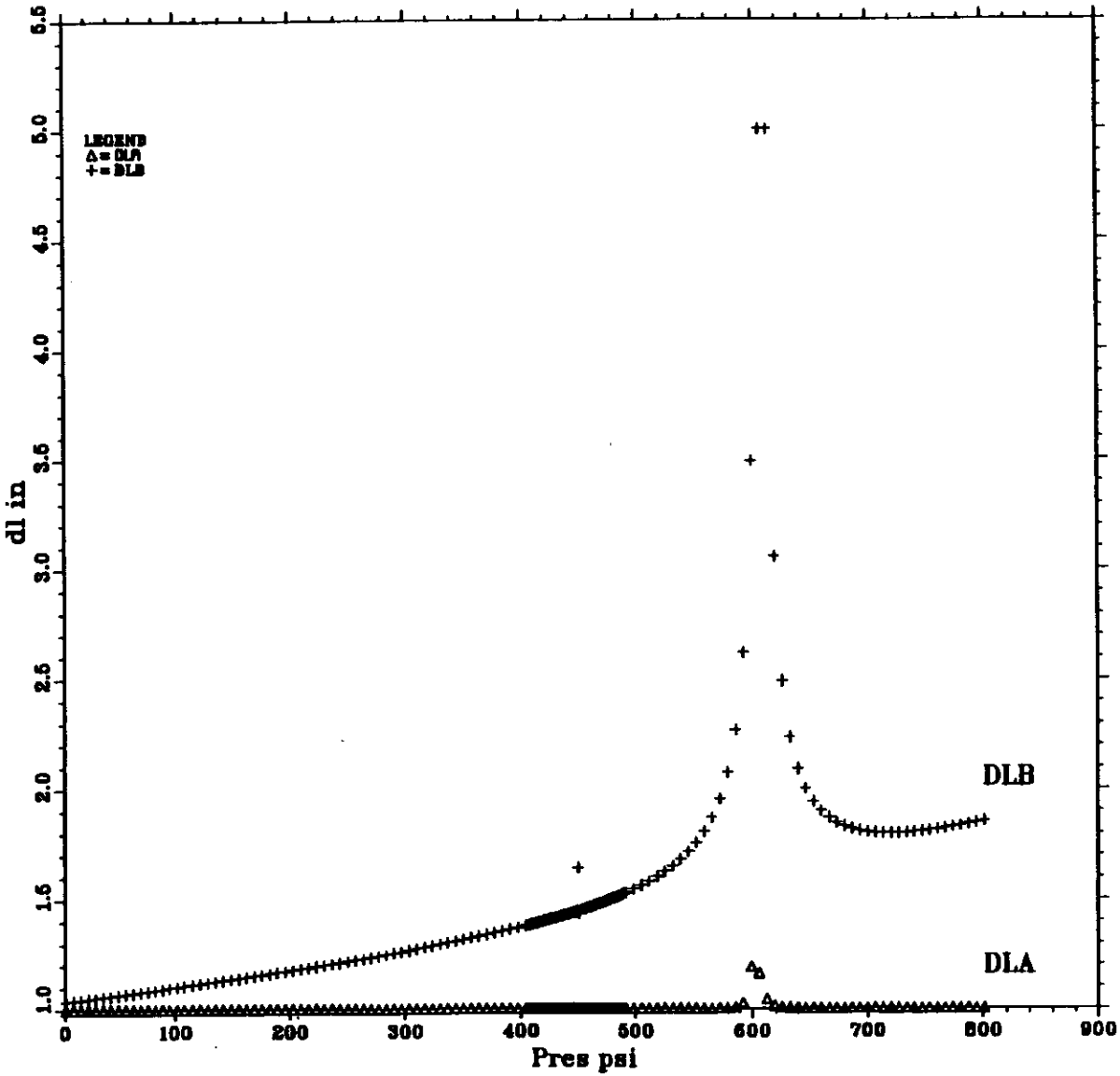

SSC ddq
zet6=0.000 in
zet7=0.000 in
zet13=0.000 in
zet14=-.030 in
et6=0.000 in
et7=0.000 in
et13=0.000 in
et14=0.000 in
ds6=0.000 in
ds13=0.020 in
f(6)= 0.0 lbs
f(13)= 0.0 lbs
K= 2759.2 lbs/in

FIGURE D8

2DUA7:<ROSSUM.BUC>FOR001.DAT;96

MAX BELLOWS LOCAL ELONGATION

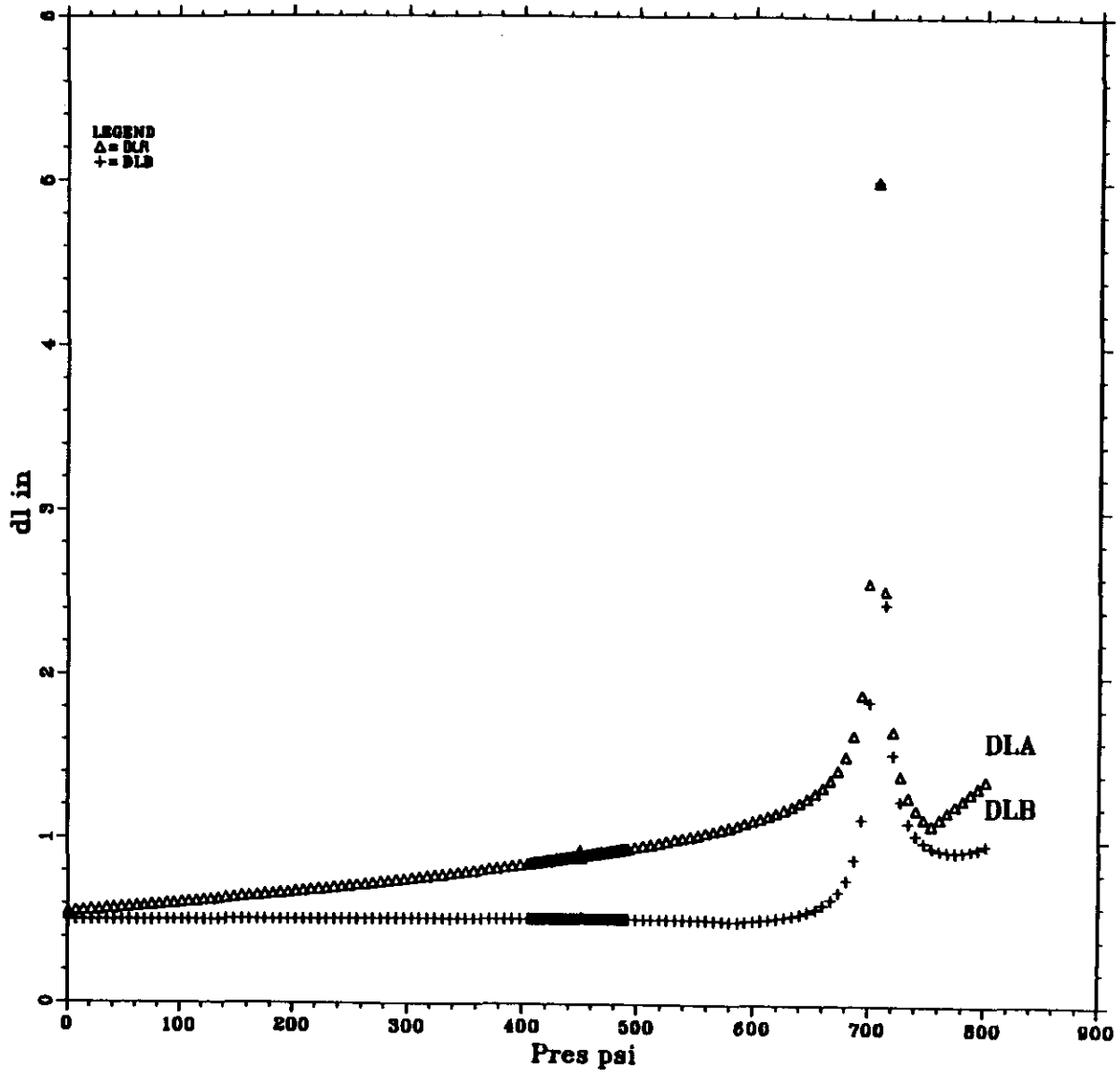

RHIC dqd
zet6=0.030 in
zet7=0.000 in
zet13=0.000 in
zet14=0.000 in
et6=0.000 in
et7=0.000 in
et13=0.000 in
et14=0.000 in
ds6=0.020 in
ds13=0.000 in
f(6)= 0.0 lbs
f(13)= 0.0 lbs
K= 1784.5 lbs/in

2DUA7:<ROSSUM.BUC>FOR001.DAT;91

FIGURE DR1

plot file: 2DUA7:[ROSSUM.BUC]FOR001.DAT;91
machine: RHIC mode: dqd

Table 1: Input: bellows design parameters

r_i in	D_i in	d in	β	l in	pcr psi	λ in	Eb psi
0.060	7.630	0.500	0.094	6.000	450.000	0.500	3.297E+07

Table 2: Results: bellows properties

Nb	r in	D in	Λ in	t in	bc in	K lbs/in	Kl in lbs	I in^4
17	0.072	8.130	0.352	0.024	0.346	1784.526	4.915E+03	5.137E+00

Table 3: Results: maximum bellows stresses at p_{op}

σ_{mas} psi	σ_h psi	σ_{pw1} psi	σ_{pw2} psi	σ_{ps}	y_{mas} in
1.066E+05	1.534E+04	6.869E+04	7.013E+04	3.071E+04	1.548E-03

Table 4: Input: bellows misalignments

$\zeta(6)$ in	$\zeta(7)$ in	$\zeta(13)$ in	$\zeta(14)$ in	$\eta(6)$	$\eta(7)$	$\eta(13)$	$\eta(14)$
0.030	0.000	0.000	0.000	0.000	0.000	0.000	0.000

Table 5: Input: bellows initial shape

d_e6 in	d_e13 in	d_c6 in	d_c13 in
0.020	0.000	0.020	0.000

Table 6: Input: dipole properties

s in	L_D in	ovh_D in	D_m in	t_m in	Im in^4	Em psi
2.00	394.	55.4	10.5	0.188	111.	3.000E+07

Table 7: Input: quadrupole properties

L_q in	ovh_Q in	D_q in	t_q in	Iq in^4	Eq psi
170.	48.0	10.5	0.188	111.	3.000E+07

Table 8: Results: bellows maximum elongation at p_{op}

p_{op} psi	dl6 in	dl13 in
3.000E+02	7.511E-01	5.139E-01

FIGURE DR1A

Table 9: Results: node location, stiffness, force at p_{op}

node	x(i) in	k(i) lbs/in	F(i) lbs
1	0.00	25000.00	404.58
2	70.80	0.10	0.00
3	141.60	25000.00	280.09
4	212.40	0.10	0.00
5	283.20	25000.00	168.42
6	338.60	0.00	0.00
7	344.60	0.00	0.00
8	392.60	25000.00	213.01
9	411.10	0.10	0.00
10	429.60	0.10	0.00
11	448.10	0.10	0.00
12	466.60	25000.00	121.71
13	514.60	0.00	0.00
14	520.60	0.00	0.00
15	576.00	25000.00	199.74
16	646.80	0.10	0.00
17	717.60	25000.00	278.03
18	788.40	0.10	0.00
19	859.20	25000.00	403.15

FIGURE DR1B

MAX BELLOWS LOCAL ELONGATION

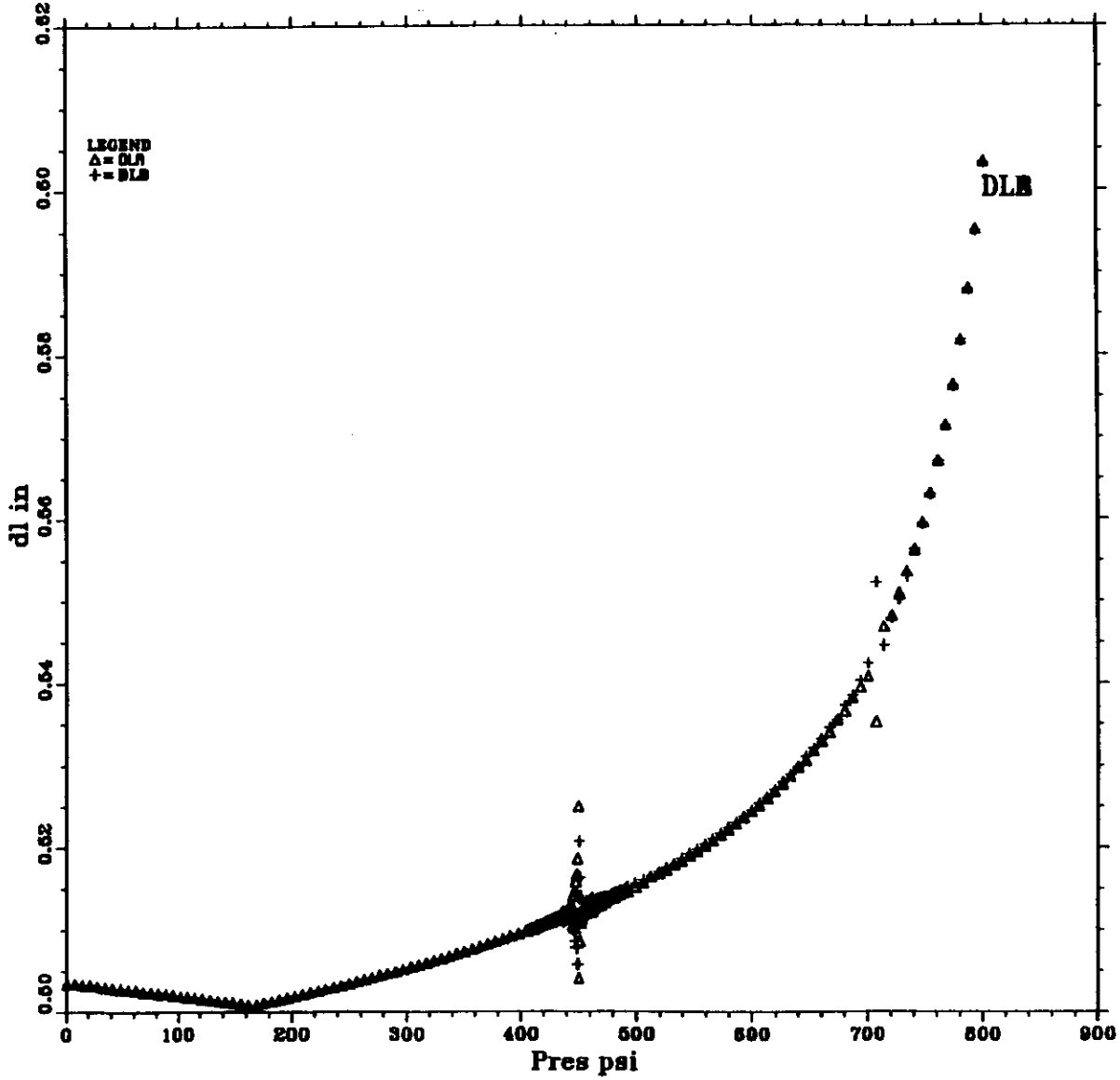

RHIC dqd
zet6=0.000 in
zet7=0.000 in
zet13=0.000 in
zet14=0.000 in
et6=0.000 in
et7=0.000 in
et13=0.000 in
et14=0.000 in
ds6=0.000 in
ds13=0.000 in
f(6)= 0.0 lbs
f(13)= 0.0 lbs
K= 1784.5 lbs/in

2DUA7:<ROSSUM.BUC>FOR001.DAT;93

FIGURE DR2

plot file: 2DUA7:[ROSSUM.BUC]FOR001.DAT;93
machine: RHIC mode: dqd

Table 1: Input: bellows design parameters

r_i in	D_i in	d in	β	l in	pcr psi	λ in	Eb psi
0.060	7.630	0.500	0.094	6.000	450.000	0.500	3.297E+07

Table 2: Results: bellows properties

Nb	r in	D in	Λ in	t in	bc in	K lbs/in	Kl lbs/in	I in^4
17	0.072	8.130	0.352	0.024	0.346	1784.526	4.915E+03	5.137E+00

Table 3: Results: maximum bellows stresses at p_{op}

σ_{max} psi	σ_h psi	σ_{pw1} psi	σ_{pw2} psi	σ_{pe}	y_{max} in
1.066E+05	1.534E+04	6.869E+04	7.013E+04	3.071E+04	1.548E-03

Table 4: Input: bellows misalignments

$\zeta(6)$ in	$\zeta(7)$ in	$\zeta(13)$ in	$\zeta(14)$ in	$\eta(6)$	$\eta(7)$	$\eta(13)$	$\eta(14)$
0.000	0.000	0.000	0.000	0.000	0.000	0.000	0.000

Table 5: Input: bellows initial shape

d_e6 in	d_e13 in	d_e6 in	d_e13 in
0.000	0.000	0.000	0.000

Table 6: Input: dipole properties

s in	L_D in	ovh_D in	D_m in	t_m in	Im in^4	Em psi
2.00	394.	55.4	10.5	0.188	111.	3.000E+07

Table 7: Input: quadrupole properties

L_q in	ovh_Q in	D_q in	t_q in	Iq in^4	Eq psi
170.	48.0	10.5	0.188	111.	3.000E+07

Table 8: Results: bellows maximum elongation at p_{op}

p_{op} psi	dl6 in	dl13 in
3.000E+02	5.051E-01	5.052E-01

FIGURE DR2A

Table 9: Results: node location, stiffness, force at p_{op}

node	x(i) in	k(i) lbs/in	F(i) lbs
1	0.00	25000.00	402.98
2	70.80	0.10	0.00
3	141.60	25000.00	276.46
4	212.40	0.10	0.00
5	283.20	25000.00	205.65
6	338.60	0.00	0.00
7	344.60	0.00	0.00
8	392.60	25000.00	149.29
9	411.10	0.10	0.00
10	429.60	0.10	0.00
11	448.10	0.10	0.00
12	466.60	25000.00	149.27
13	514.60	0.00	0.00
14	520.60	0.00	0.00
15	576.00	25000.00	205.64
16	646.80	0.10	0.00
17	717.60	25000.00	276.49
18	788.40	0.10	0.00
19	859.20	25000.00	402.96

FIGURE DR2B

MAX BELLOWS LOCAL ELONGATION

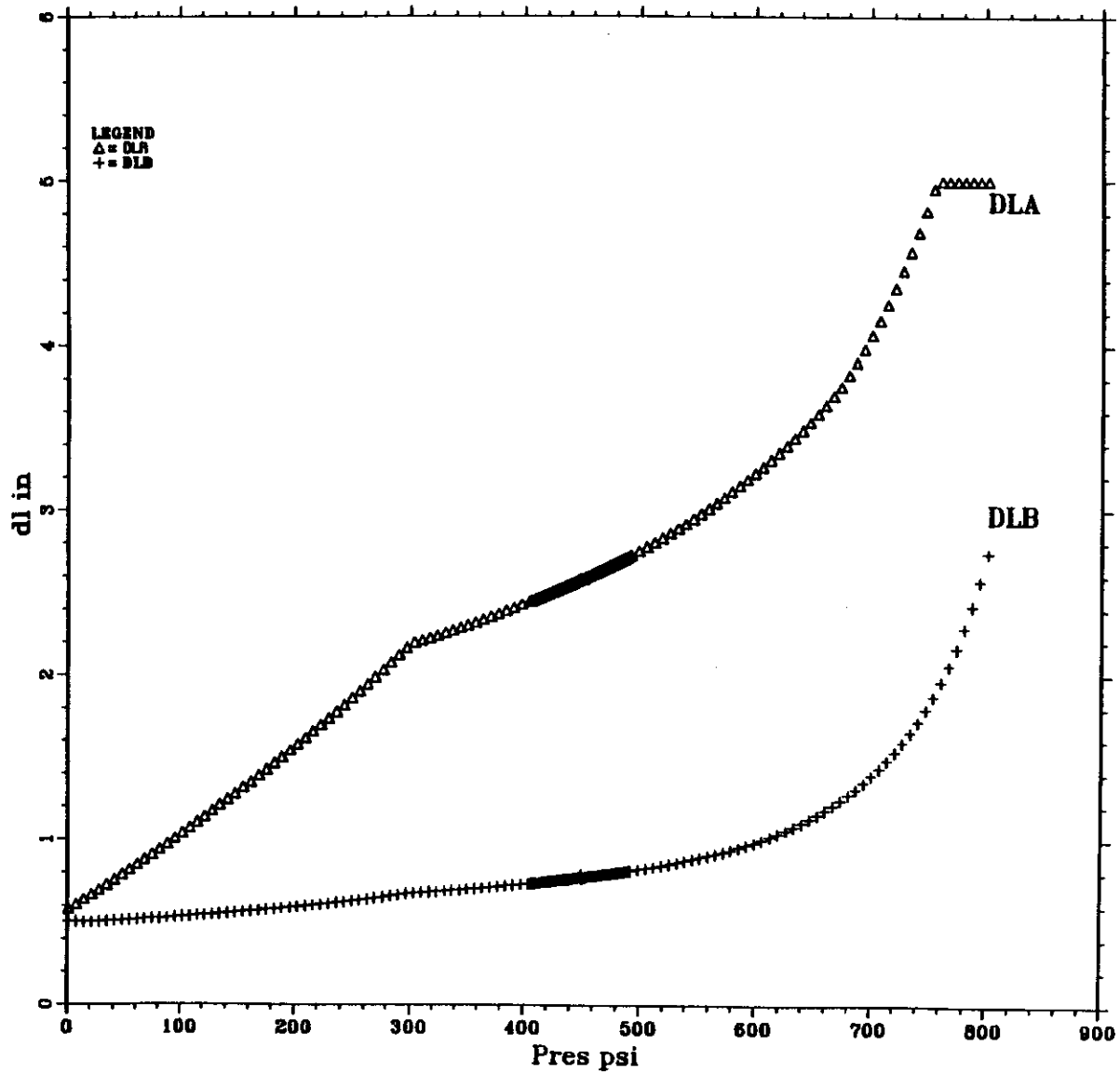

RHIC dqd
zet6=0.030 in
zet7=0.000 in
zet13=0.000 in
zet14=0.000 in
et6=0.000 in
et7=0.000 in
et13=0.000 in
et14=0.000 in
ds6=0.020 in
ds13=0.000 in
f(6)= −3000.0 lbs
f(13)= 0.0 lbs
K= 1784.5 lbs/in

2DUA7:<ROSSUM.BUC>FOR001.DAT;12

FIGURE DR3

plot file: 2DUA7:[ROSSUM.BUC]FOR001.DAT;12
machine: RHIC mode: dqd

Table 1: Input: bellows design parameters

r_i in	D_i in	d in	β	l in	pcr psi	λ in	Eb psi
0.060	7.630	0.500	0.094	6.000	450.000	0.500	3.297E+07

Table 2: Results: bellows properties

Nb	r in	D in	Λ in	t in	bc in	K lbs/in	Kl lbs/in	I in^4
17	0.072	8.130	0.352	0.024	0.346	1784.526	4.915E+03	5.137E+00

Table 3: Results: maximum bellows stresses at p_{op}

σ_{mas} psi	σ_h psi	σ_{pw1} psi	σ_{pw2} psi	σ_{ps}	y_{mas} in
1.066E+05	1.534E+04	6.869E+04	7.013E+04	3.071E+04	1.548E-03

Table 4: Input: bellows misalignments

$\zeta(6)$ in	$\zeta(7)$ in	$\zeta(13)$ in	$\zeta(14)$ in	$\eta(6)$	$\eta(7)$	$\eta(13)$	$\eta(14)$
0.030	0.000	0.000	0.000	0.000	0.000	0.000	0.000

Table 5: Input: bellows initial shape

d_s6 in	d_s13 in	d_c6 in	d_c13 in
0.020	0.000	0.020	0.000

Table 6: Input: dipole properties

s in	L_D in	ovh_D in	D_m in	t_m in	Im in^4	Em psi
2.00	394.	55.4	10.5	0.188	111.	3.000E+07

Table 7: Input: quadrupole properties

L_q in	ovh_Q in	D_q in	t_q in	Iq in^4	Eq psi
170.	48.0	10.5	0.188	111.	3.000E+07

Table 8: Results: bellows maximum elongation at p_{op}

p_{op} psi	dl6 in	dl13 in
3.000E+02	2.165E+00	6.724E-01

FIGURE DR3A

Table 9: Results: node location, stiffness, force at p_{op}

node	x(i) in	k(i) lbs/in	F(i) lbs
1	0.	60000.	447.
2	71.	0.	0.
3	142.	60000.	-725.
4	212.	0.	0.
5	283.	60000.	3457.
6	339.	0.	-3000.
7	345.	0.	3000.
8	393.	60000.	-3541.
9	411.	0.	0.
10	430.	0.	0.
11	448.	0.	0.
12	467.	60000.	1465.
13	515.	0.	0.
14	521.	0.	0.
15	576.	60000.	337.
16	647.	0.	0.
17	718.	60000.	233.
18	788.	0.	0.
19	859.	60000.	395.

FIGURE DR3B

ASSEMBLY DEFLECTIONS AT 303.5 psi

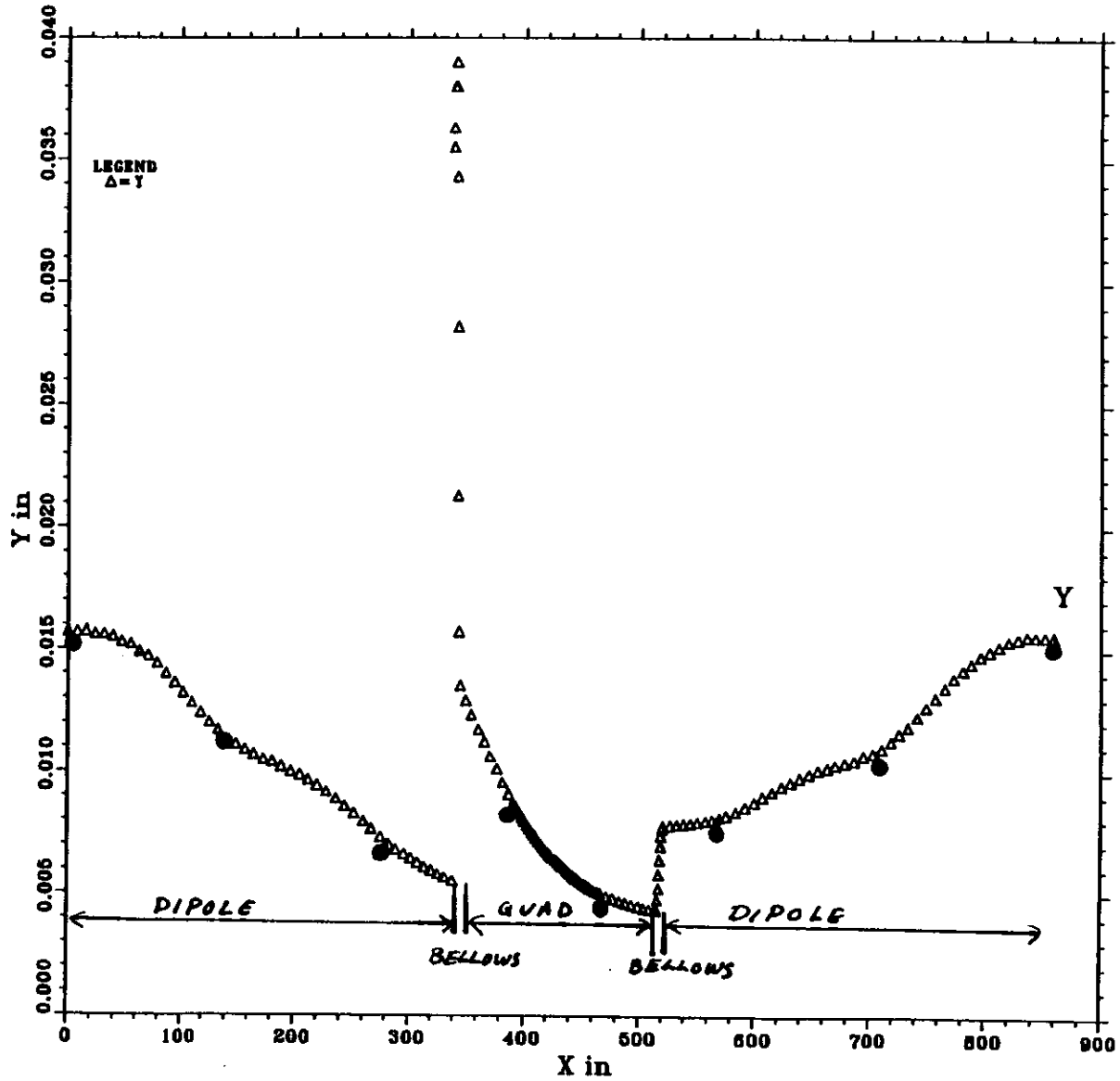

RHIC dqd
zet6=0.030 in
zet7=0.000 in
zet13=0.000 in
zet14=0.000 in
et6=0.000 in
et7=0.000 in
et13=0.000 in
et14=0.000 in
ds6=0.020 in
ds13=0.000 in
f(6)= 0.0 lbs
f(13)= 0.0 lbs
K= 1784.5 lbs/in

2DUA7:<ROSSUM.BUC>FOR001.DAT;91

FIGURE DR4

FIRST BELLOWS DEFLECTION AT 300 psi

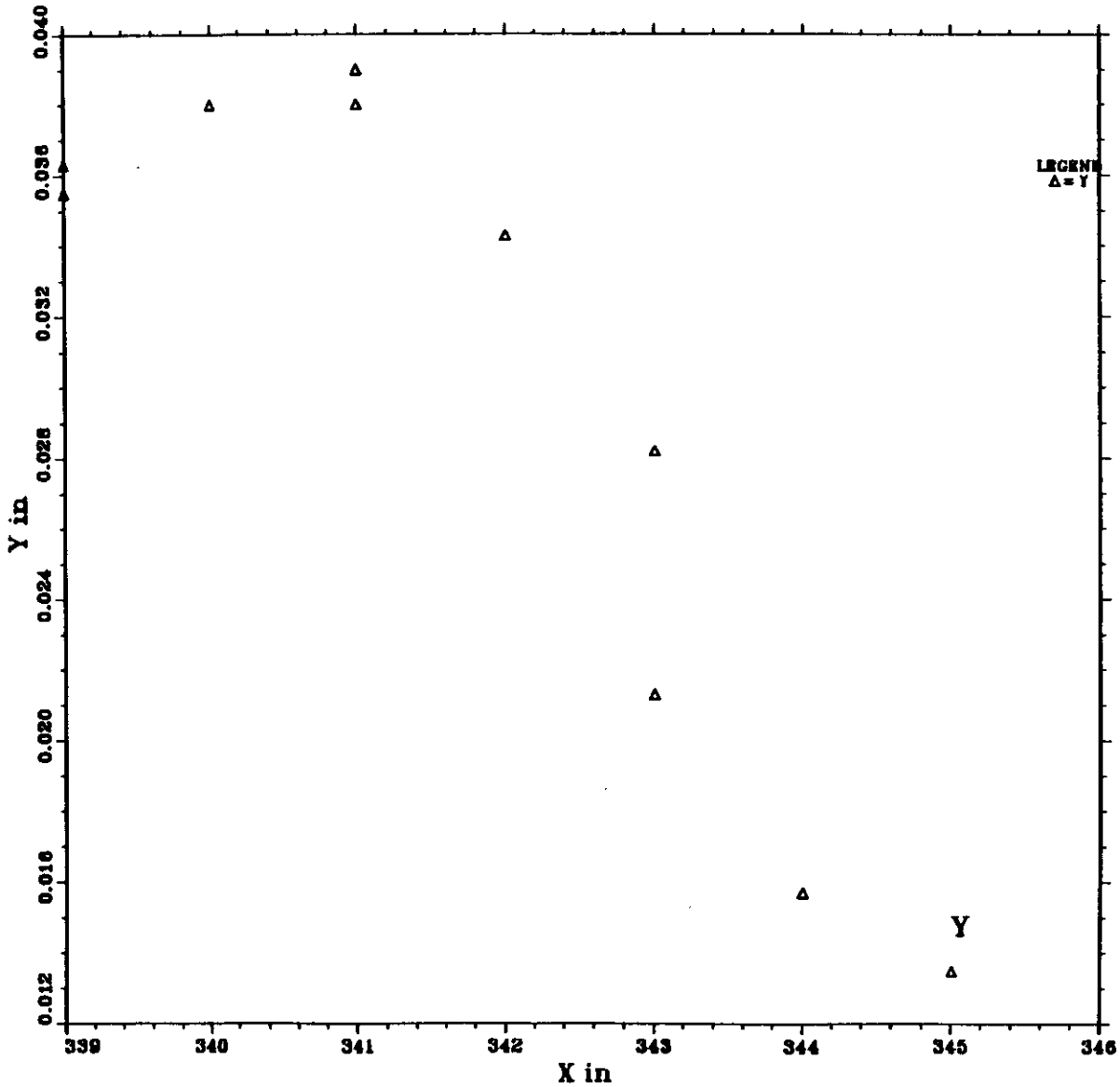

RHIC dqd
zet6=0.030 in
zet7=0.000 in
zet13=0.000 in
zet14=0.000 in
et6=0.000 in
et7=0.000 in
et13=0.000 in
et14=0.000 in
ds6=0.020 in
ds13=0.000 in
f(6)= 0.0 lbs
f(13)= 0.0 lbs
K= 1784.5 lbs/in

2DUA7:<ROSSUM.BUC>FOR001.DAT;91 FIGURE DR5

MAX BELLOWS LOCAL ELONGATION

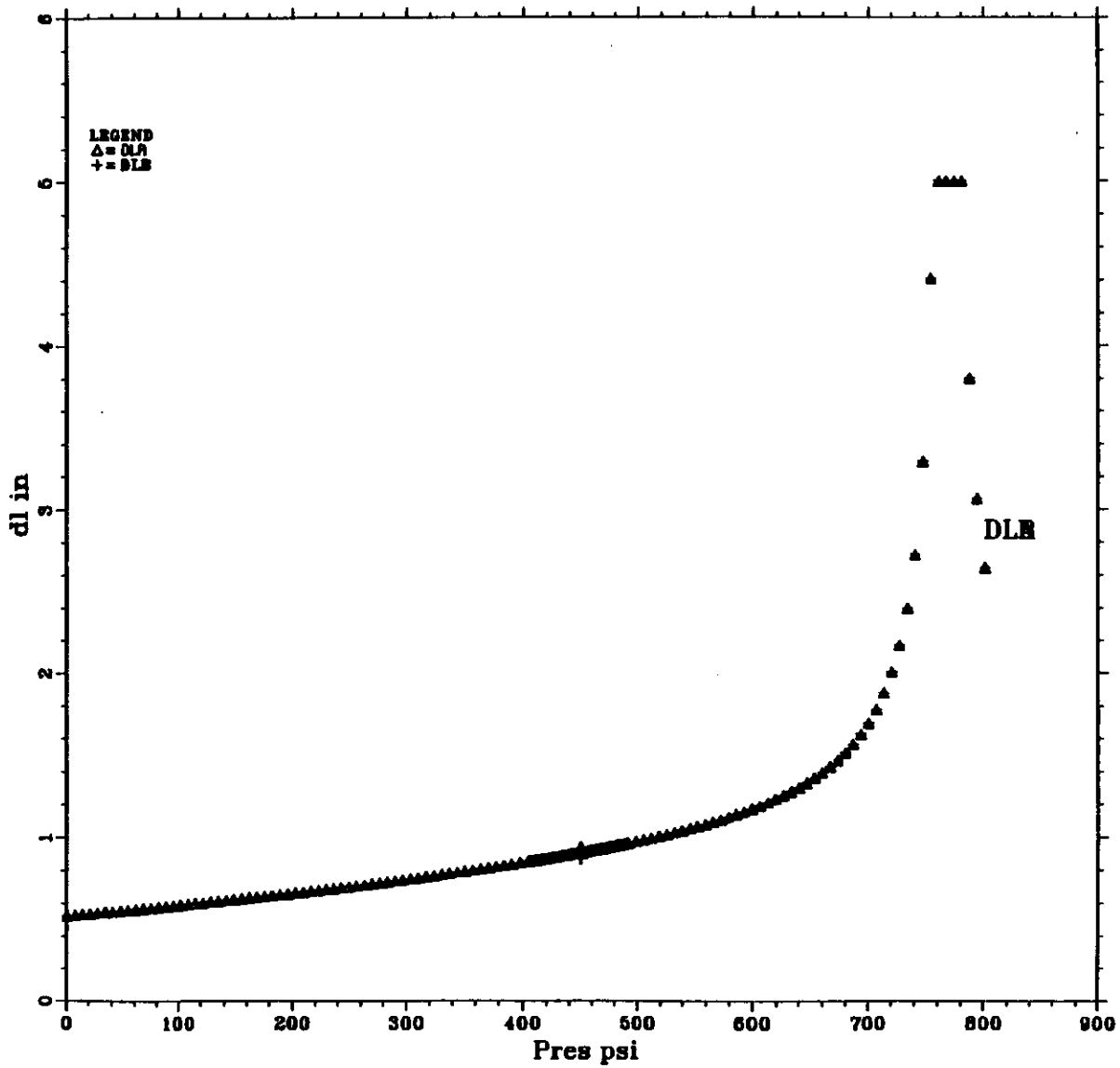

RHIC qdq
zet6=0.030 in
zet7=0.000 in
zet13=0.000 in
zet14=−.030 in
et6=0.000 in
et7=0.000 in
et13=0.000 in
et14=0.000 in
ds6=0.020 in
ds13=0.020 in
f(6)= 0.0 lbs
f(13)= 0.0 lbs
K= 1784.5 lbs/in

2DUA7:<ROSSUM.BUC>FOR001.DAT;102 FIGURE DR6

MAX BELLOWS LOCAL ELONGATION

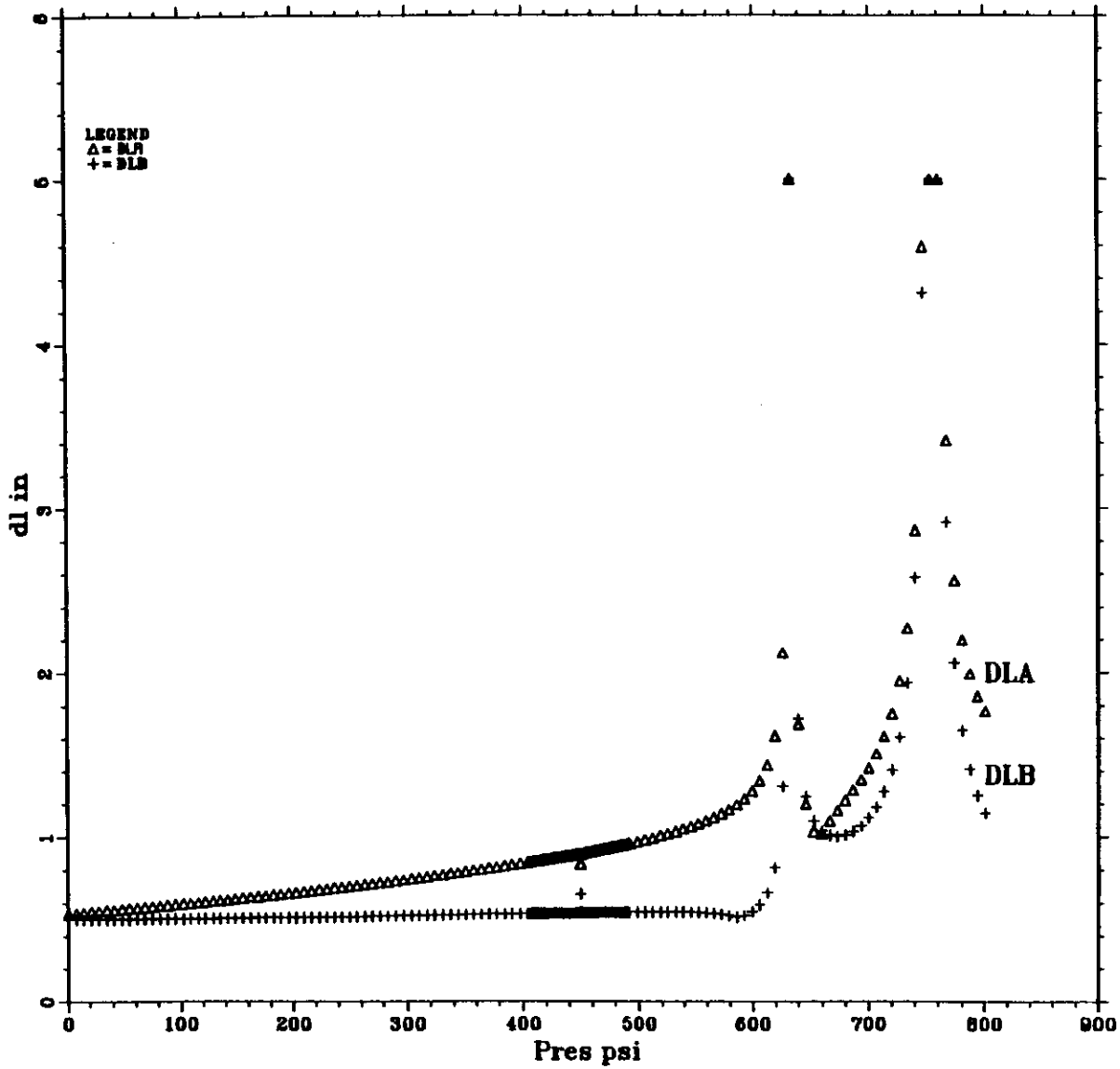

RHIC dqd
zet6=0.030 in
zet7=0.000 in
zet13=0.000 in
zet14=0.000 in
et6=0.000 in
et7=0.000 in
et13=0.000 in
et14=0.000 in
ds6=0.020 in
ds13=0.000 in
f(6)= 0.0 lbs
f(13)= 0.0 lbs
K= 2732.3 lbs/in

2DUA7:<ROSSUM.BUC>FOR001.DAT;105 FIGURE DR7

MAX BELLOWS LOCAL ELONGATION

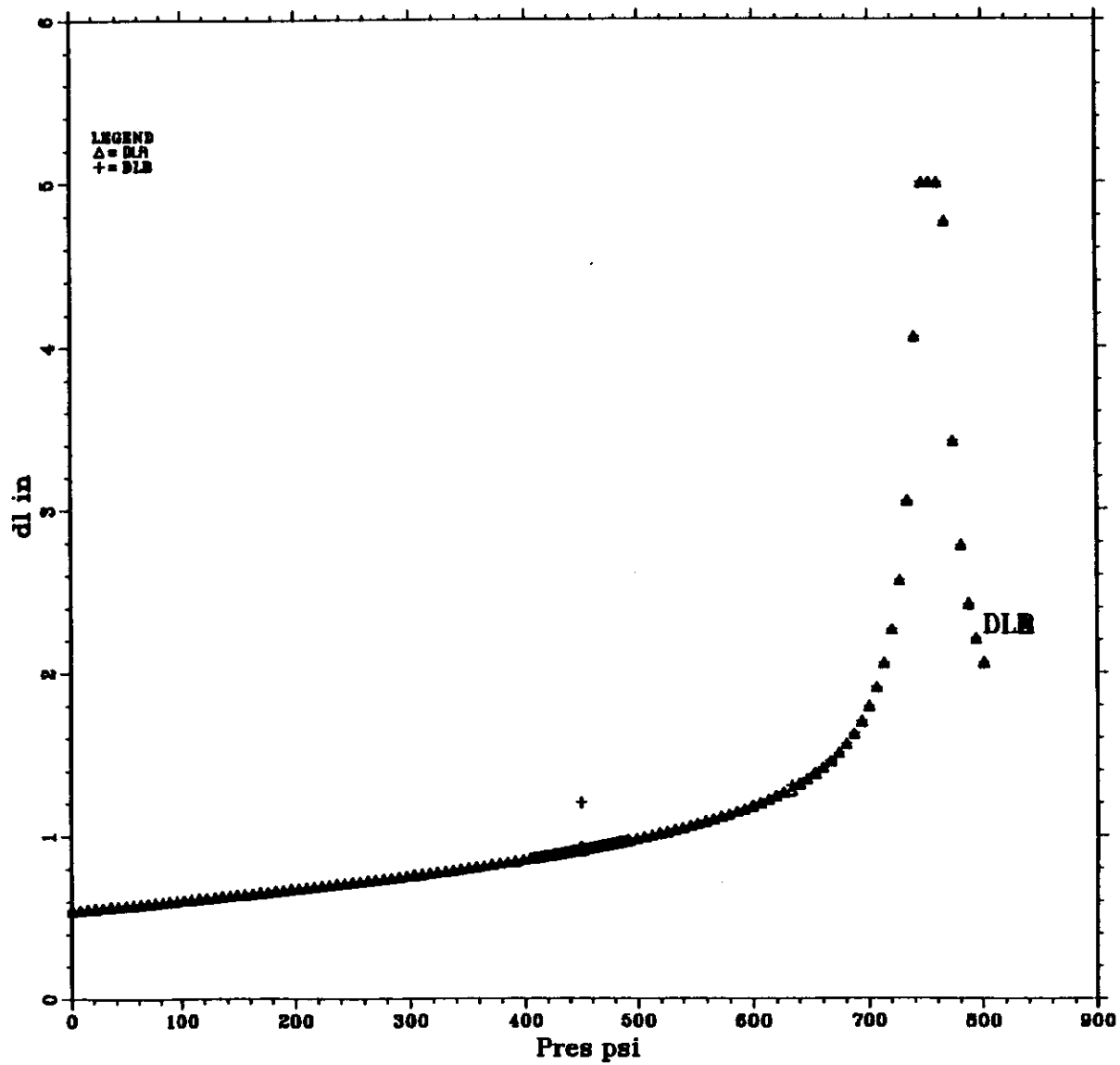

RHIC dqd
zet6=0.030 in
zet7=0.000 in
zet13=0.000 in
zet14=-.030 in
et6=0.000 in
et7=0.000 in
et13=0.000 in
et14=0.000 in
ds6=0.020 in
ds13=0.020 in
f(6)= 0.0 lbs
f(13)= 0.0 lbs
K= 2732.3 lbs/in

2DUA7:<ROSSUM.BUC>FOR001.DAT;104

FIGURE DR8

Appendix: MACSYMA code for magnet bellows assembly

There are 19 supports and 10 nodes between supports. On Fig. e5 the deflected shape of the bellows is defined as a function of i (number of the span between two supports) and j (node number on this interval). For instance if there are 10 nodes between supports, y(18,10) denotes the deflection of the last node of the eighteenth span between supports 18 and 19. y is defined in terms of three functions: one function containing the unknowns (xa, xb corresponding to A, B in eq. 64), one function which is a polynomial expression of x (denoted h), and one function of trigonometric expressions of x. y is split into three expressions to reduce the number of operations that MACSYMA has to perform, this will be shown later. Similar functions are defined for y' in Fig. e6. One could have used a command to differentiate y each time that y' is called but in order to minimize the number of operations that MACSYMA has to perform, explicit expressions for y' are provided. On Fig. e7 the functions which are called in the polynomial part of y are defined. ZG, ZC, ZD correspond to G, C, D, in eq.64.

Figure e8 shows various functions, the initial shape of the whole system denoted by y0 in the text is called here f0, all its derivatives are also explicitly provided to increase the speed of execution of the program. On Fig. e9, one finds the bellows offsets ς and η, and E_s, E_c of eq.64 . Fig. e10 shows the boundary conditions and the moment equation. In eq.62 two expressions of y for adjacent intervals but at the same x location are subtracted. Since the trigonometric functions do not cancel, operations are performed only on the polynomial part of y (function h), thus saving unnecessary operations and justifying the initial definition of y in terms of three functions.

On Fig. e11 one finds the function bc(i) calling all the boundary conditions starting with eq.58 which expresses equilibrium of forces. Function dfor() first calls a boundary condition equation bc(i), then isolates with the command coeff all the coefficients of the unknowns u(i) which it denotes by q(i,j) in the fortran expression created for further processing. These coefficients, multiplied by the corresponding unknowns, are subtracted from bc(i) to obtain the remainder w(i). w(i) is the ith component of vector W in the final matrix equation X [Q] = W which will be inverted numerically to obtain vector X containing

A, B of eq.64. Function pfor() opens a file to which the fortran expressions will be written, then calls dfor() described above, and also creates fortran expressions for C, D, Es, Ec and G which are needed in addition to A, B in eq.64 to obtain y.

Appendix: Fortran code for magnet bellows assembly

The numerical method consists of a simple matrix inversion. The system of three magnets and two bellows is modeled by a grid of 19 points. Bellows are located between nodes 6 and 7 and between nodes 13 and 14. Although there is a total of 19 nodes corresponding to the assembly of three magnets with 5 supports each, one can set the support stiffness to zero and achieve the desired combination of dipoles and quadrupoles with any number (less than 16) of supports. The program treats RHIC and SSC magnets and all applicable combinations of dipoles and quadrupoles.

The main program starts by defining the size of the matrix to be inverted, the bellows can have bent shapes of sine or cosine functions, ds6 and dc6 refer to the sine and cosine components for the first bellows while the index 13 refers to the second bellows.

The values f(6), f(7), f(13), f(14) of array f define the external forces which are applied at the bellows nodes used to study interaction between bellows.
All other values of f are the support forces on the posts. The critical pressure pcr is the pressure at which the system will first become unstable, by setting a safety factor one gets an operating pressure pop. The bellows is then designed to fail at this critical pressure. The options for machine type and magnet sequence are given next.

Subroutine GEO defines node location and material properties using the previously selected options. Subroutine AX specifies all the bellows design details to build a bellows whose axial stiffness is such that it will fail at the previously defined critical pressure. Subroutine INT applies only if one wants to know what the stresses in the bellows are once they are internally pressurized. INT calls COEFINT where MACSYMA generated expressions for the constants of integrations are given. It also calls PLOTINT and ENCINT for plotting the deflected shapes and stresses.

MAT gives the material properties. In order to clearly see the peak at the critical pressure, the mesh is refined between pressures pin2 to pfin2 which are centered around pzo=pcr. Alternatively one could have a uniformly fine mesh of icm points by setting inu=1. The overall mesh starts at pin and ends at pfin. Subroutine FORCE simply sets up the array pres of pressures with variable mesh described above.

The values for omega appearing in the solutions of the differential equations are then defined. They are needed in the subroutine COEF which are the MACSYMA generated coefficients called Q(i,j), the vector of right-hand sides is W. Q and W are copied into arrays A and B and inverted using the numerical routines LUDCMP and LUBKSB from [6]. Upon inversion of the matrix, array B contains the solutions XA, XB, F which are needed to obtain the explicit expressions for deflections, slopes and curvatures y, y', y''. Additional coefficients E, G, D, which are needed for these expressions are generated by MACSYMA are given by subroutine IND. Finally the maximum local bellows elongation DL can be computed.

Subroutine PLOT produces four types of output in addition to a table of values. Option 1 plots maximum local bellows elongation versus pressure, there are two curves, one for each bellows. Option 2 plots support deflections for each support versus pressure. Option 3 gives the deflected shape of the magnet-bellows assembly at pcr and pop. Option 4 provides the deflected shape of the bellows at pcr and pop. These are written in the plot file FOR001.DAT. The Table containing all the various design parameters and summary of the output is in the file ECHO.TEX which must be further processed with the TEX program.

Appendix: File names of additional Codes

The main program is in BEL.FOR, the common block is in BELCOM.FOR, output routines are in the file BELOUT.FOR, material and geometric properties are in BELGEO.FOR, bellows design parameters and output are in BELAX.FOR, the numerical algorithm for matrix inversion are in BELNUM.FOR, the MACSYMA code BELLOWS.MAC generates the coefficients which are in BELCOEF.FOR. BEL.COM is the command file which compiles the main program and links all the other subroutines. The bellows design parameters are computed in the main program for one bellows, they are also available for a number of cases in BELDES.FOR which includes BELDESCOM.FOR.

The spring-support model deflected shape is computed in SPRING.FOR which calls the subroutine generated by the MACSYMA code SPRING2.MAC, SPRINGCOEF2.FOR and includes SPRINGCOM.FOR as the common block. This routine also computes the three roots of the determinant=0 equation which are created by the MACSYMA code DET.MAC.

```
(c24) dispfun(bc1,bc2,bc3,bc4,bc5,bc6,eq);

                                                  m1    m2
(e24)                 bc1() := f1 + f2 - fw (--- - ---)
                                                  kt1   kt2

                                      f1   f2                m1
(e25)          bc2() := m1 + m2 - fa (-- - --) + (f1 - fw (---)) l
                                      k1   k2                kt1

                                                  m1
(e26)                       bc3() := cyp0() - ---
                                                  kt1

                                                  m2
(e27)                       bc4() := cyp1() - ---
                                                  kt2

                                                        f1
(e28)              bc5() := expand(ratsimp(cy(0) - z - --))
                                                        k1

                                                  f2
(e29)                       bc6() := cy(l) - --
                                                  k2

                                          f1            fw m1
                           fa (yx + y0 - --) + f1 x - ----- x + m1
                                          k1            kt1
(e30)   eq() := expand(ypp = - ----------------------------------------)
                                                e i

(d30)                                done

(c31) dispfun(sol,pfor);

(e31)             sol() := sol : part(solve(leq(), lunk), 1)

(e32) pfor() := (writefile("workcoef.for"),

detriq : trigsimp(denom(rhs(part(sol, 1)))),

                    detriq
detsimp : expand(---------------), fortran(determ = subst(ls, detsimp)),
                 l k1 k2 kt1 kt2

FOR k THRU 6 DO fortran(subst(ls, s3(k))), fortran(cd = subst(ls, xd)),

fortran(cq = subst(ls, xq)), closefile())

(d32)                                done
```

FIGURE E4

```
(c5) "deflected shape y, i is the interval and j the node number"$

(c6) dispfun(y);

(e6)                y(i, j) := ab(i, j) + h(i, j) + he(i, j)

(d6)                                done

(c7) "ab contains the trigonometric functions of x"$dispfun(ab);

(c8)
(e8)       ab(i, j) := xa(i) cos(om(i) x(j)) + xb(i) sin(om(i) x(j))

(d8)                                done

(c9) "h is a polynomial expression of x"$dispfun(h);

(c10)
                                                 2
(e10)             h(i, j) := zc(i) x(j) + zd(i) x (j) + zg(i)

(d10)                               done

(c11) "he contains the trigonometric expressions due to the prebent shape"$dispfun(he);

(c12)
(e12) he(i, j) := (IF i = 6 THEN xinit : x(6)

 ELSE (IF i = 13 THEN xinit : x(13)), zes(i) sin(pil (x(j) - xinit))

 + zec(i) cos(2 pil (x(j) - xinit)))

(d12)                               done
```

FIGURE E5

```
(c13) "derivative of y w.r.t. x"$dispfun(yp,pab,hp,hep);

(c14)
(e14)          yp(i, j) := pab(i, j) + hp(i, j) + hep(i, j)

(e15) pab(i, j) := - om(i) xa(i) sin(om(i) x(j)) + om(i) xb(i) cos(om(i) x(j))

(e16)                hp(i, j) := zc(i) + 2 zd(i) x(j)

(e17) hep(i, j) := (IF i = 6 THEN xinit : x(6)

 ELSE (IF i = 13 THEN xinit : x(13)), zes(i) pil cos(pil (x(j) - xinit))

 + zec(i) (- 2 pil) sin(2 pil (x(j) - xinit)))

(d17)                                done

(c18) "list of unknowns"$dispfun(u);

(c19)
(e19) u(i) := IF i <= 18 THEN xa(i) ELSE (IF i <= 36 THEN xb(i - 18)

 ELSE (IF i <= 41 THEN f(i - 36) ELSE (IF i <= 46 THEN f(i - 34)

 ELSE (IF i <= 51 THEN f(i - 32)))))

(d19)                                done
```

FIGURE E6

```
(c69) "functions called by functions h and hp"$dispfun(zq,q,zc,zd);

(c70)
                        q(i) - 2 zd(i)
(e70) zq(i) := (xqc : --------------, IF i = 6 THEN xqc - dc6
                            a(i)

                                   ELSE (IF i = 13 THEN xqc - dc13 ELSE xqc))


                                 fa f(1)
(e71) q(i) := (IF i = 1 THEN qin : -------
                                   sk(1)

                                 f(10)
 ELSE (IF i = 10 THEN qin : fb (------ + f0(10))
                                 sk(10)

      f(1)    f(10)                qin + sum(qam(j) + f(j) x(j), j, 1, i)
 + fa (----- - ------ - f0(10))), -------------------------------------)
      sk(1)   sk(10)                            aml(i)


                                b(i)              p x(19) fwa
(e72)                zc(i) := ---- - p x(19) + -----------
                                a(i)               fab(i)


(e73)                            zd(i) := p


(d73)                               done
```

FIGURE E7

```
(c50) "torsional rigidity of supports at center of the 3 magnets"$dispfun(gam);

(c51)
(e51) gam(i) := IF i = 3 THEN gam3 ELSE (IF i = 10 THEN gam10

                                        ELSE (IF i = 17 THEN gam17 ELSE 0))


(d51)                                done

(c52) "product EI for each of the 3 magnets"$dispfun(aml);

(c53)
(e53) aml(i) := IF i <= 5 THEN am ELSE (IF i = 6 THEN al

                  ELSE (IF i <= 12 THEN aq ELSE (IF i = 13 THEN al ELSE am)))


(d53)                                done

(c54) "axial force"$dispfun(fab);

(c55)
(e55)                 fab(i) := IF i <= 9 THEN fa ELSE fb


(d55)                                done

(c56) "useful functions of aml, fab"$dispfun(a,b);

(c57)
                                        fab(i)
(e57)                           a(i) := ------
                                        aml(i)


                                   sum(f(j), j, 1, i)
(e58)                     b(i) := - ------------------
                                        aml(i)


(d58)                                done

(c59) "function expressing the curvature of the magnet and derivatives"$dispfun(f0,f0p,f0pp);

(c60)
(e60)                   f0(i) := - p x(i) (x(i) - x(19))


(e61)                    f0p(i) := - (2 x(i) - x(19)) p


(e62)                          f0pp(j) := - 2 p


(d62)                                done
```

FIGURE E8

```
(c63) "bellows mounting lateral and angular misalignments"$dispfun(zet,et);

(c64)
(e64) zet(i) := IF i = 6 THEN zet6 ELSE (IF i = 7 THEN zet7

              ELSE (IF i = 13 THEN zet13 ELSE (IF i = 14 THEN zet14 ELSE 0)))


(e65) et(i) := IF i = 6 THEN et6 ELSE (IF i = 7 THEN et7

                ELSE (IF i = 13 THEN et13 ELSE (IF i = 14 THEN et14 ELSE 0)))

(d65)                                done

(c66) "terms due to initial cosine and sine shape of the bellows"$dispfun(zec,zes);

(c67)
                                   a(i)
                              dc6 (--------)
                                        2
                                  (2 pil)
(e67) zec(i) := IF i = 6 THEN - --------------
                                   a(i)
                             1 - --------
                                        2
                                  (2 pil)

                                                   a(i)
                                             dc13 (--------)
                                                        2
                                                   (2 pil)
                             ELSE (IF i = 13 THEN - --------------- ELSE 0)
                                                   a(i)
                                            1 - --------
                                                        2
                                                  (2 pil)


                                 a(i)
                            ds6 (----)
                                   2
                                 pil
(e68) zes(i) := IF i = 6 THEN ----------
                                 a(i)
                           1 - ----
                                   2
                                 pil

                                                   a(i)
                                            ds13 (----)
                                                     2
                                                   pil
                        ELSE (IF i = 13 THEN ---------- ELSE 0)
                                                   a(i)
                                            1 - ----
                                                     2
                                                   pil
```

FIGURE E9

```
(c28) "boundary condition at the supports relating force to displacement"$dispfun(ceq);

(c29)
                                                f(i)
(e29) ceq(i) := IF i <= 5 THEN expand(y(i, i) - -----)
                                                sk(i)

                                                f(i + 2)
 ELSE (IF i <= 10 THEN expand(y(i + 2, i + 2) - ---------)
                                                sk(i + 2)

                                                f(i + 4)
 ELSE (IF i <= 14 THEN expand(y(i + 4, i + 4) - ---------)
                                                sk(i + 4)

                                               f(i + 4)
 ELSE (IF i = 15 THEN expand(y(i + 3, i + 4) - ---------))))
                                               sk(i + 4)


(d29)                                done

(c30) "boundary condition for continuity of deflection"$dispfun(eq);

(c31)
(e31) eq(i) := - ab(i, i + 1) + ab(i + 1, i + 1)

 + expand(ratsimp(- h(i, i + 1) + h(i + 1, i + 1))) - he(i, i + 1)

 + he(i + 1, i + 1) - zet(i + 1)


(d31)                                done

(c32) "boundary condition for continuity of slope"$dispfun(peq);

(c33)
(e33) peq(i) := - pab(i, i + 1) + pab(i + 1, i + 1)

 + expand(ratsimp(- hp(i, i + 1) + hp(i + 1, i + 1))) - hep(i, i + 1)

 + hep(i + 1, i + 1) - et(i + 1)


(d33)                                done

(c34) "moment equation"$dispfun(mom);

(c35)
                                  f(10)    f(19)
(e35) mom() := (mom : expand(fb (------ - ------ - (f0(19) - f0(10)))
                                  sk(10)   sk(19)

      f(1)    f(10)
 + fa (----- - ------ - (f0(10) - f0(1)))),
      sk(1)   sk(10)

                                                          2
mom + sum(gam(i) - f(i) (x(19) - x(i)), i, 1, 19) + fwa p x (19))
```

FIGURE E10

```
(c38) "list of all the boundary conditions starting with equilibrium of forces"$dispfun(bc);

(c39)
(e39) bc(i) := IF i = 1 THEN sum(f(j), j, 1, 19) - (fwa + fwb) x(19) p

 ELSE (IF i <= 18 THEN eq(i - 1) ELSE (IF i <= 35 THEN peq(i - 18)

 ELSE (IF i <= 50 THEN ceq(i - 35) ELSE mom())))

(d39)                                done

(c40) "gather all the coefficients of the unknowns"$dispfun(dfor);

(c41)
(e41) dfor(i) := (s : 0, be : bc(i), FOR j THRU 51

DO (zs : coeff(be, u(j)), IF zs # 0 THEN fortran(q(i, j) = zs),

s : s + zs u(j)), smbe : ratsimp(s - be),

IF smbe # 0 THEN fortran(w(i) = smbe))

(d41)                                done

(c42) "write coefficients in fortran to file"$dispfun(pfor);

(c43)
(e43) pfor() := (writefile("belcoef5.for"), FOR i THRU 51 DO dfor(i),

FOR i THRU 18 DO (fortran(xc(i) = zc(i)), fortran(xd(i) = zd(i)),

fortran(xq(i) = zq(i)), fortran(xec(i) = zec(i)), fortran(xes(i) = zes(i))),

closefile("belcoef5.for"))

(d43)                                done
```

FIGURE E11

TECHNICAL NOTE DISTRIBUTION

Building 902

Blake, A.
Cottingham, J. G.
Garber, M.
Ghosh, A.
Greene, A.
Gupta, R.
Herrera, J.
Kahn, S.
Kelly, E.
Morgan, G.
Muratore, J.
Ozaki, S.
Prodell, A.
Rehak, M.
Rohrer, E.P.
Sampson, W.
Shutt, R.
Thompson, P.
Wanderer, P.
Willen, E.

Building 1005S

Brown, D.
Claus, J.
Courant, E.
Dell, F.
Gavigan, M.
Lee, S.Y.
Milutinovic, J.
Parzen, G.
Rhoades-Brown, M.
Ruggiero, S.
Sondericker, J.
Tepekian, S.
Wolf, L.

Building 911

AD Library, (R. Cohen)
P. Hughes (1) plus one for ea. author

Building 460

Samios, N. P.

Building 510

Banks, M.

For SSC Papers

FNAL

Mantsch, P.
Strait, J.

SSCL

Bush, T.
Coombes, R.
Goodzeit, C.
Kelly, V.
Tompkins, J.
Library Copy

LBL

Taylor, C.

S&P in Magnet Division for all MD papers

S&P in Accelerator Physics Division for all Cryogenic Papers (and J. Briggs, R. Dagradi, H. Hildebrand, W. Kollmer